Accelerometry based detection of epileptic seizures

PROEFSCHRIFT

ter verkrijging van de graad van doctor aan de
Technische Universiteit Eindhoven, op gezag van de
Rector Magnificus, prof.dr.ir. C.J. van Duijn, voor een
commissie aangewezen door het College voor
Promoties in het openbaar te verdedigen
op donderdag 11 september 2008 om 16.00 uur

door

Tamara Mathea Elisabeth Nijsen

geboren te Weert

Dit proefschrift is goedgekeurd door de promotoren:

prof.dr. R.M. Aarts
en
prof.dr. P.A.J.M. Boon

Copromotor:
dr.ir. P.J.M. Cluitmans

Drukwerk: Universiteitsdrukkerij TUE

A catalogue record is available from the Eindhoven University of Technology Library

ISBN 978-90-386-1379-6

Hab Sonne im Herzen...

CONTENTS

1 INTRODUCTION

Epilepsy is one of the most common neurological disorders. Worldwide, epilepsy affects almost 60 million people [1]. The diagnosis of epilepsy is made by the occurrence of at least 2 unprovoked seizures. Epileptic seizures are the manifestation of abnormal hypersynchronous discharges of populations of cortical neurons. These discharges impair brain function. The signs and symptoms of seizures depend upon the location and extent of the propagation of the discharging cortical neurons. A seizure can express itself in movements or one could experience sensorial sensations, like strange smells or aura's. The best known example of a seizure is a tonic-clonic seizure. During a tonic-clonic seizure the patient loses consciousness and can drop down to the floor. A phase of tetanic muscle contraction (tonic phase), is followed by a phase in which jerking of the body and limbs occur (clonic phase).
The perception that epilepsy was a neurological disorder was not widely accepted until the 19th century. In the 20th century, the development of the electroencephalograph (EEG) revealed the presence of electrical discharges in the brain. It also showed different patterns of brainwave discharges associated with different seizure types. The EEG also helped to locate the site of seizure discharges and expanded the possibilities of neurosurgical treatments. Since the 1960s, there has been an accelerating process of drug discovery, based in part on a much greater understanding of the electrochemical activities of the brain, especially the excitatory and inhibitory neurotransmitters. Most of the people affected can be treated successfully with drug therapy (67%) or neurosurgical procedures (7-8%). Nevertheless there is still 25% of the people affected that can not be treated by any available therapy [1]. For refractory patients who also continue to have frequent seizures, it is shown that intensive monitoring with EEG and video over a longer period, contributes to the management of daily care and the adjustment of drug therapy [2]. Intensive monitoring with EEG and video can be very unpleasant for patients, and analyzing large amounts of EEG/video-data is very labor intensive for medical personnel. Therefore it would be of great clinical value, if there was an automated seizure detection system available that is both reliable and patient friendly, that can be used for long-term monitoring of refractory patients with frequent seizures in their living environment. A possibility for detecting these seizures is to focus on motor signs since epileptic seizures are often accompanied by motor signs.

In this context, this thesis describes the first results of *accelerometry* based seizure detection. A detailed overview is provided on the perspectives for

long-term epilepsy monitoring and automated seizure detection. The value of accelerometry (ACM) for seizure detection is shown by means of a clinical evaluation, and methods are developed for the detection of motor activity, and two types of simple motor seizures to support off-line analysis. Naturally there will always be seizures without motor signs, where only changes in consciousness will take place. For the detection of these types of seizures the EEG will always be necessary.

In summary, in this thesis the first steps are made for accelerometry based detection of epileptic seizures. Besides extensive studies on the perspectives for automated seizure detection in long-term monitoring purposes and the value of accelerometry for seizure detection, new detection methods were developed for the detection of motor activity, myoclonic seizures and tonic seizures. Clinical information was incorporated in the feature extraction and a new model based wavelet is developed that incorporates physiological information.

1.1 SIMPLE MOTOR SEIZURES

With accelerometry (ACM) only seizures can be detected that express themselves in movements or seizures that disturb normal movement patterns. Seizures in which the main clinical manifestations are movements are called motor seizures [3]. These motor seizures can be divided into two major subgroups, simple motor seizures and complex motor seizures[1]. In simple motor seizures, motor movements are relatively 'simple' and unnatural and are caused by a relatively massive discharge in the motor structures of the cortex. Complex motor seizures are seizures in which the movements are relatively complex and simulate natural movement, except that they are inappropriate for the situation. These seizures often arise from the limbic system.
This thesis focusses on the detection of simple motor seizures. The movements during simple motor seizures tend to be stereotypical, and when movements are repetitive, they affect the same body segment [6]. Simple motor seizures can be subdivided into the following types: myoclonic, clonic, tonic, and tonic-clonic seizures. These types depend on the duration of the muscle contractions, the frequency of movement repetition, and the muscles involved.

1 To prevent confusion it should be mentioned here that the words 'simple' and 'complex' indicate the type of movement. According to the current seizure classification standard 'simple\complex' generally means 'not accompanied by loss of consciousness\accompanied by loss of consciousness'[4, 5]

1.1.1 *Myoclonic seizures*

A myoclonic seizure is characterized by a sudden jerk. Each myoclonic jerk typically involves only a few adjacent muscles, for example, only one antagonistic pair. Myoclonic jerks are most probably generated by activation of the primary or secondary motor area's in the cortex by epileptic discharges. Most of these epileptic seizures begin in the frontal lobe and then spread a.o. towards the motor cortex. The central area of the motor cortex (primary motor area) is responsible for subtle myoclonic jerks. When the frontal area of the motor cortex is involved (secondary motor area), this results in more massive jerks.
The surface EEG associated with a myoclonic seizure shows a (poly)spike-wave correlate [7]. EMG-signals reveal synchronous muscle activation in both agonist and antagonist muscle of the affected muscle group. The duration of this train of muscle action potentials is $<$100 ms and the frequency is $\approx$ 50 Hz [8].
During a myoclonic jerk flexor muscles are generally more active than extensor muscles. Also distal muscles are more affected than proximal muscles, and the arms are more affected than the legs. This stereotype expression is caused by the fact that the projection area of the motor cortex to these segments of the body is larger.
A schematic representation of such an arm movement associated with a myoclonic seizure is depicted in Fig. 1 A.

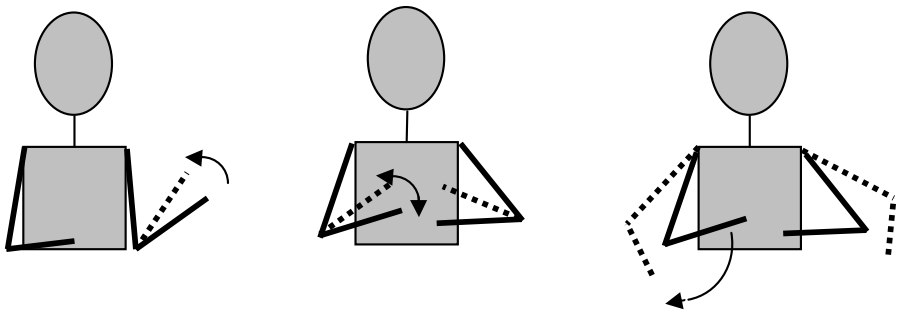

Figure 1: Schematic representation of arm movements during simple motor seizures.

1.1.2 *Clonic seizures*

Clonic seizures consist of repeated myoclonic contractions that regularly recur at a intervals between 0.2 and five times per second [6]. During a clonic seizure the affected parts of the body show repetitive jerking. Tetanic 50 Hz electrical stimulation of the motor strip in wake humans can elicit clonic muscle responses. Hamer et al. [9] used cortical electrical stimulation to investigate the pathophysiology underlying the clonus generation. They also analyzed spontaneous focal clonic seizures in humans by recording of EEG in combination with surface EMG-recordings of muscles involved in the epileptic clonus [10]. Stimulation of the motor cortex with frequencies of 20 Hz or more elicited clonic muscle response. The rhythmic clonic muscle responses consisted of bursts of muscle action potentials which occurred synchronously in agonistic and antagonistic muscles and were separated by periods of complete muscle relaxation in all muscles despite continuous stimulation. Alternating contractions of agonistic and antagonistic muscles were never observed. The frequency of muscle action potentials within each burst followed the stimulation frequency. During the spontaneous clonic seizures (poly)spike-wave complexes were observed in the EEG (Fig. 2).

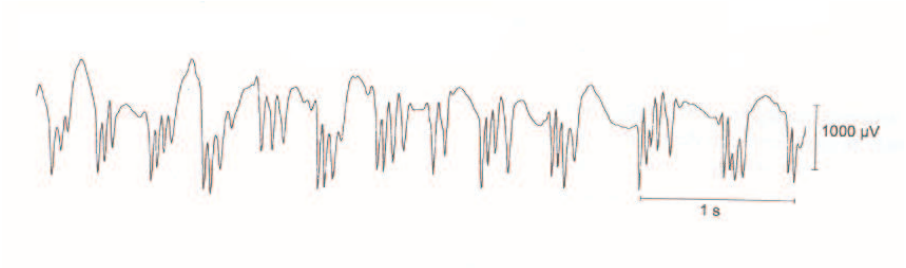

Figure 2: (Poly)spike-wave complexes in the EEG that are associated with clonic seizures [10].

These (poly)spike-wave complexes were coinciding with the appearance of clonic muscle activity. Here again the bursts of muscle action potentials occurred synchronously in agonistic and antagonistic muscles and were separated by periods of complete muscle relaxation in all muscles. Again, alternating contractions of agonistic and antagonistic muscles were never observed. The waveform of each (poly)spike-wave complex consisted of 2-6 spikes recurring with a frequency of 12-45 Hz. The series of muscle action potentials (muscle contraction) follow the spikes and the periods of muscle relaxation follow the waves of the (poly)spike-wave complexes. It is believed that the rhythmic arrest of motor activity during clonic seizures is caused by hyperpolarization of pyramidal tract cells [9, 10]. A schematic representation

of the jerking arm movements associated with clonic seizure is depicted in Fig. 1 B.

1.1.3 *Tonic seizures*

During tonic seizures a sudden sustained contraction of multiple muscle groups is seen. Often the limbs undergo a slow change of posture, but depending on how quickly the seizure starts it can also begin with a massive jerk. Tonic seizures have a duration that lies typically between 10 and 20 seconds, but can vary between 2 seconds and 60 seconds [3]. They are primarily generated by the supplementary motor area frontal in the brain. The EEG shows diffuse low voltage, fast frequency (20-40 Hz) activity, which may show a gradual increase in amplitude with decreasing frequency (Fig. 3).
Hamer et al. showed that increasing the intensity of stimulation at the same

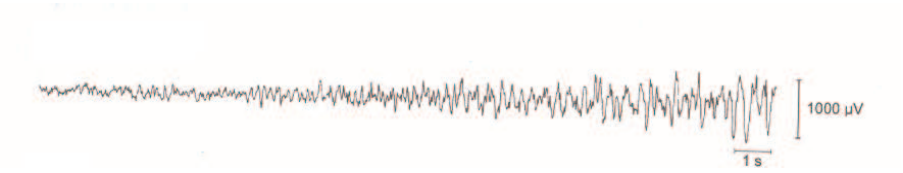

Figure 3: EEG associated with tonic seizure: diffuse low voltage, fast frequency (20-40 Hz) activity, which may show a gradual increase in amplitude with decreasing frequency [10].

frequency (50 Hz) converted an intermittent clonic muscle response to a continuous tonic muscle response [9]. High intensity cortical stimuli appeared to overcome the recurrent cortical inhibition occurring during clonus. This indicates that during tonic seizures the level of epileptic activity in the brain is so high, that the cortical inhibition that occurs during a clonic seizure fails. A schematic representation of the slow change of posture of the arms associated with tonic seizure is depicted in Fig. 1 C.

1.1.4 *Tonic-clonic seizures*

These seizures consist of an initial tonic phase during which the patient has the legs and arms in extension with the arms adducted and crossed in front of the body. The tonic phase lasts 5–10 seconds and is then followed by a series of tremor-like muscle contractions. The movements of the arms increase progressively in amplitude as the repetition rate diminishes. Eventually, this evolves to clonic contraction (flexions at the elbow), initially of a frequency of 5 Hz, and then progressively decreasing in frequency to one contraction every

1 to 3 seconds [3]. Finally the contractions disappear completely. The muscles included in the tonic and clonic phase should be essentially the same.

1.2 ACCELEROMETRY

1.2.1 *State of the art*

Accelerometers are used in many medical research areas for activity recognition [11], [12]. Information about physical activity can be used in a.o. rehabilitation medicine [13], [14], [15], geriatrics [16] and Parkinson's disease [17], [18], [19], [20]. Most recent literature focusses on physical activity in obesity [21], and preventive healthcare [22]. In geriatrics accelerometers are also applied for fall detection in the elderly [23]. Published literature concerning epilepsy, seldom mentions accelerometry (ACM) and it has never been used in a detection context [24], [25], [26]. Seizure detection literature heavily depends on the EEG-signal. Only recently other sensor modalities that focus more on the clinical symptoms and signs of seizures have become more popular [27]. Thus detection of epileptic seizures based on ACM is a research field that is open for exploration.[2]

1.2.2 *Sensor type*

The accelerometers used in this thesis, are created using the two-axis accelerometer ADXL202E from Analog devices. The three-dimensional (3-D) accelerometers described in this thesis, were created by mounting two 2D-sensors at right angles to each other. One channel is not connected during the recordings, and thus a 3-D accelerometer is created. In the studies presented in these thesis, five 3-D sensors were placed on the body. Simple motor seizures are most clearly visible on the extremities. To get a complete picture of the movements of the limbs and the body accelerometers were placed on both wrists, both ankles and on the sternum.
The output of an accelerometer attached to the human body consists of different components:

1. noise from sensor and measurement system
2. noise sources from environment:
    a. accelerations produced by external sources, like vehicles
    b. accelerations due to bumping of the sensor or the body against other objects
3. noise sources from the body:

2 An extensive overview on the literature concerning seizure detection is given in chapter 2 of this thesis.

   a. muscle tremor
   b. heart
   c. respiration
   d. blood flow
4. gravitational acceleration
5. accelerations due to movements of the body

In comparison to body movements, the noise from the sensor and measurement system can be neglected. All data used in this thesis was recorded while the patients were in their living environment, thus there were no accelerations produced by external sources. When there is no movement, physiological noise, like respiration and heart rate are clearly visible in the signal. In chapter 4, this information is used to set a threshold for motor activity. Gravitational acceleration varies between -1 g and 1 g, depending on the orientation of the measured direction of the sensor in the gravitational field.

1.3 SIGNAL PROCESSING METHODOLOGY

This thesis describes signal processing methods that can be used to detect simple motor seizures to assist off-line analysis of long-term recorded accelerometer signals in clinical practice. The information that is obtained from these off-line detections can then be used to evaluate medical treatment and daily care.
As we shall see in chapter 3 of this thesis, patterns in accelerometry (ACM) signals associated with simple motor seizures reflect the stereotypical movements that can be observed during these seizures. This results in 3 types of elementary patterns (myoclonic, tonic, clonic). Each pattern has its own characteristics of duration, intensity and frequency. Therefore it was decided to use a modular approach for the detection methodology as represented in Fig. 4. The first step is to develop an algorithm that distinguish between periods in the data with and without motor activity. When there is no motor activity, there is no motor seizure, and in this way a large part of the data can be excluded in a simple way. This results in a reduction of the amount of data that needs to be further analyzed with stronger, more complex signal processing tools. The second step is the development of separate detection modules for each seizure type. This thesis covers strategies for the detection of myoclonic and tonic seizures.

1.3.1 *Supervised learning*

For the algorithms described in this thesis a supervised learning approach is chosen. This means that appropriate features, classification algorithms,

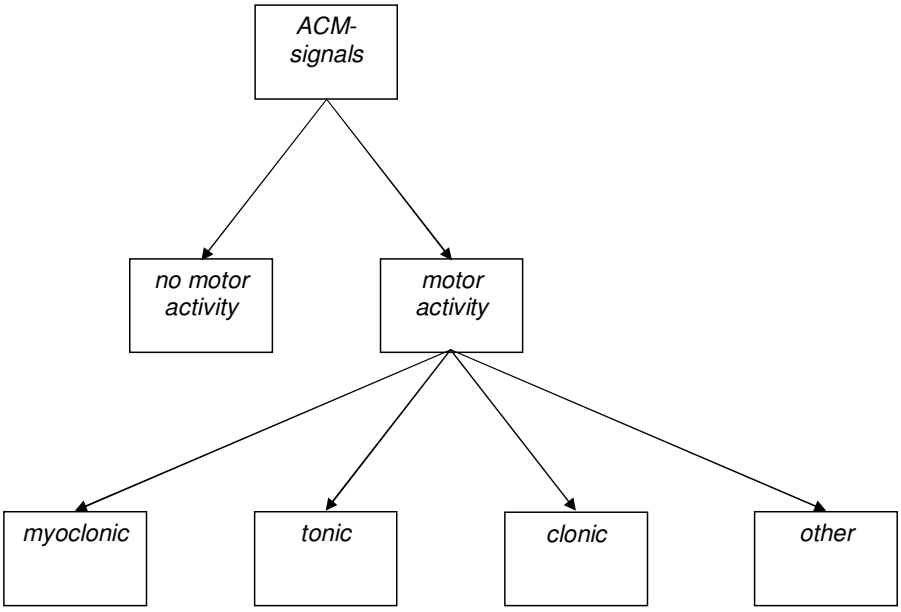

Figure 4: Modular approach: Step 1: Screening data for motor activity. Following steps: detecting presence of elementary patterns associated with seizures.

and a proper way of training the algorithms with labelled data need to be chosen. It is known that the success of classification critically depends on the choice of features and much less on the complexity of the type of classifier [28]. Therefore one of the key principles of this thesis is its main focus on the selection of suitable features. For classification straightforward classification methods are used. Furthermore, it is known that features that incorporate morphological or physiological characteristics of the pattern of interest are most successful for pattern recognition [29]. Therefore in this thesis features are used that are either based on the morphology of the patterns of interest, as described in clinical practice, by experts, or the features are based on physiological model that analytically describes the pattern of interest with parameters that are related to seizure duration and intensity.

The detection methods suggested in this thesis are all evaluated using clinical data. Figure 5 shows the setup that is used for this evaluation. ACM-signals obtained from epilepsy patients are annotated (labelled) by three experts. Besides the ACM-signals they also have acces to the gold standard EEG/video. These annotations are used as a standard to evaluate the detection methods described in this thesis. Here it has to be kept in mind that the evaluation thus heavily depends on the experts and that results based on such standard should be interpreted with care.

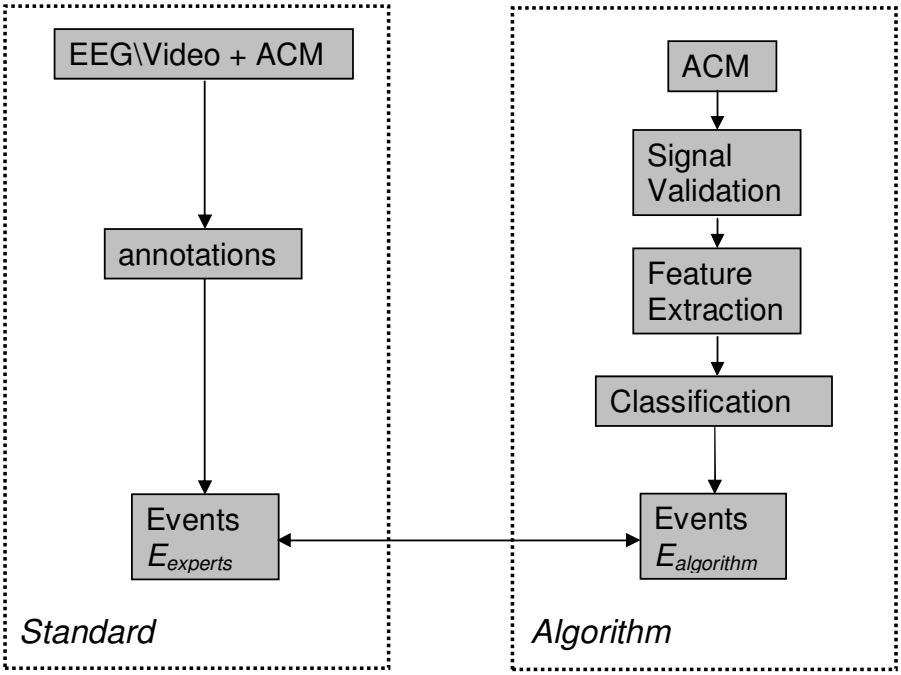

Figure 5: Complete detection and evaluation setup. Two parallel schemes: one for the video that is used for evaluation of the algorithm and one for the ACM-based detection algorithm.

1.4 THESIS OUTLINE

Seizure detection based on accelerometry (ACM) is a novel field of research. This thesis describes a number of studies that were intended to evaluate the use of accelerometers for the detection of epileptic seizures.

Chapter 2 gives an overview of the literature on seizure detection algorithms. Here it is shown that for seizure detection in living environments not only the adjustment of existing (EEG-based) techniques is important, but also the development of new methods based on other sensor modalities (e.g. ACM) and the incorporation of clinical information in the detection methodology.

Chapter 3 shows that 3-D ACM is a valuable sensing method for detection of simple motor seizures. A clinical study is carried out where 18 mentally retarded patients with severe epilepsy are intensively monitored over a period of 36 hours, using the gold standard EEG/video and 5 3-D accelerometers. It is found that 95% of the motor seizures in our population consist of one or more of three elementary patterns that are associated with simple motor seizures. The outcome of this clinical study is a good starting point for automated seizure detection.

Chapter 4 presents the first step for an automated detection algorithm for nocturnal seizures based on 3-D ACM. The main goal is to distinguish between data with and without subtle nocturnal motor activity. This results in reducing the amount of data that needs further (more complex) analysis for seizure detection.
In **Chapter 5** a model for myoclonic seizures is presented. This model consists of an electrophysiological and a mechanical part. From this model, an analytical expression is derived for the pattern that can be observed in ACM-signals during myoclonic seizures. This analytical expression is the basis for a wavelet. This wavelet can be used to analyse accelerometer signals and can contribute to the detection of myoclonic seizures.
This is shown in **Chapter 6**, where the model based wavelet is evaluated in a clinical data set. Furthermore three other time-frequency methods for the detection of myoclonic seiuzres are studied. It is found that wavelet based methods are useful for detection of myoclonic seizures. On top of that, our model based wavelet has the advantage that it consists of parameters that are related to seizure duration and intensity which is physiologically meaningful.
In **Chapter 7** features are derived that are suitable for the detection of ACM-patterns associated with tonic seizures. In contrast to the myoclonic jerks that are fast and abrupt in appearance, and short in duration, tonic movements are slow and gradual in appearance, and longer in duration. These characteristics are incorporated in the features. The results show that our approach can contribute to the detection of tonic seizures.
This thesis is concluded by **Chapter 8** with recommendations for future research.

This thesis consists to a large extent of material that over the past years is published elsewhere by the author.

- Chapter 3 as [30], and
- Chapter 4 as [31], and
- Chapter 5 consists of two short papers, that are separately published as [32] and [33].

Furthermore other parts of this thesis are submitted to scientific journals and are currently under review.

- Chapter 2 as [27], and
- Chapter 6 as [34].

2

SEIZURE DETECTION IN LONG-TERM MONITORING, FROM CLINICAL PRACTICE TO HOME ENVIRONMENT

This chapter is submitted to the Journal of Clinical Neurophysiology as:
T.M.E. Nijsen, J.B.A.M. Arends, P.A.M. Griep, P.J.M. Cluitmans, and P.A.J.M. Boon, Seizure detection in long-term monitoring, from clinical practice to home environment [27].

2.1 ABSTRACT

This chapter reviews the literature on epileptic seizure detection methodologies suitable for long-term monitoring. Both technological and clinical aspects of seizure detection methodologies are explored varying from sensor type and mathematical methods used to patient and seizure characteristics. Implications of these data for future research and development for seizure detection in clinical practice are considered. There are many methods developed for seizure detection in established application areas such as the Epilepsy Monitoring Unit and (Neonatal) Intensive Care Units. These methods are usually based on the EEG-signal. Recently, the need for seizure detection outside intensive monitoring units has lead to the use of other sensor modalities that are more patient friendly and thus more suitable for care at distance. Often detection methods are developed for specific patient or seizure types, but the extrapolation of these methods to a broader patient population is not evident. Hence, the development of seizure detection methods for application areas that are yet to be explored such as institutions and home environments is not trivial. Furthermore for monitoring in living environments alternative physiological measures such as movement and heart rate will be more important. Signal processing methods that are commonly used, focus on the calculation of features that have a physiological meaning or are morphological characteristics of the signal pattern of interest. Nevertheless patient and seizure characteristics are often omitted in the feature selection process. Hence for seizure detection outside specialized hospital units not only the adjustment of existing techniques is important, but also the development of new methods based on other sensor modalities and the incorporation of clinical information in the detection methodology.

2.2 INTRODUCTION

There is a growing need for seizure detection systems that can be reliably used in a mobile set up for monitoring refractory epilepsy patients in institutions

or home situations [35, 36, 37]. Seizure detection in patients with frequent seizures will result in better management of daily care or adjustment of drug therapy [38, 2, 39, 40]. Seizure detection can also trigger medical intervention in life threatening situations such as a status epilepticus. Historically automated seizure detection was first pursued in epilepsy monitoring units (EMU), to facilitate the analysis of 24-hours EEG recordings, and to reduce the workload of the EEG-technicians [41]. In this context information of seizure frequency and type is used for diagnostic purposes and the evaluation of candidates for epilepsy surgery. Later EEG measurements were also used in intensive care units (ICU), to monitor brain function in critically ill patients, and in neonatal intensive care units (NICU), where the occurrence of seizures can indicate neurological complications. Recent technological developments, such as wireless communication, low-power design and flexible sensors, make it easier to continuously monitor patients from a distance [42, 43]. Therefore seizure detection can be applied easier in other areas, that are outside specialized hospital units, such as institutions (INST), home situations (HOME) and in- and outpatient clinical monitoring (CLIN), where patients are temporarily monitored, for diagnostic purposes, with an ambulatory setup. In all the application areas above, the term 'long-term monitoring' is used. The meaning of 'long-term' strongly depends on the application area. For epilepsy monitoring units, (neonatal) intensive care units and outpatient clinical monitoring, the monitoring duration varies from several hours to days. In an institution or home environment the monitoring duration can be indefinite. In all these situations, a suitable seizure detection method, also has to meet different requirements for patient friendliness and costs as is depicted in Fig. 6.

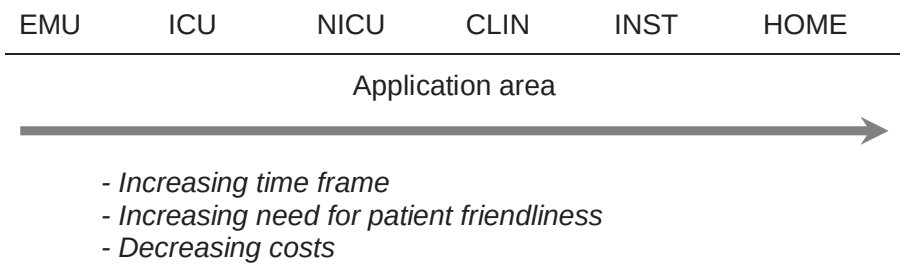

Figure 6: Monitoring duration, need for patient friendliness and cost depend on application area.

Presently, numerous alarm devices are already available, such as mechanically triggered alarms in mattresses or audio-triggered alarms, but the reliability and performance of these devices for seizure detection are not described in literature. Most published seizure detection approaches are originally based on the EEG-signal. EEG/video-monitoring is considered as the gold standard for seizure detection in clinical routine. Nevertheless, the measurement of

the EEG is not always practical, especially when the electrodes have to stay on the head for several days. Furthermore, seizures sometimes are not accompanied by EEG changes (for example elementary seizures and seizures in mentally retarded patients). Only recently, detection algorithms that use signals from alternative sensor modalities for seizure detection have been described in literature [44, 30, 45]. These articles focus more on autonomic effects (increase of heart rate) and movement characteristics. So called 'motor seizures' can be divided in elementary movement patterns (myoclonic, clonic, tonic and tonic-clonic movement patterns) and complex movement patterns [3]. Movements can be monitored with video or accelerometry (ACM). Video is part of the gold standard for seizure detection. Not only movement but also the total behavior of the patient is visible in the video, but the moving body parts have to be in the scope of the camera. Accelerometers are worn on the body, thus seizure detection is not limited to living areas with a video camera, providing more freedom in daily activities.

This chapter aims to review the literature that describes methods used for seizure detection in general and to provide practical considerations for seizure detection during long-term monitoring in a mobile environment. Previously seizure detection literature was reviewed by Gotman [46]. Here, all described methods were purely based on the EEG and most attention was paid to hospital monitoring. The focus of this article will be on the technological methodology used, such as sensor choice and signal processing strategies. It will be shown that for long-term monitoring in institutions and home environment it is important to take into account the clinical aspects of seizures and to integrate various physiological measurements and detection methods.

2.3 METHODS

2.3.1 *Search strategy and analysis variables*

Relevant studies were identified using *PubMed* and *Web of Science*. Articles included in this review were identified by using the following search query: (computerized OR automa*) AND seizure AND (detection OR prediction OR warning OR alarm OR monitoring) NOT (MRI OR CT OR MEG OR SPECT OR PET OR (antiepileptic drug) OR surgery OR animal).
With the * indicating that the search was extended to find all terms that begin with a given text string. The last search was performed on January 14th 2008. Titles and abstracts identified during the search were reviewed for relevance, and if appropriate, the full-text article was retrieved. Articles that did not have 'seizure detection' as primary topic (e.g., MRI, CT, SPECT, PET, MEG, antiepileptic drugs or epilepsy surgery) were excluded. Articles on interictal spike detection were excluded, since this review focusses on the detection

of ictal manifestations. Articles that used only intracranial EEG to evaluate detection methods were also excluded. Furthermore articles were excluded if they were published in another language than English or published before 1975. Review articles and editorials were excluded from analysis.
The remaining articles were screened for the analysis variables depicted in Table 1.
Technological variables are divided into five categories: measurement, application area, detection method, evaluation and performance. Clinical variables are patient type, epilepsy syndrome and seizure type. For a paper to be included in this review, the detection method must be clearly described and all the variables of at least two of the other technological categories should be described. Availability of clinical variables is not mandatory for an article to be included, but when they are present they are taken into account as analysis variable. After selecting the relevant articles, the PubMed function *related articles* was used to find other relevant articles. Also the references of the selected articles were checked for relevant articles. As a result of this selection procedure, in total 47 articles were included.

Table 1: Analysis variables

Technological	Measurement	Sensor type
	Application area	EMU, (N)ICU, CLIN, INST or HOME.
	Detection method	Feature extraction and classification
	Evaluation	Number of patients, number of seizures, and measurement duration
	Performance	Sensitivity, specificity, positive predictive value, false detection rate per hour or other statistical measure.
Clinical	Patient type	Age, sex and mental development level
	Epilepsy syndrome	Syndromes described by the ILAE in 2001 [5].
	Seizure type	Semiological seizure classification according to Lüders et al. [3].

Abbreviations: EMU: Epilepsy Monitoring Unit, (N)ICU: (Neonatal) Intensive Care Unit, CLIN: In- or outpatient clinical monitoring, INST: Monitoring in institution, HOME: Home monitoring.

2.4 RESULTS

Table 2 shows all analysis variables per article. Articles are listed in chronological order. For each variable the results will be described in the next sections. Striking results will be further discussed in the discussion.

2.4.1 *Measurement*

The majority of published articles described seizure detection based on the EEG signal (39 studies). Four studies used video, two used the ECG and one

study used accelerometers.
The EEG is part of the gold standard for seizure detection, that consists of the combination of video and EEG. Epileptic seizures result from abnormal synchronization of brain activity. EEG measures electrical activity of the brain, and is therefore a logical choice for monitoring epilepsy patients. Nevertheless EEG is not always practical, often many electrodes need to be placed on the head. Especially in institutions and home environments this is not practical. For monitoring neonates also the cerebral function monitor (CFM) was used, which uses two electrodes [47]. Because of this sampling bias, seizures that occur in another part of the brain than where the electrodes are positioned can be missed.
Also not all seizures are necessarily visible in the EEG-signal. Nijsen et al. described a clinical study that shows that accelerometry and EEG are complementary for seizure detection in a number of patients [30]. Also in neonates seizures can either give rise to changes in the EEG or cause specific change in movements, that can be detected from video-recordings [44].
Epileptic seizures can be accompanied by changes in heart rate. Van Elmpt et al., and Greene et al. described algorithms for seizure detection based on the ECG signal [45, 48].
Because of the widespread seizure variety, combinations of sensor types might be useful. This idea is presented by several authors [49, 45]. Practical results of such a combined setup were only presented by Greene et al. [50]. Here EEG and ECG were combined to detect seizures in newborn subjects.

2.4.2 *Application Areas*

The application areas that are most mentioned in literature are the epilepsy monitoring unit, EMU (17) and the neonatal intensive care, NICU (20). Three studies mentioned the use of their method for intensive care (ICU) [51, 52, 53]. One study mentioned the use of ambulatory EEG [54], that is mostly applied for in- or outpatient clinical monitoring(CLIN). Only 5 studies emphasized that their method may be used for patients in their living environment [55, 30, 56, 45, 57].
Chronologically EMU is the first application area where large amounts of EEG data were available. After seizure detection in EMU became more successful it was extrapolated to (neonatal) intensive care units. Technological developments made it possible to measure ambulatory EEG and therefore also patient monitoring outside the clinic became possible.

2.4.3 *Detection Method*

In the literature, many algorithms for seizure detection are described. Although various sensor types can be used, all suggested signal processing

Table 2: Characteristics of articles on long-term seizure detection

			Detection Method	
AUTHOR (YEAR)	SENSOR	APPL.	FEATURE EXTRACTION	CLASSIFICATION
Gotman (1982) [58]	EEG	EMU	HW based	RBD
Gotman (1990) [59]	EEG	EMU	Gotman(1982)	Gotman(1982)
Liu et al. (1992) [60]	EEG	NICU	autocorrelation	RBD
Pauri et al. (1992) [61]	EEG	EMU	Gotman(1982)	Gotman(1982)
Qu and Gotman (1993) [62]	EEG	EMU	Gotman (1982) + subspace	PS threshold
Gabor et al. (1996) [63]	EEG	EMU	WT based (amplitude + TF)	RBD + NN [a]
Pradhan et al. (1996) [64]	EEG	EMU	filtered EEG	NN
Webber et al. (1996) [65]	EEG	EMU	TD + FD	NN + RBD
Weng and Khorasani (1996) [66]	EEG	EMU	TD + FD	NN
Yaylali et al. (1996) [67]	EEG	EMU	autocovariance + correlation dimension	threshold
Gotman et al. (1997a) [68]	EEG	NICU	M1: FD M2: HW based features M3: filtering + HW based features	RBD
Gotman et al. (1997b) [69]	EEG	NICU	Gotman (1997a)	Gotman (1997a)
Qu and Gotman (1997) [55]	EEG	INST, HOME	TD , FD + location	nearest neighbour
Gabor (1998) [70]	EEG	EMU	Gabor (1996)	Gabor (1996)
Klatchko et al. (1998) [71]	EEG	..	Webber (1996) + clustering	Webber (1996) + clustering
Roessgen et al. (1998)[72]	EEG	NICU	model based	threshold
Celka (2002) [73]	EEG	NICU	singular value decomposition + minimum description length algorithm	threshold
Liu et al. (2002) [54]	EEG	CLIN	adaptive filtering, WT, TD	NN + expert system
Altenburg et al. (2003) [74]	EEG	NICU	synchronization likelihood	threshold
van Putten (2003) [51]	EEG	ICU	maximum nearest neighbour phase synchronization	threshold
Shoeb et al. (2004) [75]	EEG	..	WT based	SVM + temporal constraint
Smit et al. (2004) [76]	EEG	NICU	synchronization likelihood	threshold
Faul et al. (2005) [77]	EEG	NICU	M1:Gotman(1997a) M2:Liu(1992) M3:Celka(2002)	M1:Gotman(1997a) M2:Liu(1996) M3:Celka(2002)
Firpi et al. (2005)[78]	EEG	..	delay embedding + genetic programming	nearest neighbour
Karayiannis et al. (2005) [44]	Video	NICU	motion strength + trajectory (TD)	NN
Nijsen et al. (2005) [30]	ACM, EEG	INST	..	visual inspection
Saab and Gotman (2005) [56]	EEG	EMU, HOME	WT based	threshold
Subasi (2005a) [79]	EEG	EMU	WT	NN
Subasi and Erçelebi (2005b)[80]	EEG	EMU	WT	logistic regression or NN
Wilson (2005) [81]	EEG	EMU	TF features	NN
Aarabi et al. (2006) [29]	EEG	NICU	TD, FD, WT, cepstral , autoregressive coefficients	feature redundancy analysis + NN
van Elmpt et al. (2006) [45]	ECG	INST	median RRI	threshold
Karayiannis et al. (2006a) [82]	Video	NICU	motion strength (TD + FD)	NN
Karayiannis et al. (2006b) [83]	EEG	NICU	FD	RBD + NN
Karayiannis et al. (2006c) [49]	Video	NICU	motion trajectory (TD +FD)	NN
Karayiannis et al. (2006d) [84]	Video	NICU	motion strength + trajectory (TD + FD)	NN
Navakatikyan et al. (2006)[85]	EEG	NICU	parallel wave fragmentation	RBD
Slooter et al. (2006)[52]	EEG	ICU	synchronization likelihood	threshold
Subasi (2006) [86]	EEG	EMU	WT	NN [a]
Aarabi et al. (2007) [87]	EEG	NICU	TD, FD, WT, cepstral, autoregressive coefficients	feature redundancy analysis + NN + RBD
Greene et al. (2007a) [48]	ECG	NICU	RRI-based (TD + FD)	LDA
Greene et al. (2007b) [50]	EEG, ECG	NICU	RRI-based (statistical + nonlinear) + EEG-based (FD + nonlinear)	LDA
Lee et al. (2007) [57]	EEG	EMU, HOME	M1:Total power M2:Largest principal eigenvalue M3:Kolmogorov Entropy M4:Correlation Dimension	threshold
Hopfengärtner et al. (2007) [88]	EEG	EMU	integrated spectral power	threshold
Khlif et al. (2007) [89]	EEG	NICU	TF matched filter	threshold
Lommen et al. (2007)[47]	EEG	NICU	amplitude integrated EEG	threshold
Subasi (2007) [53]	EEG	ICU	WT + statistical	adaptive neurofuzzy inference system [a]

[a] Unsupervised learning method. [b] Only the numbers for the testdata are included. [c] Age groups: newborn (N), children (C), adults (A). [d] '+' if syndromes are defined as described by Engel [5]. [e] '+' if semiological seizure classification according to Lüders et al. [3] is used. [f] Mentally retarded subjects. [g] In two patients. [h] In five recordings.

AUTHOR (YEAR)	Clinical			Evaluation[b]			Performance[b]			
	Age[c]	ET[d]	ST[e]	n	MD (h)	SN	Sen	Spec	FDR/h	Other
Gotman (1982)		-	-	16	297.6					PPV 0.24
Gotman (1990)	C,A	-	-	44	4362.1	179	0.73		0.84	
Liu et al. (1992)	N	-	-	14	0.975		0.84	0.98		
Pauri et al. (1992)	C,A	+	+	12	461	253	0.81		5.38	
Qu and Gotman (1993)		-	-	10	1070.6				1.45	
Gabor et al. (1996)		-	-	22		62	0.90		0.71	
Pradhan et al. (1996)		-	-	4			0.67	0.75		
Webber et al. (1996)	A	-	-	50		34	0.76		1	PPV 0.87
Weng and Khorasani (1996)		-	-	5	5–10 days	39	0.95		0	
Yaylali et al. (1996)	C	-	-	41		22	0.86	0.95		
Gotman et al. (1997a)	N	-	-	55	281.5	679	M1:0.64 M2:0.35 M3:0.13 All:0.71		M1:0.8 M2:0.8 M3:0.2 All:1.7	
Gotman et al. (1997b)	N	-	-	54	235.5	662	0.69		2.3	
Qu and Gotman (1997)		-	-	12	31.2	36	PS:1.00 PI:0.12		PS:0.02 PI:0.46	
Gabor (1998)	C,A	-	-	65	4553.8	181	0.93		1.35	
Klatchko et al. (1998)	C	-	-	10	4.1	25	0.69			PPV 0.74
Roessgen et al. (1998)	N	-	-	2	3.1	69	0.93			PPV 0.64
Celka (2002)	N	-	-	4			0.93			FDR 0.04
Liu et al. (2002)		-	-	81	> 800		0.90			FDR 0.06
Altenburg et al. (2003)	N	-	-	22			0.85	0.75		
van Putten (2003)		+	+	16	40		0.48–0.87	0.48–0.87		
Shoeb et al. (2004)	C	-	+	36	60	139	0.94		0.25	
Smit et al. (2004)	N	-	-	20	10.9		0.66	0.90		
Faul et al. (2005)	N	-	-	13	1.3	34	M1:0.63 M2:0.43 M3:0.66	M1:0.64 M2:0.90 M3:0.56		
Firpi et al. (2005)		+	+	3	267.6	26	1.00		0.007	
Karayiannis et al. (2005)	N	-	+	43		160	MYO:0.94 CLO:0.86	MYO:0.96 CLO:0.98		
Nijsen et al. (2005)	A[f]	+	+	18	288	897				
Saab and Gotman (2005)		-	-	16	360	69	0.76		0.34	
Subasi (2005a)		-	+	5		20	best 0.93	best 0.93		
Subasi and Erçelebi (2005b)		-	+	5	452.8	20	LR:0.89 NN1:0.92 NN2:0.93	LR:0.90 NN1:0.91 NN2:0.92		
Wilson (2005)		+	+	10	80	57	0.89		0.56	
Aarabi et al. (2006)	N	-	+	6	5.1	34	0.91	0.95	1.17	
van Elmpt et al. (2006)	A[f]	+	+	3	12	58	>0.90			PPV>0.50[g]
Karayiannis et al. (2006a)	N	-	+	54			>0.90	or >0.90		
Karayiannis et al. (2006b)	N	-	-	12			best 0.84	best 0.80		
Karayiannis et al. (2006c)	N	-	+	54			best >0.90	best >0.90		
Karayiannis et al. (2006d)	N	-	+	54			all >0.90	all >0.90		
Navakatikyan et al. (2006)	N	-	-	55	24.4	97	0.84	0.48–0.77		
Slooter et al. (2006)	A	-	-	26	0.875	38				
Subasi (2006)		-	+	5		20	0.93	0.93		
Aarabi and Grebe (2007)	N	-	+	10	86	478	0.74	0.86	1.55	
Greene et al. (2007a)	N	+	-	7	101.55	520	PI:0.55 PS:0.62	PI:0.77 PS:0.72		
Greene et al. (2007b)	N	+	+	10	154.1	633	PI:0.81 PS:0.98			PI: FDR 0.29 PS: FDR 0.13
Lee et al. (2007)	C	+	-	4	245	29	M1:0–0.96 M2:0-0.58 M3:0-0.63 M4:0			FDR 0.50
Hopfengärtner et al. (2007)	A	+	+	19	3248	148	0.91		0.29	
Khlif et al. (2007)	N	-	-	6			0.92			FDR 0.02
Lommen et al. (2007)	N	+	-	13	222		> 0.90[h]		1	
Subasi (2007)		-	+	12		20	0.94	0.94		

Abbreviations: ACC:Accuracy, Appl.:Application, CLO:focal clonic seizure, ET:epilepsy type, FD:frequency domain, FDR(/h):false detection rate (per hour), HW:half wave, LDA:linear discriminant analysis, LR:logistic regression, M: method, MD:measurement duration, MYO:myoclonic seizure, n:number of patients, NN: neural network, PI:patient independent, PPV:positive predictive value, PS:patient specific, RBD:rule based decision, Sen:sensitivity, SN:number of seizures, Spec: specificity, ST:seizure type, SVM:support vector machine, TD:time domain, TF:time-frequency, WT:wavelet transform.

methods aim to detect a pattern in the signal, that is the manifestation of an epileptic seizure. Most seizure detection methods consist of a feature extraction step and a classification step. Features are characterizing measures for the pattern of interest calculated from the measured signals. In the classification step, the actual decision is made whether there is a seizure present in the signal or not. In the next sections those two steps will be separately described.

Feature extraction

The selection of discriminative features is the basis of almost all detection algorithms. Sometimes the choice for certain features was based on the physiological phenomena that need to be detected. Some authors referred to the fact that during a seizure many neurons fire synchronously. To get a measure for this 'synchronicity' they determined features such as the autocorrelation function [60], the synchronization likelihood [74] or nearest neighbour phase synchronization [51]. Other authors based their feature choice on how the pattern that needs to be detected visually can be characterized. Seizures are often visible in the EEG as rhythmic discharges or multiple spikes. For spike detection, Gotman developed an algorithm that first brakes down the signal into half waves. Then morphological characteristics of these half waves, such as amplitude and duration, were used to determine whether they are part of a seizure or not [58]. For rhythmic discharges, FFT-based, or wavelet based features were often used. Some studies did not use prior information and just used large sets of various features. Aarabi et al. evaluated a large feature set containing various types of features [29]. Their results showed that the most discriminative features for neonatal seizure detection are morphological based features, such as amplitude, shape and duration of waveforms. Also wavelet based features were relevant, especially for the detection of transients. It is also possible to select features using genetic programming. In this way features were extracted that were able to detect seizures, but these features did not have a physiological meaning [78].

Classification

Most authors chose a supervised classification method. This means that the algorithm is trained using data that was labeled on forehand by experts. Some algorithms (4) consisted of a unsupervised classification method. In this case the algorithm defines groups in the data based on similarities in the features. Classification methods varied from simple threshold, rule based decisions, or linear classifiers to neural networks that have a complex shaped decision boundary. Most algorithms described use either a neural network (17), rule based decisions (14) or a threshold (15). In 7 articles neural networks were combined with rule based decisions. Other classifiers used were support vector machine (1), logistic regression (1), linear discriminant analysis (2)

nearest neighbor classifier (2) and an adaptive neuro-fuzzy inference system (1).

2.4.4 *Clinical information*

Patients

Mental development level and sex were rarely mentioned. We defined three age groups: newborn (N), children (C), and adults (A). Most of the detection methods were developed for newborn (20 articles). In 15 articles the age was not mentioned. Eight articles contained no clinical information at all. Epilepsy type was mentioned in only 11 articles. Seizure type was mentioned in 19 articles. Only 5 articles contained information about patient type, epilepsy type and seizure type.

2.4.5 *Evaluation*

Number of patients

The number of patients included in the published papers, varied from 2 [72] to 81 [54]. It is evident that for a statistically reliable outcome, a large number of patients should be used. Only 12 articles evaluated data of more than 40 patients. Often a smaller data set was used when the algorithm described was still in an development phase.

Measurement duration

Measurement durations varied from 0.875 hours [52] to 4553.8 hours [70]. Again, in order to obtain a statistically reliable outcome, larger data sets should be used. Algorithms that were in a further development phase were evaluated in large data sets [59, 70]. In 13 studies measurement duration was not mentioned.

Number of Seizures

The number of seizures depends on measurement duration and patient type. The largest number of seizures was described by Nijsen et al. [30]. A total of 897 seizures were seen in 288 hours of data obtained from 18 refractory patients who experienced high seizure frequencies. In comparison, the largest data set in Table 2 described by Gabor contained over 4000 hours of data obtained from children and adults and only 181 seizures [70]. For proper evaluation, sufficient seizure data, but also sufficient interictal data should be included in the evaluation.

2.4.6 *Performance*

Two performance measures that were most mentioned in the literature, are sensitivity (Sen) and false detection rate per hour (FDR/h). These measures describe how well the algorithms can detect seizures and how many false alarms occur. It is difficult to compare the performance measures since they are dependent on a.o. patient type, seizure characteristics and sensor modalities used.
When a method is successful in one patient type it can not simply be applied to another patient type. Some authors extended their methods to other patient groups. Gotman initially developed a detection method for seizures in children and adults [59]. For the application in neonates the algorithm was adapted [68]. The synchronization likelihood was first evaluated for the detection of neonatal seizures [74], but the application of this measure in ICU seemed to be not evident [52]. Many methods described are developed using data from patients with a localization related (focal) epilepsy [88]. From our own experience we know that these methods may not be suitable for patients with strongly abnormal background EEG-activity, as can be the case in patients with (symptomatic) generalized epilepsy or in mentally retarded patients [90]. Furthermore Faul et al. [77] evaluated three detection methods previously reported by Gotman et al. [68], Liu et al. [60], and Celka [73] in their own data set and they were not able to reproduce the performances of the original studies. For the detection of various seizure types maybe different methods are necessary. Karayiannis et al. separately evaluated myoclonic and focal clonic seizures in neonates [84]. The algorithm suggested by Gotman et al. for neonatal seizure detection consisted of three separate methods, each for another aspect of the seizures [68].
Lee et al. compared four seizure detection methods in both scalp EEG and intracranial EEG [57]. As shown in Table 2, this comparison suggests that one can not use a similar algorithm for another sensor modality.

2.5 DISCUSSION

More than 80% of the literature concerning seizure detection is based on studies performed in epilepsy monitoring units (EMU) or neonatal intensive care units (NICU) and heavily depends on the EEG. Still, the overwhelming number of algorithms developed for seizure detection based on EEG does not completely cover the spectrum of application areas in which seizure detection is valuable. Newer application areas such as seizure detection in home environments, have to fulfill special requirements regarding measurement duration, patient friendliness and costs. Thus the use of other sensor modalities besides EEG becomes more important.

The algorithms described in literature typically consist of a feature extraction and a classification step. Most authors agree on the fact that the choice of features is critical for any detection method to be successful. Often features are chosen based on morphological aspects of the pattern of interest. For the eventual classification, most studies use a neural network based classifier, a simple threshold or rule based decisions. The published results do not prove superiority of neural network based methods over threshold or rule based classifiers, that are easier to understand and to interpret by clinicians.
Most articles focus on the technological aspects of seizure detection and in many cases no or incomplete attention is paid to clinical information, such as patient characteristics (age, mental development level), and seizure semiology. 17% of the published articles contain no clinical information at all. In 32% of the articles, the patient type is not mentioned and in 60% seizure type is omitted. Only 19% of the articles mentioned characteristics of both patients *and* seizures. Clinical factors can play an important role in how seizures express themselves electrophysiologically and clinically and thus affect the choice of a suitable detection method.
From the results presented in this review, four major points arise, that have to be taken into account when developing a seizure detection system in the future:

- First, the adaptation of existing EEG-based algorithms that are successful to other patient types is not trivial. Most of the time adaptations are necessary. Gotman et al. describe the adaptation of an existing seizure detection algorithm so that it can be used for neonates [68]. Sazonov shows that techniques that are very successful in patients with temporal lobe epilepsy can not be applied for seizure detection in mentally retarded subjects [90]. Although it may be clear that, for the use in different patient groups, adaptations of existing algorithms are necessary, it has never been systematically investigated what the demands are for such adaptations per patient group. For some groups adaptations of existing algorithms may not even be possible. These issues should be taken into account in future research.

- Second, for home monitoring, adaptation of existing methods may not be sufficient. Other sensor modalities, such as video, accelerometry and ECG become more important [44, 30, 45, 48]. The use of these alternative sensor modalities is relatively new and the algorithm development for seizure detection based on these measures is still in a premature stage.

- Third, although these new sensor modalities are promising, there will always be seizures that are only visible in the EEG. Therefore an ideal seizure detection system will consist of more sensor modalities. Greene et al. show that the combination of EEG and ECG leads to a better detection performance than each modality on its own [50]. Future

research needs to point out what combinations of sensor modalities are most suitable for various patient and seizure types.

- Fourth, for both the adaptation of existing techniques and the development of new algorithms, clinical information should be taken into account. This leads to more sensible choices regarding suitable sensors as well as algorithm development.

For example it is known that mental retardation leads to slow background EEG [90] and to a dominant presence of seizures with motor symptoms [91]. Based on this information the choice can be made to use alternative sensors for seizure detection that focus on capturing movement patterns, such as accelerometers [30]. Also the EEG of newborn differs significantly from that of the adult. Epileptic spikes tend to be of much longer duration than those in adults, and newborn seizures can also be characterized by very slow rhythmic discharges. Gotman et al. used this information for the adaptation of an existing algorithm, so that it can be used for seizure detection in newborns [68]. For newborns it is also known that they can experience seizures that are associated with characteristic movements, but no specific ictal EEG changes. Video-monitoring seems a feasible choice for detection these seizure related movements in newborns [44].

2.6 CONCLUSION

This review presents an overview of available methods for epileptic seizure detection in a long-term monitoring context. Based on the available information, we formulated recommendations that can be used in future research. In the development of seizure detection systems patient and seizure characteristics should play a more dominant role. Furthermore suitable seizure detection methods mainly depend on a specific application area. In Epilepsy Monitoring Unit and (Neonatal) Intensive Care Units, more attention should be paid to the adaptation of existing methods to other patient types. Furthermore, the growing need for clinical monitoring outside the ICU and home monitoring requires a totally different approach that incorporates the use of new sensor modalities and algorithms.

3

THE POTENTIAL VALUE OF 3-D ACCELEROMETRY FOR DETECTION OF MOTOR SEIZURES IN SEVERE EPILEPSY

This chapter is published as:
T.M.E. Nijsen, J.B.A.M. Arends, P.A.M. Griep and P.J.M. Cluitmans, The potential value of 3-D accelerometry for detection of motor seizures in severe epilepsy, Epilepsy and Behavior, 7:74–84, 2005 [30].

3.1 ABSTRACT

Seizure detection results based on the visual analysis of 3-D accelerometry (ACM)- and EEG/video-recordings are reported of 18 patients with severe epilepsy. They were monitored for 36 hours during which 897 seizures were detected. This was seven times higher than the number of seizures that was reported by nurses during the recording period. The results in this chapter show that 3-D ACM is a valuable sensing method for seizure detection in this population. 428 (48%) seizures were detected by ACM. With 3-D ACM alone it was possible to detect all the seizures in 10 of the 18 patients. 3-D ACM also had a complementary value to the EEG in our population. ACM-patterns during seizures are stereotype in 95% of the motor seizures. These characteristic patterns are a starting point for automated seizure detection in the future.

3.2 INTRODUCTION

The term 'seizure detection' can be interpreted in more than one way according to the setting it is used in. In *care* settings 'seizure detection' mostly means the *instantaneous* detection of an epileptic seizure that triggers an alarm system in order to get the right assistance in situations that need intervention. In *diagnostic* settings seizure detection is done after *a (longer) period of monitoring*. Thus information can be obtained like seizure type, seizure frequency, seizure distribution during day and night and how the seizures influence a patient's behavior and quality of life. This information can lead to better management of daily care or better titration of anti-epileptic drugs. Seizure detection is often necessary in institutions where many patients with severe epilepsy live together. Due to lack of resources the patients are not continuously supervised by nurses, especially at night. Therefore we have to rely on alarm systems. Currently audio-triggered systems are mostly used in clinical practice. Unfortunately the performance of these systems are very

poor. For the performance of the alarm system in our institute we found a sensitivity $< 30\%$ and positive predictive value (PPV) $< 5\%$ [1] [92].
On the other hand, in the diagnostic setting the gold standard for seizure detection, the measurement of the electroencephalogram (EEG) in combination with video-monitoring, is used. This method has by definition a sensitivity and PPV of 100%. Seizure detection takes place off-line and the signals and videotapes are visually analyzed by EEG-technicians. For care situations EEG/video-monitoring is not a practical detection method. It is uncomfortable for the patient and the analysis of the videos and the EEG-signals is labor-intensive and costly. Furthermore, this method can not be applied in real-time yet.
All factors mentioned above, are important reasons to search for alternative sensors that are easy to wear and can be used for reliable automatic detection of epileptic seizures. This chapter shows the potential value of 3-D accelerometry (ACM) for the detection of epileptic seizures with motor phenomena. Our eventual goal is to develop a set of systems based on e.g. ACM, ECG, EEG or other quantities, depending on the seizure type, that ensure a reliable detection of epileptic seizures with an overall sensitivity of at least 90% and a positive predictive value (PPV) of 50%. These numbers are chosen with a real-time alarm system in mind. Here sensitivity needs to be as high as possible and the number of false alarms needs to be acceptable for the medical personnel that has to check the patient each time there is an alarm. A PPV of 50% means that one out of two alarms is genuine, and this is found acceptable in clinical practice.
When we look in the clinical/(bio)medical field we find that ACM is frequently used to monitor daily activity in for example rehabilitation medicine [13], [14]. The goal of these studies is to distinguish between different activities, like standing, sitting, lying, walking, running, e.g., based on ACM-recordings. There are studies that use ACM for extracting parameters that are an indicator for energy expenditure during physical activities [93], [94] and to validate reported food intake [95]. ACM is also used to characterize dyskinesia in patients with Parkinson's disease [17], or in FES-applications (functional electrical stimulation) to trigger nerve stimulation [96]. The use of 3-D ACM for detection of seizures is not common, in epilepsy related fields ACM is rarely mentioned [24] and then ACM is not used in a detection context. Nevertheless we believe 3-D ACM has the potential to be very useful for seizure detection when motor phenomena are present [97], [98]. An advantage of 3-D ACM is that the signals contain information about motor behavior that can be directly linked to the movements that clinicians are used to observe in the video-recordings. When applying video-analysis for seizure detection, the patient needs to be constantly in the scope of one or more video cameras.

1 These numbers mean that more than 70% of the seizures is missed by in the curent detection setup, and less than 5% of all the alarms is actually a seizure.

Accelerometers can be worn on the body, resulting in more freedom to pursue normal daily activities. Another advantage of accelerometers above video is that it is possible to observe movements under blankets. The value of ACM for seizure detection in subjects with severe epilepsy is shown in our results of the visual analysis of ACM-data in combination with the gold standard EEG/video-monitoring.

3.3 METHODS

3.3.1 *Subjects and data collection*

During a clinical trial a set of data was systematically collected. This database contains 36 hours of EEG-recordings and five days of videomonitoring, 3-D ACM-recordings on five positions (upper and lower limbs and chest) and ECG-recordings of 20 patients. Inclusion criteria for the patients were that they are mentally retarded, live in a long stay environment, suffer from severe epilepsy and have a minimum seizure frequency of 20 seizures a month. The 3-D accelerometers used in this programme were created by mounting two 2D-sensors, the ADXL202E from Analog Devices Inc., at perpendicular angles to each other. This accelerometer measures inertial acceleration during movements as well as the acceleration caused by gravity. The polygraphic data were stored on portable recorders (Porti 24/36 channels, TMS, Enschede, The Netherlands) and the video on portable MPEG2 recorders. After the recordings, the polygraphic data were moved to a network based analyzing system (Brainlab, OSG, Rumst, Belgium). Seizures were visually identified by EEG-technicians. For the automated analysis the data was made available in Matlab (The Mathworks Inc.).

3.3.2 *Seizure detection by visual inspection of the data*

The gold standard for seizure detection in clinical practice is EEG/video-monitoring. EEG-technicians detect seizures using two possible paradigms. In one case they screen the video-recordings for behavioral information that corresponds to a seizure and then additionally check the EEG-signal for epileptiform activity. In the other case first the EEG-signal is screened for epileptiform activity and the video recordings provide additional behavioral information. We will refer to the seizures that are detected by the EEG-technicians according to these paradigms as clinical seizures. The analysis was performed by EEG-technicians without any automatic signal processing tool except visualization features of the Brainlab analyzing system. In our trial we combined EEG/video-monitoring and ACM-recordings during 36 hours. Before the recordings started we estimated how many seizures could

be expected per patient in this 36 hours period, based on the number of seizures that were reported by nurses the month before the recording period.

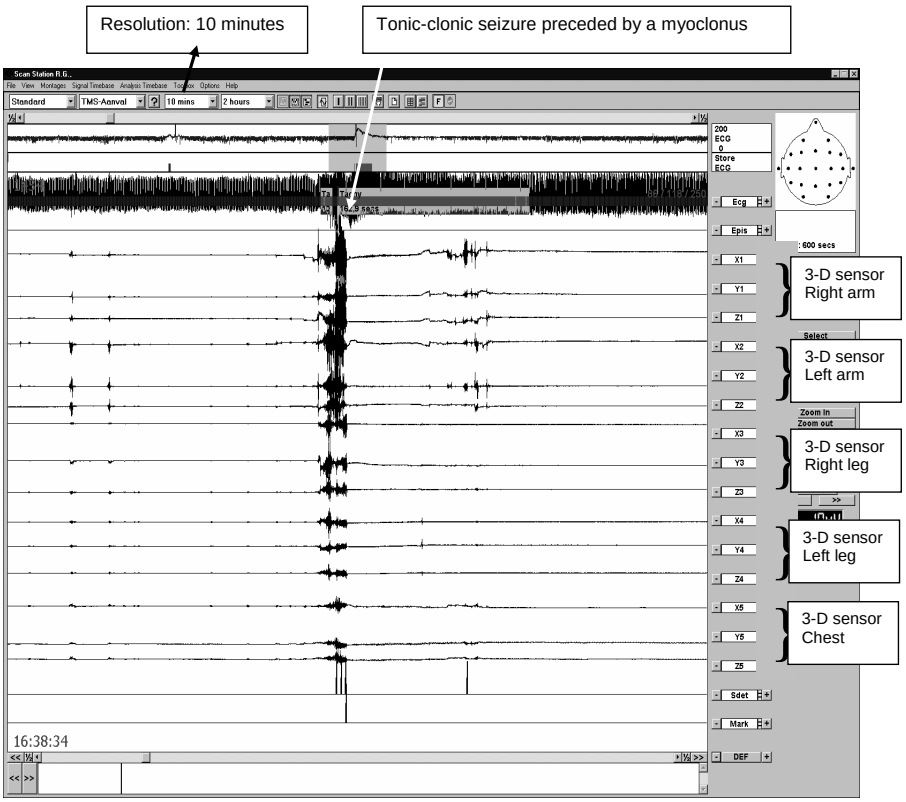

Figure 7: Patterns that can be observed in ACM-data during seizures. Here a myoclonic seizure that evolves into tonic-clonic contractions is shown.

3.3.3 *Stereotypical ACM-patterns associated with simple motor seizures*

During this trial it was observed that the patterns that are visible in the 3-D ACM signal during seizures with motor phenomena have stereotypical patterns throughout our patient population. These patterns that are so clearly visible in the ACM-data are known as simple motor seizures (myoclonic, clonic and tonic seizures) [3]. For human observers, these patterns are easy to distinguish from normal movement patterns, this is illustrated in Fig. 7. Here ACM-signals are visualized in Brainlab with a resolution of 10 minutes per page, during a tonic-clonic seizure that started out as short myoclonus. The patterns are synchronously visible at all the fifteen ACM-channels (the first two channels show a compressed ECG signal with a resolution of two hours).

One of our goals in the future is to computerize this pattern recognition process. That the patterns are stereotypical is an indication that automated seizure detection based on 3-D ACM could be feasible.

3.4 RESULTS

3.4.1 *Patients*

The initial population consisted of 20 patients. All patients were mentally retarded and suffered from severe epilepsy. The EEG of one patient could not be analyzed due to technical difficulties, 1 patient did not have any seizures during the recording period. These 2 patients were excluded from further analysis. The 18 remaining patients had a mean age of 37 years with a standard deviation of 11.8 years. There were 10 male and 8 female patients. All patients were known to have multiple seizure types.

Table 4 lists the seizure types per patient according to the international classification of epileptic seizures and syndromes as proposed by the International League Against Epilepsy (ILAE) in 1981, 1987 and modified in 2001 [4], [99], [5]. Tonic and myoclonic seizures were the dominant seizures across subjects in our population. Five patients also suffered from complex partial seizures. One patient suffered from startle seizures during daytime and myoclonic seizures during night. Two patients had many nocturnal arousals due to epileptic activity and during daytime predominant tonic seizures.

3.4.2 *Results of visual inspection of the data*

This section presents the results of the analysis of the first 36 hours of the recordings that included also the EEG. Table 5 shows the seizures that were expected on forehand, the number of seizures that were observed by nurses and the number of seizures that were detected by EEG-technicians who visually screened through the data. Also the percentage of seizures that was detected with ACM and EEG respectively are listed. From Table 5 we can make the following observations:

- In total 31 seizures were expected, 131 observed and 897 detected. 428 seizures could be detected with ACM. 824 seizures were visible in the EEG.
- In 17 of 18 cases the number of detected seizures is higher than the number of seizures that were expected and that were reported by the nurses.
  The number of detected seizures is 29 times higher than the number of seizures that was expected on forehand and 7 times higher than

Table 4: Overview of seizure class and syndrome for the patients analyzed

PATIENT	AGE	SEX	SEIZURE CLASS	SYNDROMES
1	53	F	myoclonic, tonic and complex partial seizures	symptomatic neocortical epilepsy
2	26	M	myoclonic, tonic and complex partial seizures	symptomatic neocortical epilepsy
3	37	F	tonic and complex partial seizures	Lennox-Gastaut syndrome
4	32	F	myoclonic, tonic and complex partial seizures	symptomatic neocortical epilepsy
5	51	M	startle seizures during day, during night myoclonic seizures	symptomatic neocortical epilepsy
6	25	F	myoclonic and tonic seizures	symptomatic neocortical epilepsy
7	24	M	myoclonic seizures	epilepsy with myoclonic astatic seizures
8	42	M	myoclonic and tonic seizures, series of myoclonic seizures	epilepsy with myoclonic astatic seizures
9	50	M	tonic seizures	symptomatic neocortical epilepsy
10	21	F	tonic seizures during day, during night EEG paroxysms, followed by arousals	Lennox-Gastaut syndrome
11	22	M	series of myoclonic seizures with sometimes a tonic phase	symptomatic neocortical epilepsy
12	32	F	tonic seizures during day, during night EEG paroxysms, followed by arousals	West syndrome, Lennox-Gastaut syndrome
13	43	M	myoclonic and tonic seizures	symptomatic neocortical epilepsy
14	25	M	myoclonic, tonic and tonic clonic seizures	symptomatic neocortical epilepsy
15	26	M	myoclonic, tonic and tonic clonic seizures	Dravet syndrome
16	49	F	myoclonic, tonic clonic and complex partial seizures	symptomatic neocortical epilepsy
17	57	M	tonic and complex partial seizures	tuberous sclerosis
18	43	F	myoclonic and tonic clonic seizures and complex partial seizures	symptomatic neocortical epilepsy

the number of seizures that were reported by the nurses. This result emphasizes the need of a seizure detection system.

- Of the 897 visually detected seizures, 428 seizures with motor phenomena could be detected with ACM, this is 48% of the seizures that were detected. The seizures that weren't detected with ACM were mostly complex partial seizures without motor phenomena. In 15 of the 18 patients the seizures coincide with motor phenomena that can be detected with accelerometry. ACM alone can detect all the seizures in 10 of the 18 patients (56 %). In 5 patients also the EEG was required for the detection of seizures without motor phenomena. In 3 patients ACM

Table 5: Number of expected, observed and detected seizures in 36 hours of EEG/video-monitoring combined with 3-D ACM. Per patient the number and the percentage of seizures detected with respectively ACM or EEG are listed

PATIENT	EXPECTED	OBSERVED	DETECTED	ACM	EEG
1	1	3	17 (100%)	3 (18%)	17 (100%)
2	2	9	9 (100%)	4 (44%)	5 (56%)
3	2	3	15 (100%)	9 (60%)	8 (53%)
4	1	0	280 (100%)	0 (0%)	280 (100%)
5	1	1	172 (100%)	172 (100%)	172 (100%)
6	2	18	32 (100%)	32 (100%)	0 (0%)
7	1	2	2 (100%)	2 (100%)	0 (0%)
8	2	12	22 (100%)	22 (100%)	22 (100%)
9	3	7	23 (100%)	23 (100%)	23 (100%)
10	1	0	1 (100%)	0 (0%)	1 (100%)
11	4	9	56 (100%)	56 (100%)	56 (100%)
12	1	11	33 (100%)	18 (55%)	33 (100%)
13	2	23	28 (100%)	28 (100%)	0 (0%)
14	1	15	9 (100%)	9 (100%)	9 (100%)
15	2	3	11 (100%)	11 (100%)	11 (100%)
16	2	11	11 (100%)	8 (73%)	11 (100%)
17	1	0	31 (100%)	31 (100%)	31 (100%)
18	2	4	145 (100%)	0 (0%)	145 (100%)
Total	31	131	897 (100 %)	428 (48%)	824 (92%)

had no value at all since the patients didn't have seizures with motor phenomena during the recording period.

- EEG changes are observed in 15 of the 18 patients and in 13 patients (72%) EEG alone would suffice for detection of all seizures. In 2 patients (11%) seizure detection was only possible when using the EEG-signal as well as the ACM-signal, since they had either motor phenomena during a seizure or EEG-changes. In 3 patients the EEG didn't provide useful information. Patient 13 had too many artefacts in the EEG, patients 6 and 7 lacked epileptiform activity during the seizures in the EEG.

Table 6 lists all the seizure semiologies of the patients during the trial period, based on the observed and the detected seizures. Per patient the seizure types that were reported by the nurses are indicated. From this table we can observe that there were more seizure types per patient than the nurses reported, especially seizure types that occurred during the night were missed. These were very well detectable with 3-D ACM. Furthermore we can see from

this table that there are some seizures that manifest themselves in movements of the head. These we can not detect with 3-D ACM since there was no sensor placed on the head.

Table 6: Seizure semiologies of the patients during the trial period. Per patient the seizure types that were reported by the nurses are indicated

PATIENT	SEIZURE TYPES DURING TRIAL	OBSERVED
1	1. Myoclonia of the head in combination with the head turning to the right and smacking with the mouth. 2. Series of myoclonic seizures starting in the right arm. 3. Generalized tonic seizures.	All
2	1. Myoclonia in the left arm followed by tonic contraction, followed by turning the head to the right. 2. Tonic contraction left arm, head and eyes turn to the right. 3. Tonic turning of the eyes to the left.	All
3	1. Short atypical absences with head and body turning to the left. 2. Makes noises, complex movement of the arm with extension, loss of consciousness. 3. Short myoclonia with flexion of both arms, extension of the legs, head turns down, followed by loss of consciousness. 4. Awakening from sleep, groaning, and irregular breathing.	1., 2., 3.
4	1. Eyelid myoclonias, loss of consciousness, bending of the body. 2. Generalized tonic contraction, falls backward. 3. Arousal, head turns to the right, sometimes to the left, sometimes followed by complete axial turning.	None
5	1. During the day, startle seizure to noise, starts with groaning and irregular breathing, followed by a tonic or a tonic-clonic seizure. 2. During the night, same type but not induced by noise.	1.
6	1. Myoclonic seizure with flexion of the arms, tonic extension of the arms	All
7	1. Myoclonic movements of the left hand, often subtle	All
8	1. Generalized tonic seizure with bending of the body and loss of consciousness. 2. Myoclonic seizure with flexion of both arms. 3. Type 1, followed by tonic-clonic seizure.	All
9	1. Tonic extension of arms and legs followed by irregular deep breathing. 2. Irregular deep breathing, followed by elevations of the head (at night).	1.
10	1. Generalized tonic contractions of arms and legs and flexion of the body. 2. Myoclonia of the head, with nodding.	None
11	1. Myoclonic and clonic contractions of the arms while eyes move upwards (sometimes in series). 2.Tonic extension of whole body with snoring and reddening of the face.	All
12	1.Tonic extension of the arms, with loss of consciousness, head turns to the left. 2. Arousal from sleep, snoring, myoclonia of left arm and eyes, head turning to the left.	1.
13	1. Flexion myoclonia of both arms. 2. Tonic contraction of the body followed by type 1.	All
14	1. Subtle myoclonic movements in both hands and eyes (sometimes in series). 2. Tonic extensions of both arms often in series, eyes move to the right.	All
15	1. Tonic-clonic seizure, predominantly in right arm and leg. 2.Nocturnal myoclonic seizure in both arms. 3.Nocturnal tonic extensions of the arms.	1.
16	1. Eyes turn upwards, blinking of the eyes, loss of consciousness. 2. Short screaming, tonic elevation of the arms, head turns to the left. 3. Nocturnal arousals with minimal myoclonia of the arms	1., 2.
17	1. Tonic extensions of the arms and smacking. 2. Arousal from sleep. 3. Movement of the head, motor restlessness and smacking. 4. Myoclonic movements of the right/left hand extending to the right/left arm, sometimes followed by motor restlessness and arousal from sleep.	None
18	1. Tonic extensions of both arms, bending the body followed by restlessness and hand automatisms. 2. Myoclonia of left shoulder followed by loss of consciousness and smacking. 3. Tonic flexion of the arms. 4. Short myoclonia of the head with nodding and loss of consciousness.	All

3.4.3 *Stereotypical ACM-patterns associated with simple motor seizures*

During seizures with simple motor phenomena there were clearly distinguishable patterns visible in the ACM-signal. In 'simple motor seizures' as defined by Lüders et al. [6], motor movements are relatively simple, unnatural and consist of movements similar to movements elicited by electrical stimulation of the primary motor areas. Simple motor seizures consist of a sequence of one or more elementary movement patterns: myoclonic, clonic and tonic movement patterns. An overview of definitions of myoclonic, clonic and tonic seizures obtained from literature is given below. More detailed examples of ACM-data associated with these seizures are presented in Fig. 8.

- **Myoclonic seizures**
  Myoclonic seizures consist of short muscle contraction. The electrical activation of the muscle lasts less than 50 milliseconds [7]. The actual movement that is observed takes more time. The International Classification of Epileptic Seizures states that myoclonic seizures are 'sudden, brief, shock-like contractions' [4]. These characteristics are all reflected in the ACM-signal. Figure 8 A. shows the '*sudden, brief, shock-like*' pattern of two subsequent myoclonic seizures. The myoclonus is a twitch like contraction of an antagonistic muscle pair. Flexion is dominantly innervated over extension, so the arm flexes during the seizure. After the seizure the arm falls back. In most cases the arm bumps into an object or surface (chair, table, bed) since the movement is uncontrolled. This bumping results in a sharp peak in the ACM-signal that damps out. This peak is typical for a myoclonus but it actually occurs after the myoclonus (second peak in Fig. 8 A.). A myoclonus can be isolated but can also be followed by another myoclonus, a tonic seizure (Fig. 8 B.), or a tonic clonic seizure (Fig. 8 C.). A myoclonus can occur synchronously throughout the body but often only one limb is involved. In this case only one of the five 3-D sensors shows this typical pattern.

- **Tonic seizures**
  Tonic seizures consist of sustained muscle contractions, usually lasting more than 5 to 10 seconds and lead to 'positioning' [3]. This is clearly visible in the ACM-signal (Fig. 8 B.). The acceleration is virtually constant due to the tetanic contraction of the muscles, and the arm undergoes a slow change of posture. We see a *block like* shape in the ACM-pattern due to the gravity component of the measured signal. During a tonic seizure mostly the entire body is involved and then all the five sensors show a similar pattern.

- **Clonic seizures**
  Clonic seizures consist of repeated myoclonic contractions that regularly

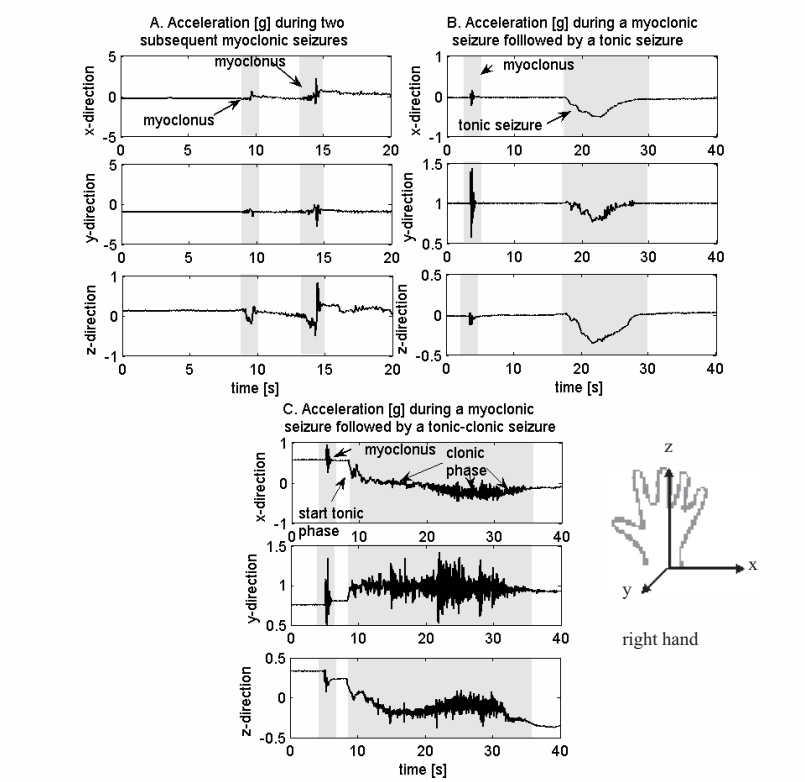

Figure 8: A. Typical pattern in the ACM-signal associated with a myoclonic seizure: a sudden *shock-like* movement of a short duration. B. Myoclonic seizure followed by typical tonic seizure pattern. The muscles are in tetanic contraction and the arm undergoes a slow change of posture. This results in a typical *block-like* pattern C. Myoclonic seizure followed by a typical tonic-clonic seizure pattern. During the clonic phase the arm is jerking repetitively, this results in a typical *burst-like* pattern. These signals are obtained from one 3-D sensor, placed at the right wrist. x-, y-, and z-directions are defined as depicted in the picture of the hand.

recur at intervals between 0.2 and 5 times per second [6]. In the ACM-signal we see that during a clonic phase there is a typical *burst-like* pattern. The acceleration pattern contains higher frequencies due to the repetitive jerking of the arm (Fig. 8 C.). Also during a clonic seizure mostly the entire body is involved and the pattern is visual at all the five 3-D sensors. The clonic seizure is often preceded by a tonic phase (tonic-clonic seizure).

These *shock-like, block-like* or *burst-like* patterns are characteristic throughout our population. Figure 9 A. shows examples of 3-D ACM-signals during

myoclonic seizures measured at the right arm in four patients. The sharp shock-like pattern is clearly visible even when there are non-epileptic movement patterns visible in the signal prior and after the seizure: patient 13 has non-specific post-ictal motor activity after the second seizure and patient 14 is carrying out normal motor behavior and then suddenly the seizure interrupts this activity. Figure 9 B. shows the patterns during a tonic seizure in four patients. The intensity and duration is different in each seizure as well as the initial slope of the block-like pattern, but in every case this stereotypical block-pattern is visible. Figure 9 C. shows stereotypical clonic patterns in four patients. In the data of patient 8 and 17 we also see a block-like tonic phase preceding the clonic phase. Again intensity and duration change but the stereotypical burst-like pattern is clearly visible.

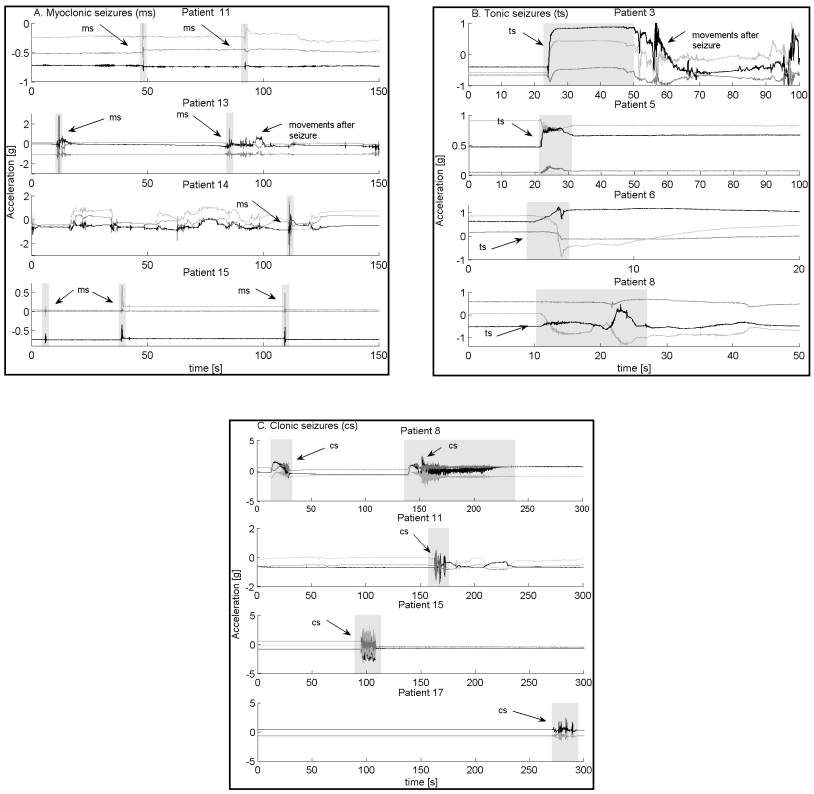

Figure 9: Stereotypical patterns during simple motor seizures occur throughout our population. A. short *shock-like* patterns during myoclonic seizures. B. *block-like* patterns during tonic seizures. C. *burst-like* patterns during clonic seizures. At the beginning of some seizures there is again the block-like tonic pattern.

As mentioned before there were 428 seizures detected by the EEG-technicians

based on the ACM-signal. These so called 'motor seizures' were observed in 15 of the 18 patients. We observed that most of these seizures were sequences of the three elementary patterns that were explained above. We observed the following categories of pattern sequences:

- myoclonic seizure (single or series)
- tonic seizure
- tonic-clonic seizure
- tonic seizure preceded by a myoclonic seizure and a pause
- tonic-clonic seizure preceded by a myoclonic seizure and a pause
- seizure that started as a myoclonic seizure but evolved into a tonic seizure without a pause
- seizure that started as a myoclonic seizure but evolved into a tonic-clonic seizure without a pause
- clonic seizure
- non stereotypical seizure pattern including complex motor phenomena as defined by Lüders [6].

Figure 10 shows the total number of seizures per category and the corresponding percentage. Only 5% of the seizures doesn't consist of a stereotypical myoclonic, tonic or clonic pattern. 78% of the seizures consist of a stereotypical tonic pattern. 74% of the seizures consist of a stereotypical myoclonic pattern and 14% of the seizures consists of a stereotypical clonic pattern. 57% of the seizures are preceded by a myoclonic seizure. On a patient basis (Fig. 11), the non stereotypical movement patterns occurred in patient 1 and 12. These patients had motor seizures that do not fall into the category simple motor seizures as defined by Lüders but are in fact complex motor seizures [6]. In eight patients (44%) tonic or tonic-clonic seizures were preceded by a myoclonic ACM-pattern. When it is known that a patient has this type of patterns, early warning could be achieved by detecting these myoclonic patterns. Figure 11 also points out once more that there are often multiple seizure types per patient (9 of 15 patients). We can conclude that the patterns in 3-D ACM-signals associated with simple motor seizures are stereotypical and can be divided into three elementary classes. Hence the patterns can be easily recognized by a human observer and the pattern-shape is an important feature for EEG-technicians while visually inspecting ACM-data. Characteristic pattern features should be taken into account in an automated seizure detection system. Another important source of information is the context surrounding a certain pattern of one or all five 3-D sensors. EEG-technicians screen through the data on a ten minutes time-basis. They screen not only for

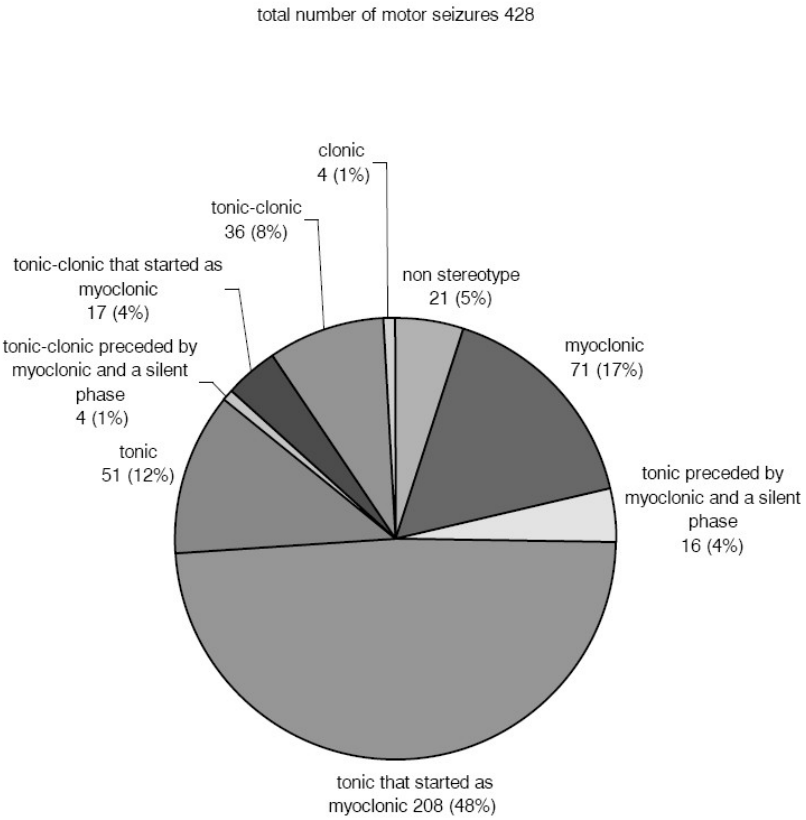

Figure 10: Number and percentages of different ACM-patterns observed in our population

characteristic patterns but also for correlated patterns between all five 3-D sensors patterns that are deviating from the rest.

During normal movements mostly there is not much synchronicity between the five sensors. It was mentioned before that especially during tonic and tonic-clonic seizures often all body parts are involved. In that case the EEG-technician thus takes into account motor activity picked up by all the sensors. This was also visible in Fig. 7. The tonic-clonic seizure is visible at all the sensors. Still the pattern itself is the main feature for seizure detection. During myoclonic seizures often only one sensor is involved and then the EEG-technician can judge only the pattern itself and decide whether or not it is deviating from surrounding movement patterns recorded by the same sensor. Sometimes also during normal movement patterns there is synchronicity between all the sensors and in that case again the movement pattern itself

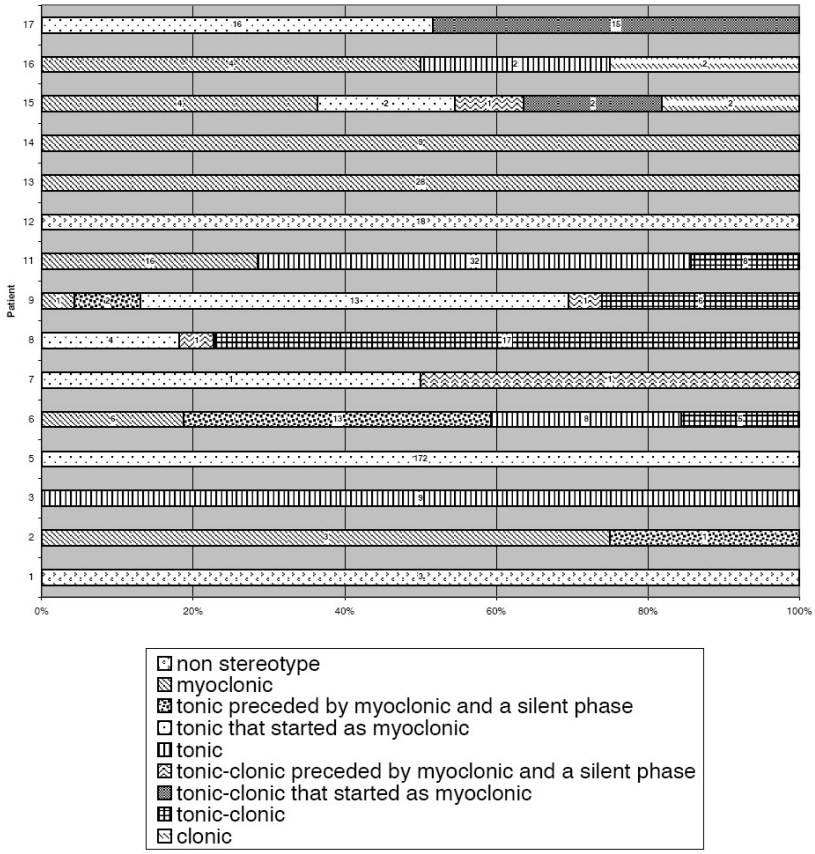

Figure 11: Different seizure-patterns per patient. The number of seizures is listed in each block.

is an important feature for the human observer. This is illustrated in Fig. 12. Figure 12 A. shows a normal walking pattern. There is activity on all the sensors that is relatively high in amplitude and frequency. The detail shows a regular pattern in both the left and right leg but with a phase difference of half a period. This is characteristic for walking and is definitely not a seizure. The high amplitude peaks are caused by the impact of the heel with the floor. These peaks appear attenuated in the chest and arm sensors. Figure 12 B. shows a tonic clonic seizure on the same scale with first a stereotypical block-like pattern in the tonic phase and then the burst-like pattern during the tonic phase, the pattern appears synchronously at all the sensors with a relatively high amplitude. The detail shows synchronicity between the sensors but no regularity in the signal pattern.

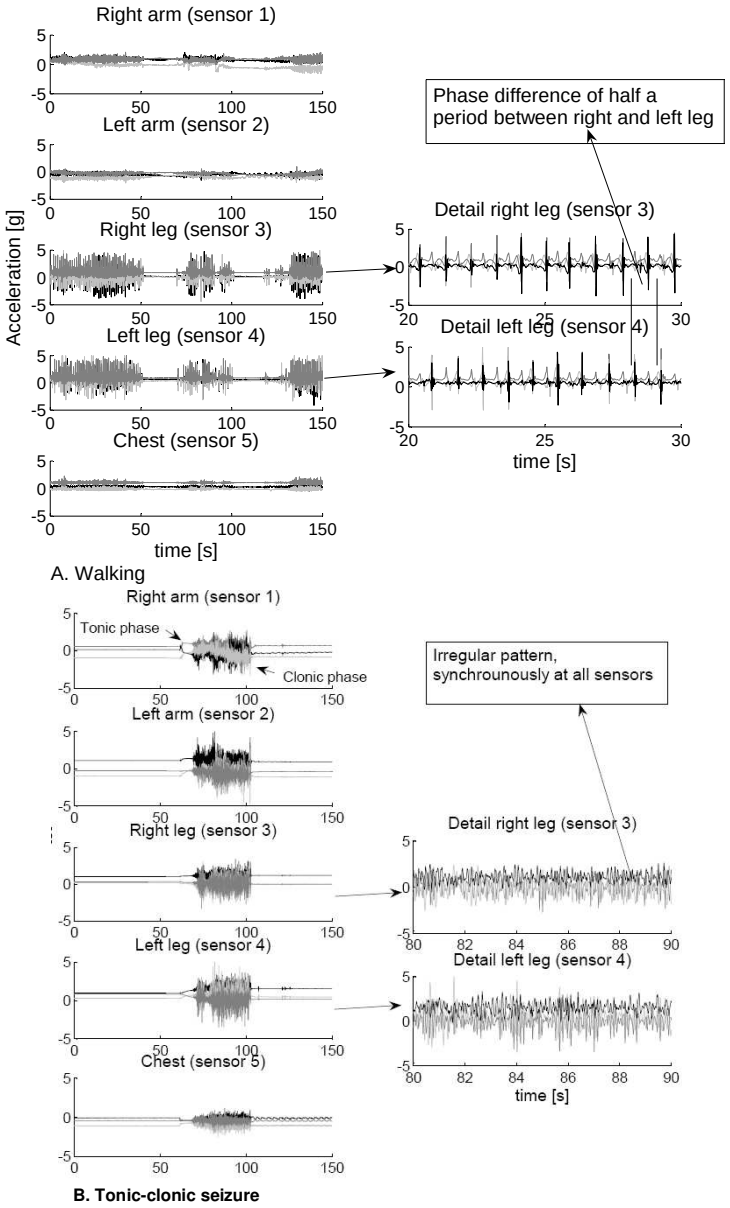

Figure 12: Pattern shape and context of all the sensors are important for distinguishing normal and epileptic patterns. A. Walking and B. Tonic-clonic seizure.

3.5 DISCUSSION

Our results show that 3-D accelerometry is very useful for seizure detection in mentally retarded subjects with severe epilepsy. Of the 897 seizures that

were detected in this trial 428 (48%) could be detected with ACM. ACM alone detected all the seizures in 10 of the 18 patients (56%). Only in 3 patients ACM had no value at all since they did not have any seizures with motor phenomena. The results also imply that ACM is possibly a valuable addition to detect the percentage of seizures with motor phenomena that are not always visible in the EEG in this population. Another striking outcome presented is the large number of detected seizures versus the number of seizures that was expected on forehand and the number of seizures that was observed by the nurses. These results underscore the need for an automatic seizure detection device since in the current situation many seizures are missed and therefore it is possible that patients do not get the right (medical) treatment. In our population such a device can never consist of only EEG. ACM would be a valuable addition, since in mentally retarded subjects seizures often express themselves with motor phenomena [91]. We observed that ACM-patterns during simple motor seizures are sequences of three elementary patterns: myoclonic, tonic and clonic patterns are stereotypical throughout our population. Only 5% of 428 motor seizures was not stereotypical. Human observers are able to easily recognize a seizure-pattern due to these stereotypical shapes. Nevertheless, visual analysis of the ACM-signals is very labor intensive and eventually we want to work towards an automatic detection algorithm. Although the ACM-patterns during seizures are relatively easy to recognize by the human eye it is more difficult to find suitable parameters that make computerized detection possible. In this trial it was also observed that 81% of the tonic and 37% of the tonic-clonic seizures were preceded by a myoclonic seizure. Thus, recognition of myoclonic ACM-patterns can be important for early detection. For seizures that do not express themselves in motor phenomena 3-D ACM can never suffice, but in our research programme also other systems are examined like EEG and ECG [45]. The eventual goal is a tailored seizure detection signals that takes into account prior clinical knowledge, so that per individual patient the best seizure detection is achieved. If real time detection becomes available, we also have a powerful tool to study complications, for instance SUDEP (sudden unexpected death in epilepsy), and general health consequences in mentally retarded patients with severe epilepsy.

4

DETECTION OF SUBTLE NOCTURNAL MOTOR ACTIVITY FROM 3-D ACCELEROMETRY RECORDINGS IN EPILEPSY PATIENTS

This chapter is published as:
T.M.E. Nijsen, P.J.M. Cluitmans, J.B.A.M. Arends, and P.A.M. Griep, Detection of subtle nocturnal motor activity from 3-D accelerometry recordings in epilepsy patients, IEEE Transactions on Biomedical Engineering 54(11),2073–2081, 2007 [31].

4.1 ABSTRACT

This chapter presents a first step towards reliable detection of nocturnal epileptic seizures based on 3-D accelerometry (ACM) recordings. The main goal is to distinguish between data with and without subtle nocturnal motor activity, thus reducing the amount of data that needs further (more complex) analysis for seizure detection. From 15 ACM signals (measured on five positions on the body), two features are computed, the variance and the jerk. In the resulting 2-D feature space a linear threshold function is used for classification. For training and testing the algorithm ACM data along with video data is used from nocturnal recordings in seven mentally retarded patients with severe epilepsy. Per patient the algorithm detected 100% of the periods of motor activity that are marked in video recordings and the ACM-signals by experts. From all the detections, 43% - 89% was correct (mean = 65%). We were able to reduce the amount of data that need to be analyzed considerably. The results show that our approach can be used for detection of subtle nocturnal motor activity. Furthermore our results indicate that our algorithm is robust for fluctuations across patients. Consequently there is no need for training the algorithm for each new patient.

4.2 INTRODUCTION

Epilepsy affects almost 60 million people worldwide. Some of the people affected can be treated successfully with drug therapy (67%) or neurosurgical procedures (7-8%). Nevertheless 25% of the people affected cannot be treated by any available therapy [1]. A substantial part of this last group is also mentally retarded. These people are at high risk for physical injuries or even lethal outcome. They are often unable to live independently and a large number is institutionalized. In these cases, seizure detection is important for the management of daily care. Detections can be used to trigger an

alarm during severe seizures that require medical assistance. Furthermore information about seizure frequency can be used to evaluate treatment effects. In clinical practice the gold standard for detecting epileptic seizures is the measurement of the electroencephalogram (EEG) in combination with video monitoring. For long-term monitoring this is not practical since patients are impeded in pursuing activities of daily living (ADL). Furthermore the analysis of EEG/video-monitoring requires considerable effort. In this context we explore alternative methods for automatic detection of epileptic seizures. Choosing an alternative method, we take into account that our target population is mentally retarded. It is known that in mentally retarded subjects, seizures often manifest themselves in movements [91], [30]. Seizures in which the main semiological characteristic is movement, are referred to as *motor* seizures [3]. An alternative detection system in our population therefore might be based on the detection of movements or, in other words, *motor* activity. In our seizure detection setup 3-D accelerometry (ACM) is used for the recording of motor activity. Previously we presented clinical results that show the feasibility of seizure detection based on 3-D ACM in our patient population [30]. It was observed that 48% of the 897 seizures that were detected based on the gold standard, were motor seizures. Furthermore, 95% of these seizures had stereotypical waveforms in the ACM-signals. In 10 of the 18 patients (56 %) seizure detection based on ACM alone was sufficient.

In literature ACM is sporadically mentioned in epilepsy related fields and then ACM is not used for seizure detection [24], [25], [26]. The few publications that do focus on the detection of seizure movements are based on video-analysis [100], [101]. Nevertheless accelerometers are popular for detection purposes in many other application areas. A well known example is the airbag industry [102]. Accelerometers can be found in laptop hard drive protection systems that protect hard drives from shock [103] and in car navigation systems, to extrapolate the position when the GPS signal is lost for short intervals [104]. They are used in a wide range of medical application areas to monitor ADL [13], [14], [11], [12], [16]. In Parkinson's disease, studies aim at distinguishing pathological (periods of hypokinesia, bradykinesia and dyskinesia) and normal movements [17], [18], [19], [20]. In this chapter a first step towards automatic seizure detection based on 3-D ACM is presented. The aim is to distinguish periods in nocturnal data with and without motor activity with a sensitivity of at least 95% and a positive predictive value of at least 50%. Eventually, the complete motor seizure detection scheme will consist of several steps. First data are screened for motor activity. Next, detected motor activity events are checked for the presence of stereotypical waveforms that can be seen in the ACM-signal during *myoclonic*, *clonic* and *tonic* seizures, as described in our clinical study [30]. We have chosen for these separate steps, since the detection of motor activity can be tackled in a relatively simple way. This first step reduces the amount of data that needs to be further analyzed with stronger, more complex signal processing tools. The

purpose of this algorithm for now is to support off-line analysis for diagnostic and evaluation purposes. Eventually in the future it can be part of a real-time detection system for long-term monitoring.

4.3 METHODS

4.3.1 *Measurement setup and patient population*

Video and ACM-data are used from seven mentally retarded patients who suffer from severe epilepsy and have minimally 20 seizures per month (2 male and 5 female, mean age 30.3 years $\pm$ 14.2 years). The patients are monitored with the same setup described in our previous clinical study [30]. The nocturnal video- and 3-D ACM-recordings on five positions (upper and lower limbs and sternum) obtained in the first night are used, because only during this night also the EEG-signal is available. In this way we have the best possible reference for determining whether a movement is actually a seizure. The sample frequency f_s of the ACM-signals is 100 Hz. Video- and ACM-data are synchronized by means of a marker in the ACM-data and a corresponding 'beep' in the video. Our definition of night is the period the patient is in bed. For each patient two data episodes are chosen: one episode containing at least one seizure (according to experts who inspected both video and EEG recordings), and one randomly chosen episode containing a non-seizure movement. The total duration of both episodes together is 5 minutes. The total amount of data is 35 minutes. We are restricted to use this small subset of the data since human experts need to judge this data, and the experts are only available for a limited time period.

4.3.2 *Evaluation of video and ACM as standard*

Ideally, the detection performance of the algorithm should be compared to a gold standard. Unfortunately, when working with real patient data such a gold standard is not always available. For seizure detection the visual inspection of the combination of EEG and video by experts is accepted as gold standard. For evaluating an ACM-based motor activity detection algorithm, a good standard would be the visual interpretation of the combination of video registrations and ACM-signals by experts. To get the best possible reference, we investigate the validity of using these qualitative interpretations as a standard for evaluating the performance of our automated detection algorithm for motor activity based on 3-D ACM. Three experts are asked to judge the set of video fragments and ACM-signals described in section 4.3.1 independently and mark the periods that they consider movement. This results in scores on a second time resolution, that have value 1 when there is motor activity and value 0 when there is none. Based on these scores, for each

expert periods in the data are defined as motor activity *events*. The remaining periods are considered as no motor activity events. Thus we construct scores, on an event time basis. Here we take into account that there can be minor differences between two expert's scores that are not relevant. Experts can score the same event, but score a different on- or offset. We tolerate a timing difference of 3 seconds and then these events are considered as the same event. When one expert scores more events than the other in the same time interval, these events are considered as one event if the timing difference between the events of the more precise expert is within 3 seconds. Eventually the scores on event basis are used to compute the interrater agreement for each pair of experts. The measure that is used for the agreement is Cohen's kappa κ [105]. This statistic is most often used to measure agreement and takes into account the agreement that can occur by chance. The range of κ is from -1 till 1, with larger values indicating better reliability. In general when $\kappa > 0.61$ the interrater reliability is considered satisfactory [106]. Computations of κ are done with SPSS 14.1, κ is calculated for video and ACM separately. Finally we evaluate our algorithm with a standard based on both ACM and video scores. Events are only taken into account when at least two experts marked the period as motor activity in either the video or the ACM-signal.

4.3.3 *Detection algorithm for ACM*

Problem description and performance measures

The detection of motor activity from ACM-recordings, as a first step before distinguishing between various activities, is described by several authors. The features, classification method, number of sensors, and sensor positions used, are diverse and depend on the type of motor activity the authors aim to detect. Mostly an algorithm is used that sets a threshold to one derived feature of the ACM-signal obtained from a single position on the body (waist, sternum) [13], [14], [12]. Some authors suggest more complex methods like discriminant analysis using more features [11] or neural networks [107]. Fahrenberg et al. use patient-specific reference-pattern based classification [11]. The studies that use a movement protocol with predefined movements [11], [12] have better results than the studies that use spontaneous movements [18], [13]. Obviously, evaluation and tailoring automated signal analysis methods for motor activity detection during nocturnal (sleep) recordings are not compatible with assessment protocols. Therefore we use movements that occur spontaneously during the night. In our population not only voluntary activities with a relatively 'long' duration and 'high' intensity need to be detected, but also involuntary movements that can be short or even epileptic of nature. These can be very subtle in duration and intensity. Often only part of one limb is involved in these subtle movements. ACM-signals without motor activity visually appear to be flat, but can contain noise caused by autonomic func-

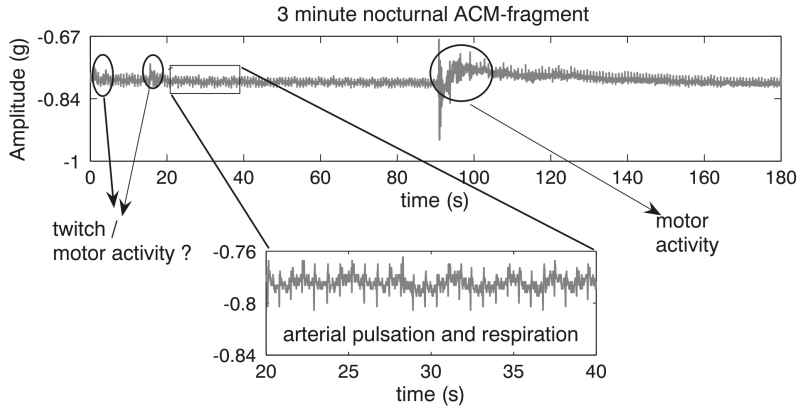

Figure 13: Nocturnal ACM-fragment measured on the sternum. We see subtle motor activity as well as accelerations caused by respiration and arterial pulsation.

tioning of the body like breathing, and the pulsation of the arteries. Hence our detection algorithm needs to detect every part of the data that might contain subtle motor activity and discard data that only contains noise caused by autonomic processes. Figure 13 shows these autonomic noise components in a 3 minute nocturnal ACM-fragment together with subtle motor activity. To tackle this detection problem we have chosen for a solution inspired by methods suggested by other authors [14], [12]. We believe a threshold based detection method that sets a threshold just above the noise caused by autonomic functioning seems feasible to use for the detection of all possible interesting subtle motor activity events.

Using supervised learning techniques to define a model for the data without motor activity, the algorithm classifies part of the data as no motor activity. This data is excluded from further analysis. The remaining part possibly contains motor activity and needs further analysis. In practice such an algorithm can be used to reduce the amount of data that needs to be visually analyzed by the experts. Figure 14 A is a schematical representation of the original data that is divided by experts into two categories: data with motor activity M_1 and data without motor activity NM_1. Figure 14 B shows the output of the detection algorithm. The data without motor activity is excluded from further analysis. The remaining data consists of data M_2 that the experts actually scored as data with motor activity and data NM_2 that the experts regarded as data without motor activity. A minor part of M_1 is not included in M_2, this is the part of the data that actually is motor activity according to the standard, but is missed by the algorithm. In the training phase the detection algorithm is constructed in such a way that 98% of the motor activity M_1 is preserved. We choose 98% instead of 100% to compensate for possible outliers in the data. Consequently in the training phase $M_2 = 0.98M_1$. In the testing phase

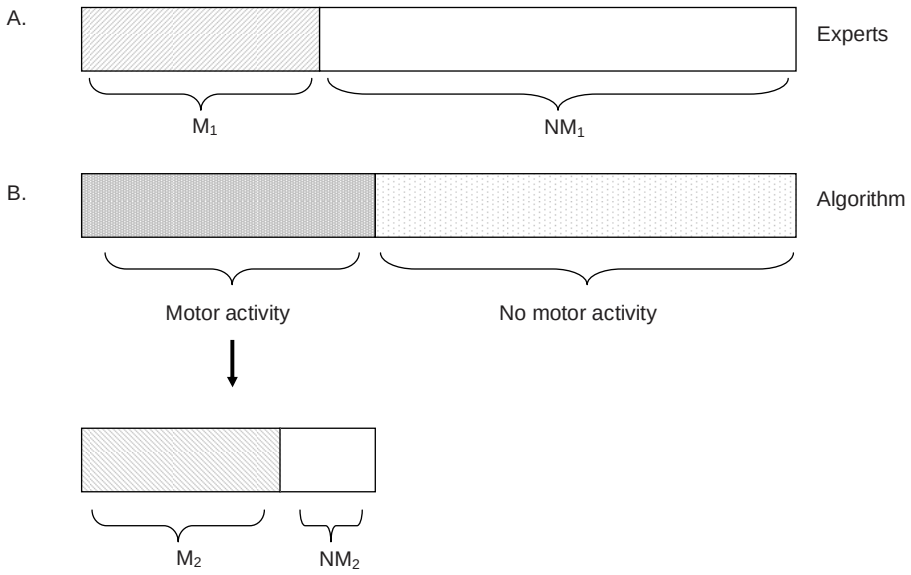

Figure 14: A. Data divided into two categories by experts, M_1 is the data containing motor activity, NM_1 is the data without motor activity. B. After applying the detection algorithm the data classified as 'no motor activity' is excluded from further analysis. The remaining part contains most of the original data with motor activity M_2. The amount of data without activity is strongly reduced NM_2.

we aim that at least 95% of the motor activity is preserved. The percentage of data preservation, DP, is expressed in M_1 and M_2:

$$DP = \frac{M_2}{M_1} \, . \tag{4.1}$$

After applying the algorithm the amount of data that needs further analysis is reduced. We aim at discarding as much of the original data without motor activity NM_1 as possible. The percentage of data reduction DR is expressed in NM_1 and NM_2:

$$DR = 1 - \frac{NM_2}{NM_1} \, . \tag{4.2}$$

The measures above are calculated on a time resolution of 1 second. Successive seconds in the experts score or the algorithms output that have the same value actually belong to the same *event*. We define positive events when subsequent seconds are scored/detected as motor activity and negative events when subsequent seconds are scored/detected as no motor activity. We define a

score function on event basis for the algorithms output in a similar way as the score function for the experts was defined in section 4.3.3. For the algorithms output a positive event can either be a true detection when it coincides with a positive event scored by the experts or a false detection when it coincides with a negative event scored by the experts. For evaluating the performance of our algorithm we also compare the occurrence of events in the output of the algorithm in time with the scores of the experts. Here we have to realize that timing differences occur between events in the data that are scored by the experts and detected by our algorithm:

- due to inaccuracy of the experts,
- due to a small synchronization error between the video and ACM-data, of approximately one second that cannot be corrected for.

The first point is intercepted as much as possible by calculating the agreement between the experts, and only use scores of events that are annotated by at least two experts. Nevertheless there still can be some inaccuracy in the precise on- and offset of the event in the ACM-signals. Also the fact that the ACM-signals and video signals are not completely synchronous contribute to this inaccuracy. To compensate for these inaccuracies, a discrepancy of 3 seconds between the on- or offset in the output of the algorithm and the scores of the experts is tolerated. Furthermore from now on we refer to the used performance measures as estimates. Hence, the estimates of the sensitivity SEN and positive predictive value PPV of the motor activity events are computed. The estimated sensitivity is the ratio between the number of annotated motor activity events that where detected by our algorithm TD (true detected events), and the total number of scored motor activity events P_{Total}:

$$SEN = \frac{TD}{P_{Total}} . \tag{4.3}$$

The estimated positive predictive value is an expression for the false alarm rate. Our aim is to obtain a PPV of at least 50%. This means that more than 50% of the detected events should be genuine. The positive predictive value PPV is expressed in the number of true detected events TD, and the number of false detected events FD:

$$PPV = \frac{TD}{TD + FD} . \tag{4.4}$$

Thus in total the performance of our algorithm is expressed by four different measures. DP and DR are based on second by second basis. The first represents the percentage of the data with motor activity that is preserved, the

second is a measure for how much the workload would be reduced, using this algorithm. DR gives the percentage of data that does not need to be analyzed anymore, in contrast to the situation without the algorithm. SEN and PPV are measures that indicate the performance on event basis, thus how many of the separate movements are actually detected, and how many of the detected *events* are true detections.

Signal validation

The signals from the 15 1-D accelerometers are represented by $x_i[n]$, $i \in \{1, ..., 15\}$. Sometimes during the recordings a sensor malfunctions. This can be easily detected since the offset value of the raw ACM-signal x_i is too high ($|x_i| > 5$ g) and the signal is clipped. In all patients, one of the five 3-D sensors was malfunctioning (arm or leg sensor). In two patients even two. We selected these disconnected sensors by visually inspecting the raw ACM-signals and excluded them from further steps in the algorithm.

Feature extraction

The choice of suitable features is guided by the descriptions of human experts on how they classify parts of ACM-data by visually screening through the data. Figure 15 shows a screenshot of the analyzing program the experts use to screen through the data, together with a picture that shows the locations and orientations of the 15 ACM-sensors. Three important aspects of this visual screening are taken into account when selecting features. Firstly, features are chosen based on characteristics that, according to experts, are important when visually interpreting the data. Experts describe motor activity as 'change in the signal'. Quantitative measures are chosen that can represent this qualitative description. Secondly, it is important to realize that experts evaluate the presence of pattern combinations along many channels at the same time. Subtle movements need to be detected, even when not all the sensors are involved in the movement. Therefore features are calculated for all the sensors. Then per feature, per time unit the maximum value across the 5 sensors is taken. The third aspect is that experts observe the data on various time scales. Therefore two different features are chosen. One that is more sensitive for slower variations in the signals and another that is more sensitive for short, fast, subtle variations. Before the features are calculated the data is divided into nonoverlapping segments. We have chosen for a segment length of 1 second. The shortest seizures have a duration of approximately 1 second and we want to be able to detect them as well as the seizures with a longer duration.
Based on the qualitative description 'change in the signal', a suitable feature for motor activity might be the 'jerk', the first derivative of acceleration and thus an indicator for the rate of change. The jerk is a quantitative measure

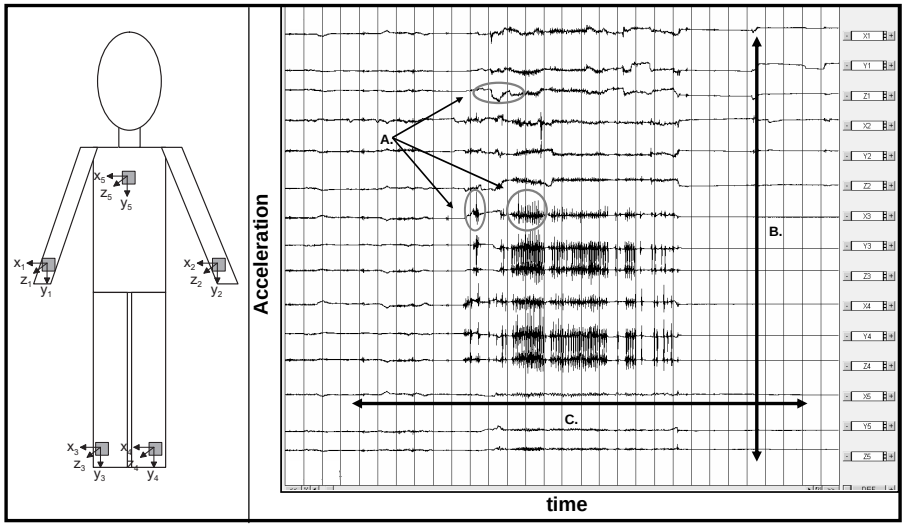

Figure 15: Illustration of three important aspects of the visual analysis of 3-D ACM data. A screenshot of the analyzing program the experts use to screen through the data, together with a picture that shows the locations and orientations of the 15 ACM-sensors is depicted. The duration of the data fragment is 5 minutes. The depicted pattern is typical during walking. Judging data, experts take into account characteristic patterns (A), how they occur in relation to patterns seen on other body parts (B) and how they occur in time (C).

for the steepness of the deviation and should be more sensitive for short, fast, subtle variations. The signals from the 15 1-D accelerometers are represented by $x_i[n]$, $i \in \{1,...,15\}$. The features are calculated per 3-D set $y_j[n]$, $j \in \{1,...,5\}$.
The magnitude of the jerk is defined by

$$Jy_j[n] = \sqrt{\sum_{k=3j-2}^{3j} \left(\frac{x_k[n] - x_k[n-1]}{\Delta t} \right)^2} \tag{4.5}$$

where $j \in \{1,...,5\}$ and Δt is the sampling interval.
Per segment of N samples we calculate the mean magnitude of the jerk $\overline{Jy_j}$:

$$\overline{Jy_j} = \frac{1}{N} \sum_{n=1}^{N} Jy_j[n] \ , \ j \in \{1,...,5\} \ , \ N = 100 \ . \tag{4.6}$$

In our case, $N = 100$, since a segment length of 1 second is chosen, and the sampling frequency f_s of the signal is 100 Hz.

Another quantitative measure that possibly covers the qualitative description 'change in the signal', is the variance. The variance is an important feature for detecting the non-flatness during a movement and is more sensitive for slower variations in the signals. We calculate the variance for the magnitude Y of each 3-D sensor set. The magnitude of each 3-D set y_j is then:

$$Y_j[n] = \sqrt{\sum_{k=3j-2}^{3j} x_k^2[n]} \ , \ j \in \{1, ..., 5\} \ . \tag{4.7}$$

Per 1 second segment the mean magnitude $\overline{Y_j}$ is calculated:

$$\overline{Y_j} = \frac{1}{N} \sum_{n=1}^{N} Y_j[n] \ , \ j \in \{1, ..., 5\} \ , \ N = 100 \ . \tag{4.8}$$

Secondly, the variance of the magnitude $S^2_{Y_i}$ is calculated for each segment:

$$S^2_{Y_j} = \frac{1}{N} \sum_{n=1}^{N} (Y_j[n] - \overline{Y_j})^2 \ , \ j \in \{1, ..., 5\} \ , \ N = 100 \ . \tag{4.9}$$

Because J_y is a linear measure and $S^2_{Y_j}$ quadratic we use the square root S_{Y_j}.

The output of our algorithm is compared to scores that are made based on video-data, therefore there are some issues that need to be resolved in the feature extraction. First we have to realize that it is possible that motor activity occurs on only one sensor but all the sensors have the score motor activity at that time. Since the visual scores are not made for each sensor, detecting motor activity for each sensor is not possible. To solve this problem the maxima of both features are taken across all the 5 sensors:

$$J_{y\,max} = \max_{j \in \{1,...,5\}} [J_{y_j}] \ , \tag{4.10}$$

$$S_{Y_{max}} = \max_{j \in \{1,...,5\}} [S_{y_j}] \ . \tag{4.11}$$

Another issue is that timing differences can occur between events scored by experts and events detected by the algorithm as already mentioned in section 4.3.3. Still we take the labels as defined by the experts as our standard, but the corresponding feature values we use are the maximum values of the set of three segments (the one that corresponds to the label and the two surrounding segments).

Classification

Classification is performed in the 2-D vector space that results from the feature extraction process. Figure 16 shows an example of a scatter plot of the 2-D vector space. Every point represents a feature vector $\underline{f_i}$ that was calculated per data segment. In our case the feature vector $\underline{f_i}$ consists of $J_{y_{max}}$ (f_1)

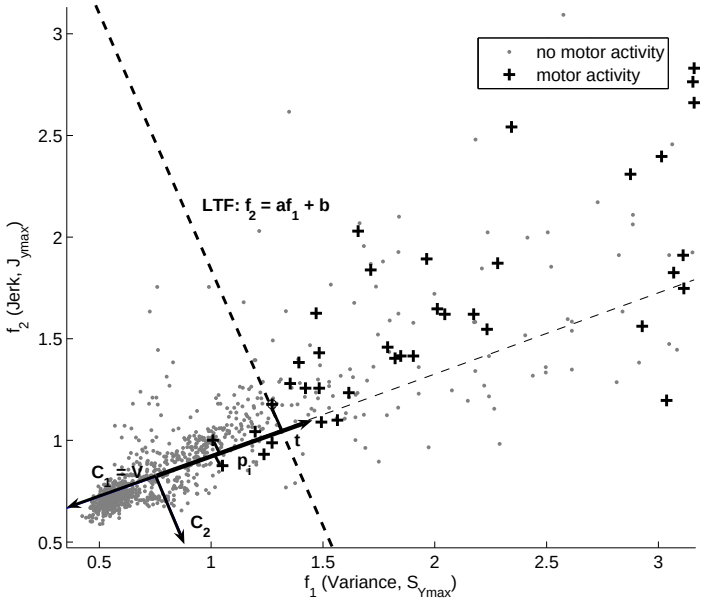

Figure 16: Graphical representation of computation of linear threshold function (LTF) in 2-D feature vector space. First the eigenvectors C_1 and C_2 of the covariance matrix of the cluster corresponding to 'no motor activity' are determined. The LTF is set perpendicular to the eigenvector corresponding to the largest eigenvalue $\underline{V}$. The LTF is set in such a way that 98% of the 'motor activity' is on the right side of the LTF.

and $S_{Y_{max}}$ (f_2). Vectors corresponding to segments with motor activity are marked with '+'. Vectors corresponding to segments without motor activity are marked with '·'. There are two clusters with an area of overlap. The shape and alignment of the cluster representing the data with motor activity depends on the motor activity type, the body parts involved and intensity of the movement. Since these properties can be very diverse, this cluster shows a high intra- and inter-patient variability. Factors that influence the shape and the alignment of the cluster without motor activity are pulsation of the arteries, respiration and involuntary muscle twitching. The first two are restricted since these are all processes regulated by the autonomous nervous

system. Therefore this cluster is more stable in the same patient and between patients. The area where the clusters overlap contains data segments with involuntary muscle twitches. This area also contains subtle motor activity events. To refer to our goal presented in section 4.3.3, we want to reduce the amount of data segments without motor activity and preserve as much of the data with motor activity as possible. Thus in our training data a linear threshold function is constructed in such a way that 98% of the data with motor activity is preserved. To ensure this threshold function is robust for fluctuations across patients, we base it on the shape and the direction of the cluster without motor activity, since this is the most stable cluster. First the covariance matrix Σ is calculated for this cluster:

$$\Sigma = \begin{bmatrix} \frac{1}{N}\sum_{i=1}^{N}(f_{1i}-\bar{f}_1)^2 & \frac{1}{N}\sum_{i=1}^{N}(f_{1i}-\bar{f}_1)(f_{2i}-\bar{f}_2) \\ \frac{1}{N}\sum_{i=1}^{N}(f_{2i}-\bar{f}_2)(f_{1i}-\bar{f}_1) & \frac{1}{N}\sum_{i=1}^{N}(f_{2i}-\bar{f}_2)^2 \end{bmatrix} \tag{4.12}$$

where f_{1i} and f_{2i} are the two features in feature vector $\underline{f}_i$ and $\bar{f}_k = \frac{1}{N}\sum_{i=1}^{N} f_{ki}$. The eigenvalues λ_1, and λ_2 and eigenvectors C_1 and C_2 of the covariance matrix are computed. The eigenvectors represent the orientation of the cluster. The eigenvalues are an indication of the spread of the feature values in the direction of the corresponding eigenvector. The eigenvector corresponding to the largest eigenvalue is chosen as principal component vector $\underline{V}$. The linear threshold function is set perpendicular to $\underline{V}$. For all the points $\underline{f}_i$ that have a label 'motor activity' the projection $\underline{p}_i$ on this vector is calculated. The point t where the linear threshold function intersects $\underline{V}$ is set so that 98% of $\underline{p}_i$ lies above t.

The linear threshold function (LTF) $f_2 = af_1 + b$ is constructed based on training data. We aim at an algorithm that is robust for fluctuations across patients. Therefore the training and test data is obtained from different patients. A sequence of training and testing is performed where the data of six patients are used for training and the data of the remaining patient are used for testing. Besides the estimated performance measures that were explained in section 4.3.3, also the slope a and the intercept b of the LTF are computed. When the variations of these two parameters are less then 10% between patients we consider the parameters consistent. This is considered as an indication that the algorithm can be used across patients. In that case we also investigate the outcome per patient for the parameters with a 10% deviation, to see if these outcomes are stable. We have chosen for a bivariate detection setup using two features, for comparison to previously suggested methods that are based on only one feature, the results are also computed for setting a threshold on the features separately. In this univariate case, threshold th is computed, instead of parameters a and b.

4.4 RESULTS

4.4.1 *Evaluation of standard*

Table 7 lists the values of κ for each pair of experts, for both the video and the ACM scores. The agreement can be considered good if κ lies between 0.61 and 0.8 [106]. Therefore we consider the annotations to be reliably enough to be

Table 7: Interrater agreement for video and ACM, for each pair of experts expressed in Cohen's Kappa κ

EXPERTS	κ_{Video}	κ_{ACM}
1 and 2	0.75	0.81
1 and 3	0.71	0.62
2 and 3	0.70	0.70

used as a reference for validation of our algorithm. In the combination video and ACM events, there are 14 events that do not overlap. Twelve events were only marked in the video, two events are only marked in the ACM-signal. The two events marked in the ACM-signal are subtle, steep patterns, that could be related to an epileptic seizure. These aren't visible in the video because the involved body part is not in the scope of the camera, or the view is blocked by blankets. The events marked in the video and not in the ACM-signal, are mostly slow movements that are clearly visible in the video, but have a relatively low amplitude and more smoother patterns in the ACM-signal. For evaluation of our algorithm we use the standard based on both ACM and video. In this reference we use only the motor activity events that are scored by at least two experts.

4.4.2 *Performance of ACM-based detection algorithm*

Figure 17 shows an example of original accelerometry (ACM) data together with the output of our algorithm and the scores of the experts. The results of the classification performed per patient (the data of the other patients is used as training data) are depicted in Table 8. Also the slope a and the intercept b of the linear threshold function LTF are depicted. In the training phase we set the percentage of data preservation DP to 0.98. In our test data we were able to detect all the annotated events (sensitivity SEN = 1) and perform data reduction varying per patient from 52% to 93%. False positive rates were acceptable. In six cases the PPV was higher or equal to the desired 50 %. The slope a and the intercept b of the linear threshold functions are

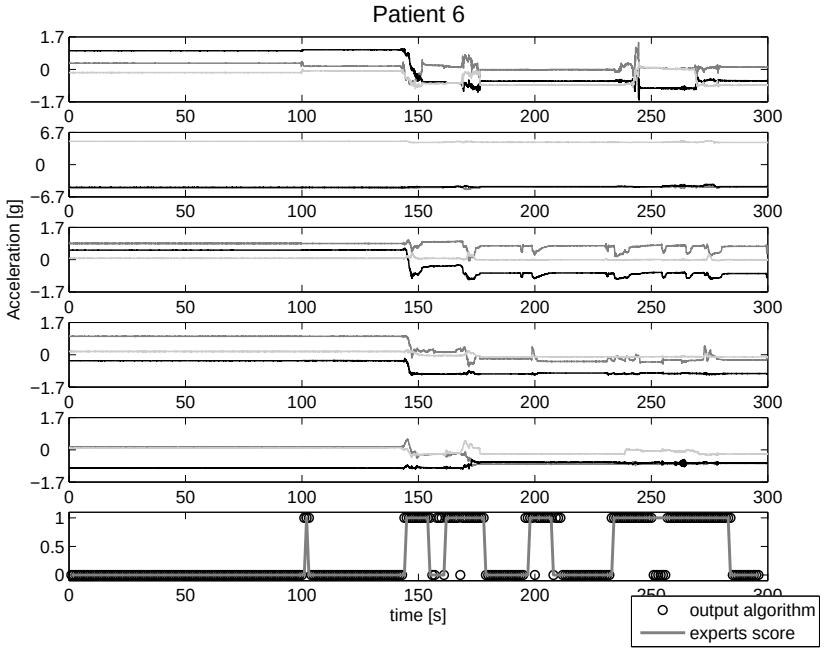

Figure 17: ACM-data of patient 6. The output of the algorithm and the experts score are plotted together in the last subplot. The value 0 indicates no motor activity whereas the value 1 indicates motor activity.

Table 8: Percentage of data reduction DR, percentage of data preservation DP, estimated sensitivity SEN and estimated positive predictive values PPV for the test data set. The slope a en the intercept b of the linear threshold function are also depicted for each case. Per data set the numbers of the corresponding patients are depicted

TRAIN DATA	TEST DATA	DR	DP	SEN	PPV	a	b
2, 3, 4, 5, 6, 7	1	0.86	1	1	0.66	-1.96	4.00
1, 3, 4, 5, 6, 7	2	0.93	0.95	1	0.89	-1.92	3.96
1, 2, 4, 5, 6, 7	3	0.91	0.95	1	0.50	-1.99	4.08
1, 2, 3, 5, 6, 7	4	0.93	1	1	0.71	-1.96	3.93
1, 2, 3, 4, 6, 7	5	0.52	1	1	0.43	-1.90	3.61
1, 2, 3, 4, 5, 7	6	0.93	0.91	1	0.71	-2.02	4.43
1, 2, 3, 4, 5, 6	7	0.78	1	1	0.66	-2.13	3.89

consistent throughout our population, the variations are less than 10%. When we perform the detection with 10% variation in the parameters a and b we observe that for every patient the sensitivity and PPV remain constant, DR and DP vary around 1%. These results imply that the algorithm can be used across patients. We analyzed the video and the ACM-signals of all the false detections. The total number of false detections was 24. Seventeen of these false detections were movements that were annotated by the experts in ACM- or video, but the detection output is longer in duration. The remaining seven false detections were periods where the patient is very restless (awake, moving the head etc.). The experts only marked the distinct movements, and not the periods of restlessness. Comparing the results of our 2-D LTF with the

Table 9: Percentage of data reduction DR, percentage of data preservation DP, estimated sensitivity SEN and estimated positive predictive values PPV for the test data set for an algorithm based on the use of respectively the Variance and the Jerk alone. The threshold th is also depicted for each case

A. Threshold on one single feature (Variance).

TRAIN DATA	TEST DATA	DR	DP	SEN	PPV	th
2, 3, 4, 5, 6, 7	1	0.85	1	1	0.66	1.41
1, 3, 4, 5, 6, 7	2	0.95	0.95	1	1	1.42
1, 2, 4, 5, 6, 7	3	0.90	0.97	1	0.50	1.42
1, 2, 3, 5, 6, 7	4	0.93	1	1	0.71	1.40
1, 2, 3, 4, 6, 7	5	0.53	1	1	0.41	1.35
1, 2, 3, 4, 5, 7	6	0.92	0.91	1	0.62	1.49
1, 2, 3, 4, 5, 6	7	0.75	1	1	0.57	1.27

B. Threshold on one single feature (Jerk).

TRAIN DATA	TEST DATA	DR	DP	SEN	PPV	th
2, 3, 4, 5, 6, 7	1	0.81	1	1	0.57	1.12
1, 3, 4, 5, 6, 7	2	0.87	0.95	1	0.57	1.18
1, 2, 4, 5, 6, 7	3	0.83	0.95	1	0.33	1.20
1, 2, 3, 5, 6, 7	4	0.94	1	1	0.71	1.10
1, 2, 3, 4, 6, 7	5	0.36	1	1	0.35	1.09
1, 2, 3, 4, 5, 7	6	0.92	0.92	1	0.71	1.26
1, 2, 3, 4, 5, 6	7	0.77	1	1	0.57	1.04

detection of an algorithm based on only one feature (Table 9) we notice that in the case for the variance alone the results are similar to the 2-D case. In patient 5, 6, and 7 extra false detections are detected and when this is checked in the ACM-signal we notice that a regularly respiratory cycle is detected. For only the jerk, additional false detections are detected in five patients (1, 2, 3, 5, 7), but in these cases there is no motor activity visible in the ACM-signal or the video. The algorithm actually detects activity caused by the pulsation of the arteries. The combination of the variance and the jerk leads to less false detections than in the univariate cases in three patients (5, 6, 7). Figure 16 supports this observation, the linear threshold function clearly depends on both the variance and the jerk, therefore both features contribute to the detection.

4.5 DISCUSSION

Our goal was to develop an algorithm for 3-D accelerometry (ACM) recordings that detects local subtle motor activity of the body with a sensitivity of at least 95% and a positive predictive value (PPV) of at least 50%, thus reducing the amount of data that needs to be further analyzed for motor seizure detection. We compared the results of our algorithm to the scores of human experts that visually analyzed the ACM-signals and simultaneously recorded video-recordings. Using the algorithm we obtained a sensitivity of 100% of the motor activity that was seen in the video by experts. Per patient the data reduction ranged from 52% to 93% (mean = 84%). The positive predictive value ranged from 43% to 89% (mean = 65%). These results indicate that our approach satisfies the requirements stated above.

The high sensitivities are not surprising since in the training phase we aimed at preserving 98% of the data with motor activity. But despite the high sensitivities our positive predictive value was higher than our criterium of 50% in 6 out of 7 patients. Furthermore 17 of the 24 false detections were actually a prolongation of a correctly detected event. We defined that these prolongations were a new event, and thus a false detection, when the duration was longer than 3 seconds. When we exclude these 17 false detections, since they probably belong to a correctly detected event, the mean PPV increases from 65% to 85%.

When we compare our results to results that were obtained by other authors that used a spontaneous movement protocol we see that although we obtain a similar PPV, our sensitivity is much higher. Bussmann et al. [13] obtained a sensitivity of 58% and a PPV of 64% for distinguishing between periods with and without movement. As a standard they also used annotated video images. Dunnewold et al. [18] determined periods of immobility in patients with Parkinsons Disease. They state that with their method between 66.7% and 80.7% of the immobility periods were correctly classified.

The data reduction numbers DR, together with the observation that the false detections are actually motor activity imply that our algorithm can be used to assist off-line analysis for diagnostic purposes since the amount of data (both ACM and video) that needs further analysis can be significantly reduced. Here we make a comment that data reduction might also be possible by a simple automatic analysis of the video images itself, by calculating the differences between successive frames. This is a familiar preprocessing step in automatic video-analysis [100], [101]. Nevertheless, interpreting the images when a moving body part is not in the field of the camera, because blankets are blocking the view, is still a problem.

The linear threshold function we used for classification was very consistent throughout our population. The slope a and the intercept b of the linear threshold function did not vary significantly per set of training data. In the training configurations we used there was overlap, so some degree of similarity can be expected, but the performance of the detection in the test data when we varied the parameters $\pm$ 10% indicates that the linear threshold function is robust for fluctuations across patients. Consequently there is no need for training the algorithm for each new patient. From a physiological point of view this means that the jerk and the variance of the acceleration caused by breathing and pulsation of the arteries lie in a certain range for all the patients. Since these are processes that are regulated by the autonomous nervous system this is also what we expected.

Our goal was to detect every possible interesting motor activity event. We hypothesized that a bivariate method would perform better than a method based on one single feature. Comparing the detection results of the bi-and univariate algorithms we can not completely confirm this hypothesis. An algorithm based on the jerk alone, detected all motor activity events, but there were 18 more false detections than in the bivariate algorithm. These false detections were introduced since this feature is susceptible for fast acceleration changes caused by the pulsation of the arteries. Nevertheless PPV was $>$ 50% in 5 out of 7 cases. An algorithm based on the variance alone had a similar performance than our bivariate approach. Although, compared to the bivariate algorithm there was an extra false detection introduced in three patients. Combined with the jerk, the algorithm does detect these small subtle events. Thus in three patients (5, 6, 7) it was better to use the combination of the two features instead of only one. Although we can not confirm our hypothesis based on these results we still believe that the bivariate performs better for our goal than an algorithm based on variance or jerk alone.

The performance measures that are used in this chapter were obtained using a qualitative standard: the visual analysis of video and ACM. Since this standard depends on the accuracy of the experts during scoring, we investigated the validity of using these interpretations as a standard for evaluating the performance of our algorithm. The interrater agreement κ between three experts was calculated as a measure for this validity. According to literature a

κ between 0.6 and 0.8 can be considered *good* [106]. Since $\kappa > 0.7$ in all cases of the video and in two cases of the ACM, and the remaining κ was 0.62, we consider the scores to be reliable enough to use as a reference for validation of our algorithm. Nevertheless we must realize that using this standard might introduce false detections that are actually motor activity, since the agreement was not 1. Therefore performance measures based on such a standard should be interpreted with care.
In the validation step of our algorithm, we excluded data from sensors that were malfunctioning. This decreases the number of sensors that are used for movement detection. Nevertheless our algorithm was able to detect all the movements that were scored by the experts. This shows that not all the five 3-D sensors are needed for movement detection in this case.

4.6 CONCLUSION

A first step is presented towards reliable detection of nocturnal epileptic seizures based on 3-D accelerometry (ACM) recordings. With a simple supervised learning detection approach we were able to distinguish between data with and without subtle motor activity. For training and evaluating of the algorithm nocturnal ACM- and video-data are used that are recorded from mentally retarded subjects with severe epilepsy. A 3-D sensor is placed at both wrists and ankles, and at the sternum. From the resulting 15 ACM signals, two features were derived for each second, and in the resulting 2-D feature space a linear threshold function was used for classification. Our algorithm showed a sensitivity of 100% compared to the motor activity that was seen in the clinical standard. The positive predictive value ranged from 43% - 89% (mean = 65%). The detection results also indicated that the algorithm is robust for fluctuations across patients, so no training for every new patient is necessary. Data reduction for each patient was substantially and ranged from 52% - 93% (mean = 84%). This algorithm can already be of great value for supporting off-line analysis in clinical setting for diagnostic and evaluation purposes, since a substantial part of the data can be excluded from further analysis thus reducing the amount of work. Important issues were tackled regarding the use of clinical standards for validation of automated algorithms. According to current practice, for accelerometry the best available standard is visual interpretation of the combination of video-recordings and ACM-signals by experts. However, such a standard has its limitations since the experts interpretations are qualitative and depend on the accuracy of the experts during scoring. Furthermore, the use of video as a reference is also limited since body parts can be out of the cameras field. These limitations can degrade performance measures based on such a method, and the use of accelerometry can overcome these problems.

5

A MODEL FOR MYOCLONIC SEIZURES THAT CAN BE USED AS MATCHED WAVELET TRANSFORM

This chapter is composed of:
T.M.E. Nijsen, R.M. Aarts, J.B.A.M. Arends, and P.J.M. Cluitmans. Model for arm movements during myoclonic seizures. 29th Annual International Conference of the IEEE EMBS [32], and T.M.E. Nijsen, A.J.E.M. Janssen, and R.M. Aarts. Analysis of a wavelet arising from a model for arm movements during epileptic seizures. ProRisc, 2007 [33].

5.1 ABSTRACT

A model is formulated for arm movements during myoclonic seizures. The system described in the model, consists of a mechanical and an electrophysiological part. The model output is compared with real patient accelerometry (ACM)-data from six epilepsy patients. Eight out of ten myoclonic seizures have a good fit to the model. The values of the model parameters tuned to the real seizures are physiologically feasible. Two of the four parameters seem to be robust for variations in patients and seizures. The model is used to formulate a matched wavelet transform. Due to the simple analytical form of the wavelet, $x(t)$, explicit computations are feasible for the frequency response $X(\omega)$, the admissibility condition and admissibility constant, the wavelet transform of x itself using x or its time-reversed version x_- (matched filter) as analyzing wavelet etc. The new wavelet is expected to yield better detectability for the problem at hand than general purpose wavelets would do. We show one example of how the new wavelet performs on clinical data and we intend to follow up this study with a more elaborate demonstration of its efficacy. The new wavelet, and some of its variants (such as the odd extension of it and a Gaussian smoothed version of it), are briefly compared with certain wavelets presented in existing literature. Our preliminary conclusion, is that the wavelet has potential in the detection of myoclonic seizures from accelerometric data of arm movements of epileptic patients.

5.2 INTRODUCTION

In this chapter an analytical model is formulated for accelerometric output associated with myoclonic seizures. This model is used to derive a matched wavelet transform that can be used to derive salient features for the detection of myoclonic seizures.
A myoclonic seizure consists of one single muscle jerk. Myoclonic seizures are

associated with clearly visible stereotypical patterns in accelerometry (ACM) signals [30]. For the choice of suitable features for automated detection of these seizures from the ACM-signal, knowledge about these patterns is important.
The suggested model can be used to study important characteristics of accelerometric waveforms associated with myoclonic seizures. It can contribute to a better understanding of the patterns that are observed in the ACM-recordings. Hence, the model makes it also possible to derive parameters from the ACM-signal that have a physiological meaning. Therefore this model-based approach can contribute to a robust detection of myoclonic seizures.
The system described in the model consists of a mechanical and an electrophysiological part. The electrophysiological part contains the definition of stimuli and a muscle response to these stimuli during a myoclonic seizure. The mechanical part is based on kinematic and kinetic relations for the lower arm, modeled as a rigid body system. The model output is compared to real patient accelerometry data. The sensitivity of the parameter settings is studied in order to get an indication whether the model is robust across patients and seizures. The next step is to use the model to derive a matched wavelet transform. An overview of some mathematical properties of this wavelet is given and a comparison to other wavelets in literature is made. Finally, an example is given on how this matched wavelet can be used for the detection of myoclonic seizures.

5.3 MODEL OVERVIEW

During a motor seizure the distal segments of the limb are more affected than the proximal ones, and arm movements are dominant over leg movements. Video observations confirm that myoclonic seizures very often manifest themselves as short abrupt flexions involving only the lower arm. It is also frequently observed that a seizure starts with myoclonic jerking in one arm followed by tonic, clonic or tonic-clonic contractions that spread towards the other arm, the trunk and the legs. Based on the above statements and observations, it was decided to include only the forearm in the model for myoclonic seizures. Figure 18 is a schematic overview of all the components of the model. The central nervous systems sends signals to the muscles. The muscles contract as a result of the stimuli and apply force on the skeletal system. These forces cause movement of the limb. For evaluation of the movement model, the choice was made to record movements with accelerometers, thus in the model also the accelerometer output corresponding to the movements is calculated.

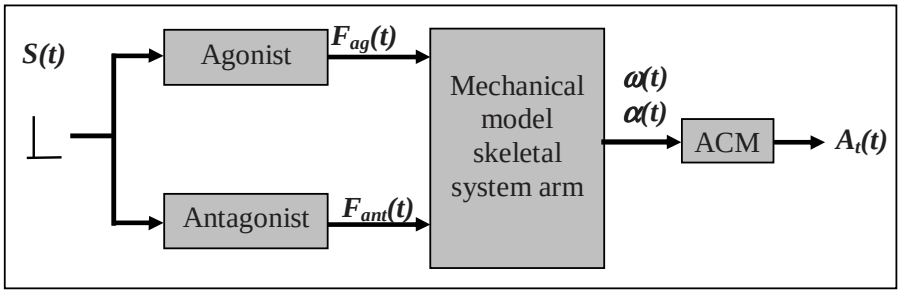

Figure 18: Schematic representation of model. $S(t)$ is the innervation pattern sent from the central nervous system to the muscles. $F_{ag}(t)$ and F_{ant} represent the muscle force produced by the agonist and antagonist muscle. $\omega(t)$ and $\alpha(t)$ are the angular velocity and the angular acceleration of arm, and $A_t(t)$ is the accelerometer output in the movement direction.

5.3.1 *Innervation patterns during myoclonic seizures*

Generally a myoclonic seizure is preceded by spike-wave (or a poly spike-wave) pattern in the EEG signal. It is believed that during the spike part of the spike-wave discharge, trains of action potentials are sent down to the motor units and the muscles contract in reaction to this stimulation [10]. The agonists and antagonists in the muscle groups involved contract synchronously. During the wave part there is a central inhibition, and no action potentials are descending to the motor units. This results in complete relaxation of all the muscles involved. The EMG activation during an epileptic myoclonus is < 50 ms [7]. Based on the above observations it was decided to model the innervation pattern during a myoclonic seizure as a pulse.

5.3.2 *Muscle contraction during seizures*

In literature [108, 109], many complicated muscle models are described. Most of these models go deeply into the muscle's structure and physiology. To use such an extensive model would go far beyond the scope of this chapter. The choice was made to use a simple approximation for muscle force in time, based on the response of a motor unit to one single stimulation pulse [110]:

$$F(t) = F_0 \frac{t}{\tau_0} e^{\frac{-t}{\tau_0}} . \tag{5.1}$$

This simplification is based on the fact that during a seizure the muscles are much more stimulated than under normal circumstances. One burst of epileptic activity can cause a sudden jerk of a limb. The entire muscle consists of many motor units. During the myoclonus they are all activated synchronously. Thus, the impulse responses of all the motor units should be

added together. For simplicity it is assumed that during a myoclonic seizure the impulse response of all the activated motor units together can then be approximated by: $F(t) = F_{sum}\frac{t}{\tau}e^{\frac{-t}{\tau}}$, with F_{sum} the weighted sum of all the F_0's of all the different motor units, and τ a general time constant for al the units together. An advantage of the use of this impulse response is that it is possible to simulate physiological-like muscle responses to different types of stimuli.
In the model one agonistic muscle pair is included that is synchronously innervated during the seizure [7]. The muscle force of the agonist muscle $F_{ag}(t)$ is modeled as:

$$F_{ag}(t) = F_{sum}\frac{t}{\tau}e^{\frac{-t}{\tau}} \ . \tag{5.2}$$

It is necessary to create an alternating positive and negative net muscle movement, to generate the typical myoclonic 'shock-like' pattern. Therefore for modeling the antagonist muscle force $F_{ant}(t)$ a similar equation would yield, but with different values for F_{sum} and τ:

$$F_{ant}(t) = F_{sum_{ant}}\frac{t}{\tau_{sum_{ant}}}e^{\frac{-t}{\tau_{sum_{ant}}}} \ . \tag{5.3}$$

Equation 5.3 can be expressed in F_{sum} and τ by:

$$F_{ant}(t) = \frac{1}{A}F_{sum}\frac{t}{\tau}e^{\frac{-t}{B\tau}} \ . \tag{5.4}$$

where A and B –as we shall see in section 5.4 – are dimensionless constants approximately equal to 1.

5.3.3 *Mechanical model of the skeletal system of the arm*

The most dominant element in a myoclonic seizure is the flexion of the elbow. The elbow is modeled as a hinge joint that is fixed at its position. This means that the movement of the wrist is a pure rotation around the elbow axis, a two-dimensional planar movement. Figure 19 shows the rigid body that represents the lower arm and the hand. The box is the fixed accelerometer that measures acceleration components in the tangential (A_t) direction. The forces that act on the rigid body are the agonist muscle force (F_{ag}), the antagonist muscle force (F_{ant}), and the joint reaction force (F_j). The length of the rigid rod is represented by L.

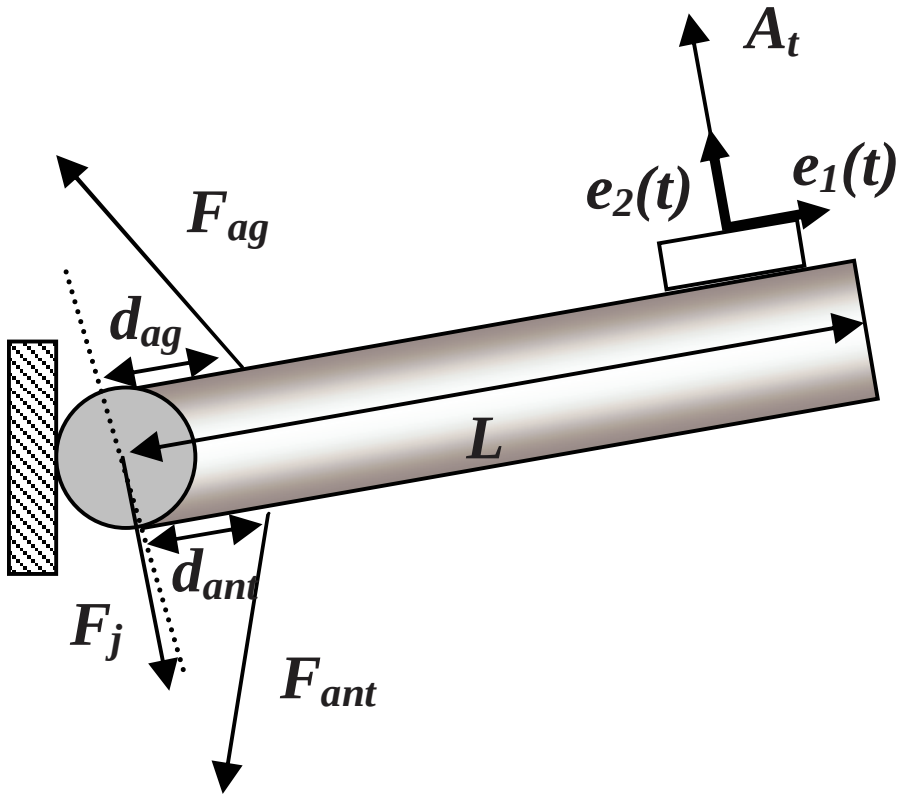

Figure 19: Schematic overview of the mechanical part of the model.

Kinematic relations for the rigid body system

The kinematic relation for position $x(t)$, during a 2-D rotation in a time-dependent, moving frame of reference $\{\mathbf{e}_1(t), \mathbf{e}_2(t)\}$, is:

$$\mathbf{x}(t) = R\mathbf{e}_1(t) \,, \tag{5.5}$$

with R, the distance of the elbow to the accelerometer. The corresponding velocity $v(t)$ is:

$$\mathbf{v}(t) = \omega R\mathbf{e}_2(t) \,, \tag{5.6}$$

where $\boldsymbol{\omega}(t)$ is the angular velocity of the moving frame. The corresponding acceleration $a(t)$ is:

$$\mathbf{a}(t) = \alpha R\mathbf{e}_2(t) - \omega^2 R\mathbf{e}_1(t) \,, \tag{5.7}$$

where $\boldsymbol{\alpha}(t)$ is the angular acceleration of the moving frame. This means that during a pure rotation, acceleration A_t (at the position of the accelerometer) in the tangential direction $\mathbf{e}_1(t)$ equals αR. The acceleration A_n in the normal direction $\mathbf{e}_2(t)$ equals $-\omega^2 R$.

Kinetic relations for the rigid body system

When there is an input force, the sum of all moments can be calculated by multiplying all the tangential components of the acting forces with their moment arms. The muscle forces described in section 5.3.2 are linked to Eq. 5.7 by Eq. 5.8:

$$\Sigma \mathbf{M} = \mathbf{I}\boldsymbol{\alpha} \,, \tag{5.8}$$

where I is the mass moment of inertia about a parallel z-axis through the fixed rotating point. For the model in this chapter this means that:

$$\Sigma \mathbf{M} = F_{ag\perp} \cdot d_{ag} - F_{ant\perp} \cdot d_{ant} = I\alpha \,. \tag{5.9}$$

The joint reaction force F_j, acts on the fulcrum and does not contribute to the sum of moments.

Since the output of interest is α, Eq. (5.9) is rewritten:

$$\alpha(t) = \frac{F_{ag\perp} \cdot d_{ag} - F_{ant\perp} \cdot d_{ant}}{I} \,. \tag{5.10}$$

For a rigid rod, of length L, rotating around one end, the moment of inertia is constant and equal to $\frac{1}{3} m L^2$, with m the mass of the lower arm. The length L and the mass m of the lower arm, can be expressed in terms of full body length (BL) and full body mass (BM) using anthropometric data [110]. Using average values from literature [111] for d_{ag} and d_{ant} Eq. 5.10 can be rewritten as:

$$\alpha(t) = \frac{4.5}{BM\ BL^2}(F_{ag} - F_{ant}) \,. \tag{5.11}$$

The measured output of the ACM-sensor caused by the myoclonic seizure equals αR. The actual accelerometer output measures also an acceleration component caused by gravity. During such a subtle movement, the displacement of the arm is very small and thus the rotation with respect to the gravity field can be neglected. Therefore for a comparison of simulated movements with real accelerometer output, Eq. 5.11 needs to be multiplied with R, the distance from the elbow to the wrist, that is equal to $0.146BL$ [110]. Thus the ACM-pattern observed during a myoclonic seizure is of the shape:

$$A_t(t) = K\left(te^{\frac{-t}{\tau}} - \frac{t}{A}e^{\frac{-t}{B\tau}}\right) \,, \tag{5.12}$$

where constant $K = \frac{0.66}{BM\ BL}\frac{F_{sum}}{\tau}$.

5.4 COMPARISON OF MODEL TO REAL DATA

Equation 6.1 was fitted to real patient data with an optimization algorithm in MATLAB.
ACM-data are used from six mentally retarded patients who suffer from severe epilepsy. This data is described in [30]. In order to get an indication whether the model needs to be tuned for every patient or seizure, the sensitivity of the parameter settings is studied. Figure 20 shows real accelerometer output compared to the modeled myoclonic seizures. The data is first filtered with a first order high-pass filter with a cut-off frequency of 0.1 Hz. Table 10 shows for every myoclonic seizure the values of K, τ, A, B, F_{max}, and the correlation coefficient R^2 between the modeled myoclonic seizure and the corresponding real myoclonic seizure. F_{max} is determined by filling out $t = \tau$ in Eq. 5.2. F_{max} represents the maximal muscle force applied to the arm by the agonist muscle. Eight out of ten myoclonic seizures have a correlation coefficient > 0.7, with a p-value $<< 0.01$. Myoclonus no. 6 and 9 have a poor fit. No. 6 is not a single muscle twitch, but there is a more repetitive movement visible in the ACM-signal. This is also the case for No. 4 although in this case the fit to the first part of the repetitive pattern is good and the correlation coefficient is 0.73. The shape of No. 9 seems to consist of two subsequent twitches. The values of τ are physiologically meaningful. The contraction time τ for motor units in the arm are in the range of 16–68 ms for the triceps and in the range of 16–85 ms for the biceps [110]. Also the values of F_{max} are physiological feasible forces. The values of A and B are all > 1. A needs to be > 1 since the arm first flexes during a myoclonic seizure. This means that when a seizure starts the force delivered by the agonist is larger than the force delivered by the antagonist. This phenomenon can possibly be explained by the fact that the projection area of the motor cortex through the pyramidal tract that belongs to the agonist muscles is larger [112]. For generating an alternating positive and negative net muscle movement, there must hold $A = B^2$. Therefore also $B > 1$. From the simulation results we can also observe that $A \approx B^2$.

To study the robustness of the model and the sensitivity of the parameters, the correlation coefficients between the real data and a simulated myoclonus with the mean values of Table 10 filled in for the parameter settings are calculated. This leads to correlation coefficients > 0.8 in 6 myoclonic seizures. The fit was poor for myoclonus No.'s 4, 6, 8, and 9. No.'s 6 and 9 already had a bad fit. In Table 10 No. 4 has a relatively large value for τ compared to the other waveforms, therefore the correlation to the mean parameters is poor. In Table 10 No. 8 has a relatively large value for K compared to the other waveforms, hence the correlation to the mean parameters is also poor. Keeping all the parameters fixed at the mean value and only the value of K to be optimized leads to similar results. Keeping all the parameters fixed at the mean value and only the value of τ to be optimized leads to poor fits with

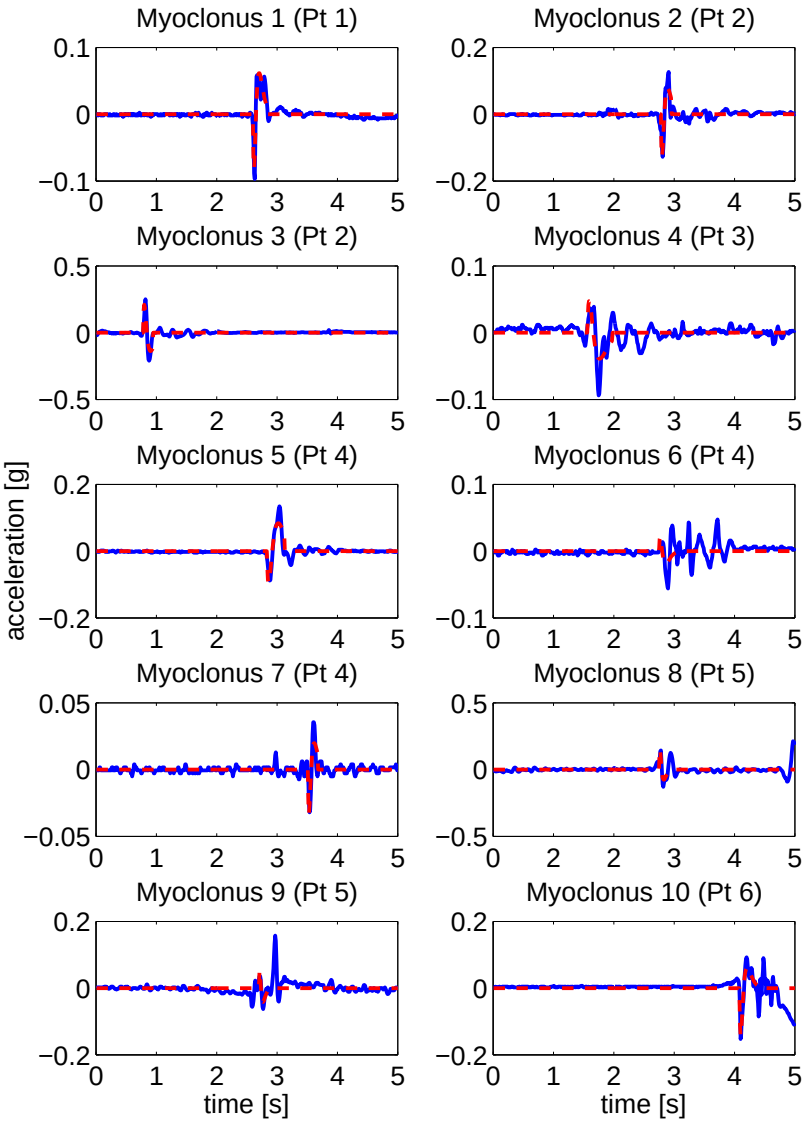

Figure 20: Simulation results (red dashed line) compared to real ACM-data (blue solid line). 'Pt #' indicates the patient where the data is from.

erratic values of τ in 5 cases. Keeping only A and B fixed, and the values of K

Table 10: Parameters of model fitted to real data

Myocl.	K [N/(kg s)]	τ [s]	A	B	F_{max}[N]	R^{2*}
1	47.8	0.035	1.025	1.017	96	0.88
2	49.9	0.035	1.036	1.022	131	0.88
3	67.8	0.040	1.038	1.024	203	0.85
4	30.7	0.070	1.011	1.008	116	0.73
5	32.3	0.065	1.024	1.017	92	0.88
6	34.5	0.038	1.109	1.006	58	0.34
7	32.9	0.034	1.015	1.009	49	0.83
8	81.6	0.024	1.038	1.025	56	0.71
9	11.6	0.022	1.114	1.076	7	0.51
10	36.9	0.039	1.046	1.025	74	0.91
Mean	42.6	0.040	1.045	1.023	88	0.75

* with a p-value $<< 0.01$

and τ to be optimized leads to similar results as those presented in Table 10. Therefore A and B might be fixed across patients, and appear to be typical for myoclonic seizure movements.

5.5 USING THE MODEL AS WAVELET

A possible way to use the model from the previous sections to derive salient features for seizure detection, is to use the model as a matched wavelet transform. In this section we analyse the wavelet that arises from our model:

$$\left(te^{-t/\tau} - \frac{1}{A}te^{-t/(B\tau)}\right)\chi_{[0,\infty)}(t)\,, t \in \mathbb{R}. \tag{5.13}$$

In Eq. 5.13, $\chi_{[0,\infty)}(t) = 0$ for $t < 0$ and $\chi_{[0,\infty)}(t) = 1$ for $t \geqslant 0$. The parameters A and B are positive, and so is τ. In particular the case is considered when $A \approx B^2$. In the case that $A = B^2$, the signal in Eq. 5.13 is admissible [113], [114] as a wavelet since then

$$\int_0^\infty \left(te^{-t/\tau} - \frac{1}{A}te^{-t/(B\tau)}\right) dt = \tau^2\left(1 - \frac{B^2}{A}\right) = 0. \tag{5.14}$$

From our experimental results in Table 10 it can be see that $A \approx B^2$ and thus our model can be considered as an admissible wavelet. In the next

section some mathematical properties of this wavelet will be presented. For computation purposes we may suppose $\tau = 1$, and consider:

$$x_{A,B}(t) := \left(te^{-t} - \frac{1}{A} te^{-t/B} \right) \chi_{[0,\infty)}(t)\,, t \in \mathbb{R}, \tag{5.15}$$

and the admissible cases

$$x_C(t) := \left(te^{-t} - C^2 te^{-Ct} \right) \chi_{[0,\infty)}(t)\,, t \in \mathbb{R}. \tag{5.16}$$

5.6 WAVELET CHARACTERISTICS

5.6.1 *Normalization and approximation by admissible wavelet*

We want to approximate a general $x_{A,B}$ by an admissible x_C. To that end

$$\int_0^\infty (x_{A,B}(t) - x_{D^{-1}}(t))^2 dt \tag{5.17}$$

is minimized ($D = C^{-1}$). We compute

$$\int_0^\infty (x_{A,B}(t) - x_{D^{-1}}(t))^2 dt = \frac{1}{4B} \left[s^2 - \frac{16sx}{(1+x)^3} + \frac{1}{x} \right] ,$$
$$s = \frac{B^2}{A} \approx 1\ ,\ x = \frac{D}{B} \approx 1\ . \tag{5.18}$$

There is the Taylor expansion

$$s^2 - \frac{16sx}{(1+x)^3} + \frac{1}{x} =$$
$$(s-1)^2 + \sum_{l=1}^{\infty} (1-x)^l \left\{ \frac{(l+1)(l-2)}{2^l} s + 1 \right\} =$$
$$(s-1)^2 + (x-1)(s-1) + (x-1)^2$$
$$-(x-1)^3 (\frac{1}{2}s + 1) + (x-1)^4 (\frac{5}{8}s + 1) + \dots\ . \tag{5.19}$$

The leading quadratic form in the last member of Eq. 5.19 can be written as

$$\left(x - 1 + \frac{s-1}{2} \right)^2 + \frac{3}{4}(s-1)^2 \tag{5.20}$$

and is minimal $\frac{3}{4}(s-1)^2$ when $x = \frac{3-s}{2}$. We are thus led to take $x = \frac{3-s}{2}$. Assuming A and B are known, we now have an expression for D (and C). Hence, we have an approximation x_C of $x_{A,B}$.

5.6.2 *Computations for x_C*

In this section an overview is given of some characteristics of x_C.

Energy

The energy $\|x_C\|^2$ is

$$\|x_C\|^2 = \int_0^\infty (te^{-t} - C^2 te^{-Ct})^2 dt = (1-C)^2 \frac{1+6C+C^2}{4(1+C)^3} \,. \tag{5.21}$$

Fourier transform

The Fourier transform $X_C(\omega)$ of x_C is given by:

$$\begin{aligned} X_C(\omega) &= \int_0^\infty (te^{-t} - C^2 te^{-Ct}) e^{i\omega t} dt \\ &= \left(\frac{1}{1-i\omega}\right)^2 - \left(\frac{C}{C-i\omega}\right)^2 \\ &= -2i\omega(1-C)\frac{C - \frac{1}{2}i\omega(1+C)}{(1-i\omega)^2(C-i\omega)^2} \,. \end{aligned} \tag{5.22}$$

Observe that $X_C(\omega) = 0$ at $\omega = 0$, which again shows that x_C is an admissible wavelet.

Admissibility constant

The admissibility constant C_{x_C} is computed as

$$\begin{aligned} C_{x_C} &= \int_{-\infty}^\infty |X_C(\omega)|^2 \frac{d\omega}{|\omega|} \\ &= \left(\frac{1-C}{1+C}\right)^2 \left\{ 2 - (1+4C+C^2)\frac{\ln C^2}{1-C^2} \right\} \,. \end{aligned} \tag{5.23}$$

This admissibility constant is required when one wants to invert the wavelet transform

$$f(\tau) \to CWT_{x_C}[f](t,a) = \frac{1}{\sqrt{a}} \int_{-\infty}^\infty f(\tau) x_C \left(\frac{t-\tau}{a}\right) d\tau \tag{5.24}$$

according to the inversion formula

$$f(\tau) = \frac{1}{C_{x_C}} \int_0^\infty \int_{-\infty}^\infty CWT_{x_C}[f] \left(\frac{\tau - t}{a}\right) \frac{da\, dt}{a^2\sqrt{a}} \,. \tag{5.25}$$

Vanishing moments

A further issue in Wavelet analysis is the desirability of vanishing moments. We compute for $k = 0, 1, ...$

$$\int_0^\infty t^k x_C(t)dt = (k+1)!\left(1 - \frac{1}{C^k}\right) \ ; \tag{5.26}$$

when $k = 0$ this vanishes for all C. When $k = 1, 2, ..$ this vanishes only when $C = 1$. In the latter case we have $x_{C=1} \equiv 0$. Therefore, except in the trivial case C=1, only the 0^{th} moment vanishes.

5.6.3 *Limiting case* $C \to 1$

As said, we have $x_C = 0$ when $C = 1$. Experimental evidence [31] shows that $C \approx 1$, hence we consider the renormalized wavelet $\frac{1}{1-C}x_C$, and in particular, its limit when $C \to 1$. There holds

$$\begin{aligned} x(t) &:= \lim_{C\to 1} \frac{1}{1-C} x_C(t) \\ &= -\frac{d}{dC}[te^{-t} - C^2 te^{-Ct}]_{C=1}\chi_{[0,\infty)}(t) \\ &= t(2-t)e^{-t}\chi_{[0,\infty)}(t) \ . \end{aligned} \tag{5.27}$$

More precisely, we have

$$\frac{1}{1-C} x_C(t) = x(t) + (1-C)te^{-t}R(t,C), \tag{5.28}$$

where

$$R(t,C) = -1 + (1+C)t + C^2\frac{1-(C-1)t - e^{-(C-1)t}}{(1-C)^2} \ . \tag{5.29}$$

Now there holds for this $R(t,C)$ that

$$R(t,C) = R(t) + \epsilon(t) = -1 + 2t - \frac{1}{2}t^2 + \epsilon(t) \ , \tag{5.30}$$

where the error $\epsilon(t)$ is of the order $\frac{1}{6}|1-C|t^3e^{|1-C|t}$ or less. For the leading behavior R of $R(t,C)$ we have

$$\begin{aligned} &\int_0^\infty te^{-t}R(t)dt = 0 \ ; \\ &-1 \leqslant R(t) \leqslant 1 \ , \ 0 \leqslant t \leqslant 4 \ . \end{aligned} \tag{5.31}$$

Next an overview is given, of some characteristics of $x(t)$. We compute

$$\|x\|_2^2 = \int_0^\infty (t(2-t)e^{-t})^2 dt = \frac{1}{4} , \tag{5.32}$$

$$\|x\|_1 = \int_0^\infty |t(2-t)e^{-t}| dt = \frac{8}{e^2} = 1.082682266 . \tag{5.33}$$

Furthermore, for the Fourier transform $X(\omega)$ of x we find

$$X(\omega) = \int_0^\infty e^{i\omega t} t(2-t)e^{-t} dt = \frac{-2i\omega}{(1-i\omega)^3} . \tag{5.34}$$

The spectral version of Eq. 5.28 and 5.29 reads

$$\frac{1}{1-C} X_C(\omega) = X(\omega) - 2i\omega(1-C)\frac{C - \frac{1}{2}i\omega + \frac{1}{2}\omega^2}{(1-i\omega)^3(C-i\omega)^2} . \tag{5.35}$$

The admissibility constant C_x of x is given by:

$$C_x = \int_{-\infty}^\infty |X(\omega)|^2 \frac{d\omega}{|\omega|} = 2 . \tag{5.36}$$

The wavelet transform of x, using x itself or the time-reversed signal x_- as wavelet are given by

$$\begin{gathered} CWT_x[x](t,a) = \frac{1}{\sqrt{a}} \int_{-\infty}^\infty x(\tau) x\left(\frac{t-\tau}{a}\right) d\tau = \\ \frac{e^{-t/a}}{a^2\sqrt{a}}[-2at(t-2)e_2(-\alpha,t) \\ +(2t^2 + (8a-4)t - 8a)e_3(-\alpha,t) - 12(t+a-1)e_4(-\alpha,t) \\ +24e_5(-\alpha,t)], \ t > 0 , \end{gathered} \tag{5.37}$$

while $CWT_x[x](t,a) = 0$ for $t \leqslant 0$. In Eq. 5.37 we have set

$$\begin{aligned} e_l(\beta,t) &= \frac{1}{\beta^l}\left(e^{\beta t} - 1 - \beta t - \ldots - \frac{(\beta t)^{l-1}}{(l-1)!}\right) \\ &= t^l \sum_{j=0}^\infty \frac{(\beta t)^j}{(j+l)!} \end{aligned} \tag{5.38}$$

which is to be read as $\frac{t^2}{1!}$ when $\beta = 0$ in accordance with the last member of Eq. 5.38. Also we have $\alpha = 1 - a^{-1}$ in Eq. 5.37. Furthermore we have

$$
\begin{aligned}
&CWT_{x_-}(t,a) = \frac{1}{\sqrt{a}} \int_{-\infty}^{\infty} x(\tau) x\left(\frac{\tau - t}{a}\right) d\tau = \\
&t \geqslant 0 \ : \ \frac{e^{-t}}{a^2\sqrt{a}} [-2a \left(\frac{a}{a+1}\right)^2 t(t-2) \\
&+ \left(\frac{a}{a+1}\right)^3 (2t^2 - (8a+4)t + 8a) \\
&+12 \left(\frac{a}{a+1}\right)^4 (t - a - 1) + 24 \left(\frac{a}{a+1}\right)^5] \, , \\
&t \leqslant 0 \ : \ \frac{e^{-t/a}}{a^2\sqrt{a}} [-2a^2 \left(\frac{a}{a+1}\right)^2 t(t+2a) \\
&+ \left(\frac{a}{a+1}\right)^3 (2t^2 + (8+4a)t + 8a) \\
&-12 \left(\frac{a}{a+1}\right)^4 (t + a + 1) + 24 \left(\frac{a}{a+1}\right)^5] \, .
\end{aligned}
\tag{5.39}
$$

We finally compute the moments of x as

$$
\int_0^{\infty} t^k x(t) dt = -(k+1)!k \, , \ k = 0, 1, .. \, , \tag{5.40}
$$

and this vanishes for $k = 0$ only.

5.7 COMPARISON TO OTHER WAVELETS IN LITERATURE

In this section, the new wavelet x, a smoothed version of x and its odd extension are compared to some wavelets described in literature.
Figure 21 shows the Cauchy wavelet and its Fourier transform [113].

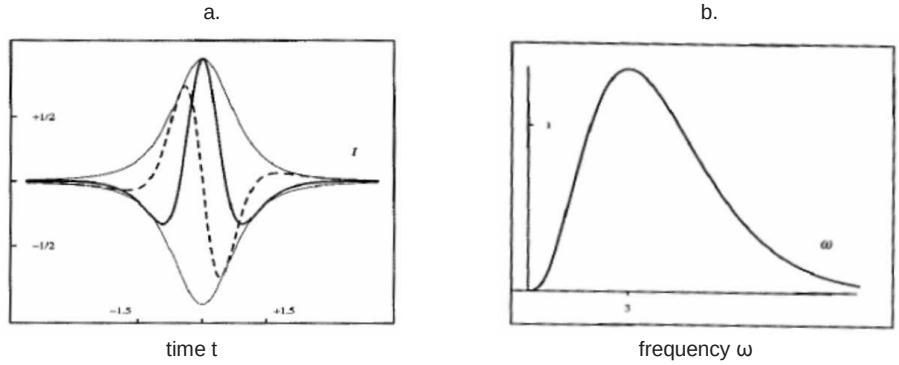

Figure 21: Cauchy wavelet $x(t) = \frac{1}{2\pi(1-it)^3}$ (imaginary part dashed), and its Fourier transform $X(\omega) = \omega^2 e^{-\omega}$, from [113].

Figure 22 shows the Bessel wavelet and its Fourier transform [113].

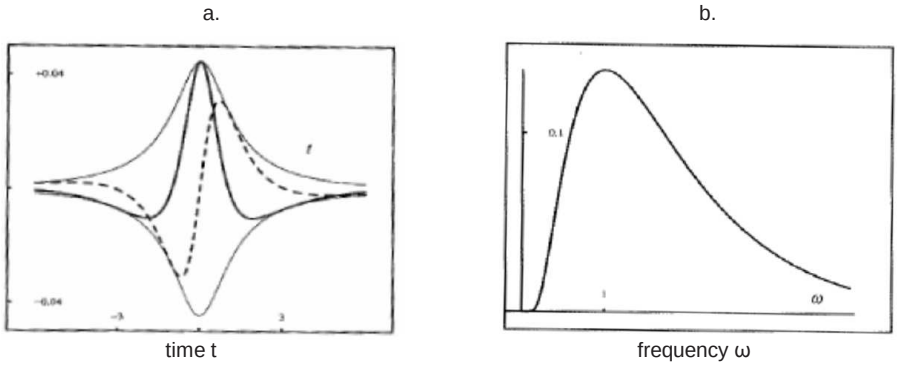

Figure 22: Bessel wavelet $x(t) = \frac{1}{\pi\sqrt{1-it}} K_1(2\sqrt{1-it})$ (imaginary part dashed), with K_1 a modified Bessel function of order 1, and its Fourier transform $X(\omega) = e^{-(\omega+1/\omega)}$, $\omega > 0$, from [113].

Observe that x is real, causal and of simple form so that relevant data concerning x can be computed analytically. Figure 23 shows the signal $x(t)$ and its Fourier transform $|X(\omega)|$ (solid lines). It can be seen that $|X(\omega)|$ decays rather slowly, roughly like $2/\omega^2$, as $\omega \to \infty$. This is due to the abrupt rise of $x(t)$ at $t = 0$.

In Fig. 23 (a) also a Gaussian window g is depicted (dashed line) by which x(t) is to be smoothed. The resulting spectrum $|X(\omega)G(\omega)|$ is depicted in Fig. 23 (b) (dashed line) and decays quite a bit faster. Smoothing $x(t)$ with a Gaussian g yields a non-causal signal; also, it is certainly not so that a

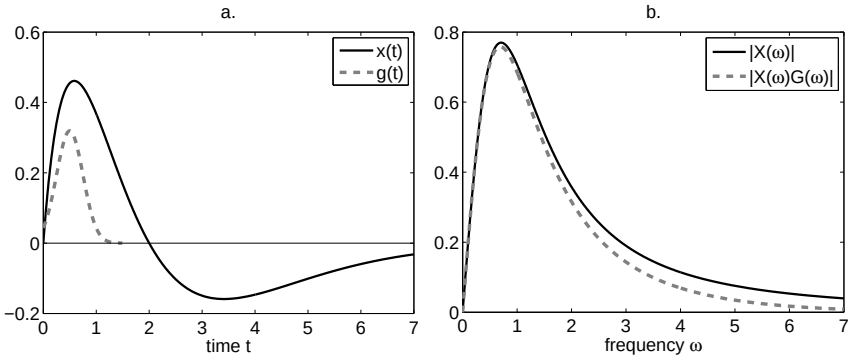

Figure 23: a. $x(t)$ and a Gaussian window g. b. $|X(\omega)|$, and $|X(\omega)G(\omega)|$.

Gaussian g is optimal and/or in complete agreement with physiology.

Odd extension of x

A different sort of modification is obtained when we consider the odd extension of x,

$$x_{odd} = x(t) - x(-t)\ ,\ t \in \mathbb{R}\ , \tag{5.41}$$

whose spectrum is given by

$$X_{odd}(\omega) = 2i\ \mathrm{Im}[X(\omega)] = 4i\frac{3\omega^3 - \omega}{(1+\omega^2)^3}\ , \omega \in \mathbb{R}\ . \tag{5.42}$$

Figure 24 shows $x_{odd}(t)$ and $|X_{odd}(\omega)|$. Note that x_{odd} looks quite similar to (the imaginary part) of certain wavelets that can be found in literature. Compared to $X(\omega)$, $X_{odd}(\omega)$ decays more rapidly, like $12/\omega^3$, as $\omega \to \infty$. Furthermore, $X_{odd}(\omega)$ has a peak value that is 1.5 times larger than the peak value of $X(\omega)$, and this peak value occurs at an ω that is more than 1.5 times larger than the ω at which $X(\omega)$ has its peak value.

5.8 APPLICATION TO CLINICAL DATA

Figure 25 shows three visual representations of the wavelet transform of a modeled myoclonic seizure, using x as a model and two accelerometric patterns from clinical data that are associated with a myoclonic seizure and an other movement. The wavelet used is the time reversed version of x (matched wavelet).

For the myoclonic seizure, the coefficients with the highest values lie in the

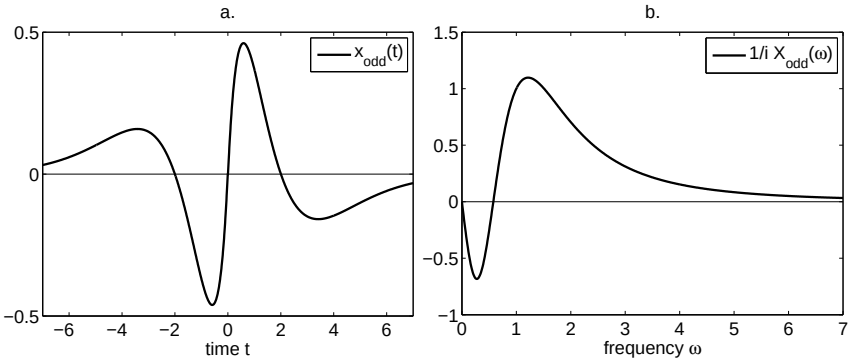

Figure 24: $x_{odd}(t)$ and $\frac{1}{i}X_{odd}(\omega)$.

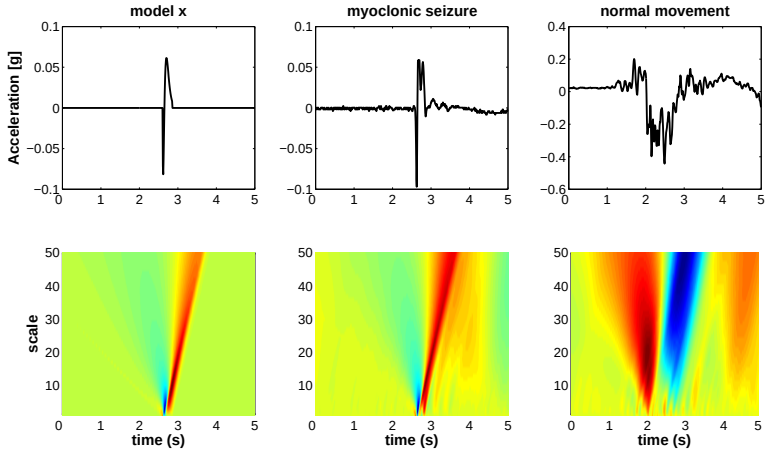

Figure 25: Wavelet transform of x, an accelerometric pattern that is associated with a myoclonic seizure, and an accelerometric pattern that is associated with a movement that is not a myoclonic seizure.

2–8 range of scales. This agrees with the findings presented in [31]. Similar behavior can be observed between the modeled myoclonic seizure and the real myoclonic seizure. In the scalogram of the other movement we see high values at high scales. This example shows that it is possible to distinguish between myoclonic seizures and other movements using the wavelet presented in this chapter.

5.9 DISCUSSION

This chapter presents an analytical model for accelerometric patterns associated with arm movements during myoclonic seizures. The model output is compared to real patient accelerometer data from six patients. The values of the model parameters tuned to real seizures are physiologically feasible. Eight out of ten myoclonic seizures have a good fit to the model (correlation coefficient > 0.7). The ACM-pattern associated with myoclonic seizures is typical [30], although some myoclonic seizures are somewhat longer in duration and have a more repetitive pattern (No. 4, 6, and 9). Maybe in these cases the neural input modeled as a pulse does not yield, but the input should be represented by a series of pulses. This corresponds with the fact that a myoclonic seizure can have either a spike and wave correlate in the EEG or a poly-spike and wave correlate [7]. Using mean parameter values leads to agreeable fits in six out of ten myoclonic seizures. The results imply that some of the parameters might be robust for patient and seizure variability. Further research will be done, with larger amounts of data to refine and optimize these findings.

By choosing other types of stimuli for an input, the model has the possibility to be extended for other types of simple motor seizures (clonic and tonic seizures). Clonic seizures consist of repeated myoclonic contractions that regularly recur at intervals between 0.2 and 5 times per second [3]. They have series of (poly)spike-wave patterns as an EEG-correlate. The ACM-pattern is rhythmic and the limbs show repetitive jerking. Tonic seizures consist of sustained muscle contractions, and the EEG shows fast frequency activity. The ACM-pattern has a typical block-like shape.

The presented analytical model can be helpful for feature extraction for detection of myoclonic waveforms from ACM-signals. The model can be used to study important characteristics of accelerometric waveforms during myoclonic seizures. It contributes to a better understanding of the patterns that are observed in the ACM-recordings, and the model makes it possible to derive parameters from the ACM-signal that have a physiological meaning. Therefore this model-based approach can contribute to a solid detection of myoclonic seizures. Furthermore a new wavelet, based on an analytical description for accelerometric patterns associated with myoclonic seizures has been introduced. Explicit computations are feasible for the frequency response $X(\omega)$, the admissibility condition and admissibility constant, the wavelet transform of x itself using x or its time-reversed version x_- (matched filter) as analyzing wavelet. The new wavelet, a Gaussian smoothed version of it, and the odd extension of it, have similar appearances as wavelets known in literature. It seems possible to distinguish between myoclonic seizures and other movements using the wavelet presented in this chapter. Thus the wavelet has potential in the detection of myoclonic seizures from accelerometric data of arm movements of epileptic patients.

6

TIME-FREQUENCY ANALYSIS OF ACCELEROMETRY DATA FOR DETECTION OF MYOCLONIC SEIZURES

This chapter is submitted to IEEE Transactions on Information Technology as:
T.M.E. Nijsen, R.M. Aarts, P.J.M. Cluitmans, and P.A.M. Griep. Time-frequency analysis of accelerometry data for detection of myoclonic seizures [27].

6.1 ABSTRACT

A newly introduced model based matched wavelet transform (MOD) is studied for its ability of detecting myoclonic seizures from accelerometric (ACM) data. MOD is especially designed for myoclonic waveforms in ACM-signals. This model based wavelet is compared to three other time-frequency methods: the short-time Fourier transform (STFT), the Wigner distribution (WD), and the continuous wavelet transform (CWT) using a Daubechies wavelet. Real patient data are analyzed using these four time-frequency measures. To obtain quantitative results, all four time-frequency methods are evaluated in a linear classification setup. Data from 15 patients are used for training and data from 21 patients for testing. Using features based on the CWT and MOD the succes rate of the classifier was 80%. Using STFT or WD based features, the classification succes is less. Analysis of the false detections revealed that they were either clonic seizures, the onset of tonic seizures, or sharp peaks in 'normal' movements indicating that the patient was making a jerky movement. The results show that both CWT and MOD are useful for detection of myoclonic seizures. On top of that, MOD has the advantage that it consists of parameters that are related to seizure duration and intensity that are physiological meaningful. Furthermore, in future work, the model can also be useful for the detection of other motor seizure types.

6.2 INTRODUCTION

Epilepsy is a common neurological disorder that is characterized by recurrent seizures, that are caused by hypersynchronous neuronal activity in the brain. The clinical signs of seizures depend upon the location and extent of the propagation of the discharging cortical neurons. Previously we reported the potential value of accelerometry (ACM) for detecting seizures that have movement as the most important clinical manifestation, so called *motor* seizures [30]. It was found that 95% of the motor seizures consisted of characteristic elementary patterns. These elementary patterns can be divided into three

groups: myoclonic, clonic and tonic patterns. It was found that 74% of the motor seizures detected, consisted of at least one myoclonic element. Myoclonic seizures are brief, shock-like jerks of a muscle or a group of muscles. Muscles of the face, the neck, shoulders, and arms can be involved. During a myoclonic seizure, the electrical activation of the muscles involved lasts less than 50 milliseconds [7]. It is of clinical importance to detect these subtle seizures. Often a patient has many myoclonic seizures during the night and thus the sleep pattern can be disturbed. Severe motor seizures are often preceded by myoclonic seizures and thus the detection of myoclonic seizures could be used for early warning. Counting myoclonic seizures may also be an important measure for successful medical treatment, especially in patients that do not become seizure free after medical treatment.

This chapter presents a first approach for the detection of myoclonic patterns from accelerometric data. The purpose of the methods under study, is to support off-line analysis for diagnostic and evaluation purposes. In our detection setup, a supervised learning approach, which requires choosing appropriate features and a classifier, is used.

Experience from more explored research areas, such as speech and audio, shows that the success of classification critically depends on the choice of features and much less on the complexity of the type of classifier [28]. Therefore we focus on the study of suitable features rather than on classification methods. In ACM-literature the choice for features depends on the type of activities that are to be detected. For distinguishing between normal daily activities, such as sitting, standing, lying, and movement in general, statistical properties of the amplitude of the signal such as mean and standard deviation seem to be effective [14]. When distinguishing between various complex movement patterns, features derived from time-frequency measures such as the short-time Fourier transform [20], or a wavelet transform [16] are also applied.

Seizure detection literature dominantly describes seizure detection based on the EEG-signal. Seizure detection based on the ACM-signal is new and new detection algorithms need to be developed. From EEG-based detection methods we can learn that features based on morphological features (such as amplitude and duration of a waveform and frequency) and wavelet based features are successful to detect the sharp peaks and rhythmic discharges that occur in the EEG-signal during epileptic seizures [59],[29].

Myoclonic seizures may be very subtle movements, and the amplitude in the ACM-signal during such a seizure can be very low. Nevertheless, a small transient can be visible in the signal, a short 'shock-like' pattern. A model was developed that describes the accelerometric output during a myoclonic seizure [32]. In this chapter this model is used to formulate a matched wavelet transform. This matched wavelet transform is used to derive features for the detection of myoclonic seizures. Furthermore in this work three other time-frequency measures are studied if they are suitable to derive salient features for seizure detection. A comparison is made between the short-time Fourier

transform, the continuous wavelet transform, and the Wigner distribution. All four feature sets are evaluated in a discriminant analysis setup on clinical data.

6.3 ACCELEROMETRIC WAVEFORMS

A myoclonus can affect muscles throughout the body but often only one limb is involved, in most cases the arm. Figure 26 shows examples of ACM-data during myoclonic seizures and other movements measured on the arm. A myoclonic seizure is a twitch like contraction of an antagonistic muscle pair. Flexion is dominantly innervated over extension, so the involved limb flexes during the seizure. After the seizure the limb suddenly stops. This suddenly stopping results in a sharp peak in the ACM-signal. Waveforms associated to myoclonic seizures have a short duration (0.5–2 s), are asymmetric and seem to damp out exponentially at the end. They can occur isolated (Fig. 26 A) or in a sequence of other movement patterns (Fig. 26 B). Normal movements have various appearances. Slow movements cause a block-shaped pattern in the ACM-signal (Fig. 26 C). Rhythmic or jerky movements can cause sharp peaks in the ACM-signal (Fig. 26 D).

6.4 MODEL FOR MYOCLONIC ARM MOVEMENTS

A model was developed that describes the ACM-output —measured on the arm— during myoclonic seizures [32]. The model description consists of a mechanical part and a electrophysiological part. The electrophysiological part contains the definition of stimuli and a muscle response to these stimuli during the myoclonic seizure. The mechanical part is based on kinematic and kinetic relations for the lower arm modeled as a rigid body system. This part contains rigid body parameters that can be linked to body mass and body length. In the model one agonistic muscle pair is included that is synchronously innervated during the seizure [7]. The ACM-pattern $X(t)$ in the dominant movement direction, observed during a myoclonic seizure can be analytically expressed by:

$$X(t) = K\left(te^{\frac{-t}{\tau_0}} - \frac{t}{A}e^{\frac{-t}{B\tau_0}}\right)\chi_{[0,\infty)}(t)\,, t \in R, \tag{6.1}$$

where constant $K = \frac{0.66}{BM\ BL}\frac{F_0}{\tau_0}$, F_0 represents the intensity of muscle contraction, the relaxation time τ_0 is related to the duration of muscle contraction, BM represents the full body mass, and BL represents the full body length, A and B are dimensionless constants. Both A and B are > 1. In this way an alternating positive and negative net muscle movement is generated that is necessary to generate the typical myoclonic 'shock-like' pattern. In Eq. 6.1, $\chi_{[0,\infty)}(t) = 0$ for $t < 0$ and $\chi_{[0,\infty)}(t) = 1$ for $t \geqslant 0$.

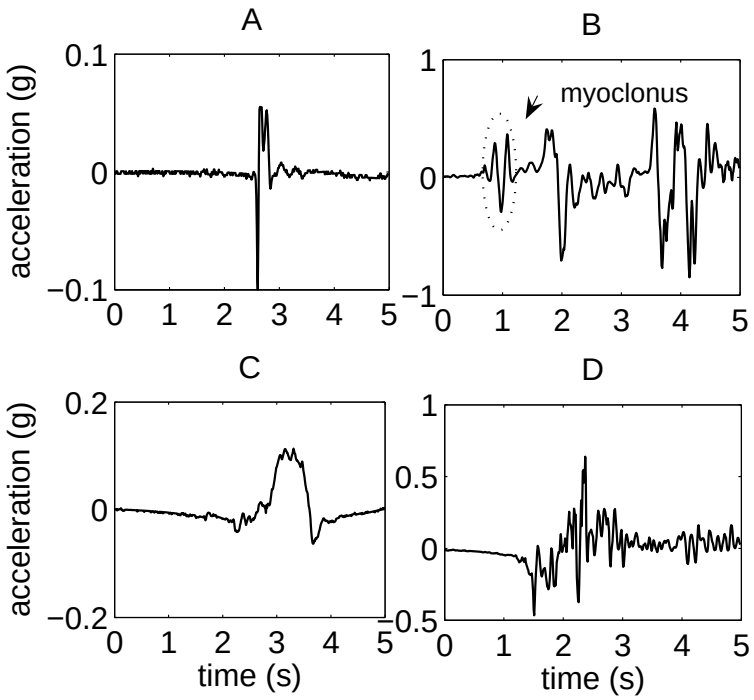

Figure 26: A. An isolated myoclonic waveform. B. Myoclonic waveform in sequence with other pattern. C Slow movement. D Non-myoclonic waveforms containing sharp peaks.

Figure 27 shows this model fitted to an accelerometric waveform associated to a myoclonic seizure. In a previous study it was shown that the values of τ_0 varied between 20 and 70 ms, and that this corresponds to physiological values of motor units of a muscle responding to a twitch [32].

6.5 TIME-FREQUENCY METHODS

This section describes four different time-frequency measures that will be used to analyse accelerometric waveforms. One of them is based on the model described in section 6.4.

6.5.1 *Short-time Fourier transform*

For the short-time Fourier transform (STFT) of signal f, the signal is multiplied by a window function h and then the Fourier transform of the product function is taken [115]. By translating the window along the signal, the STFT

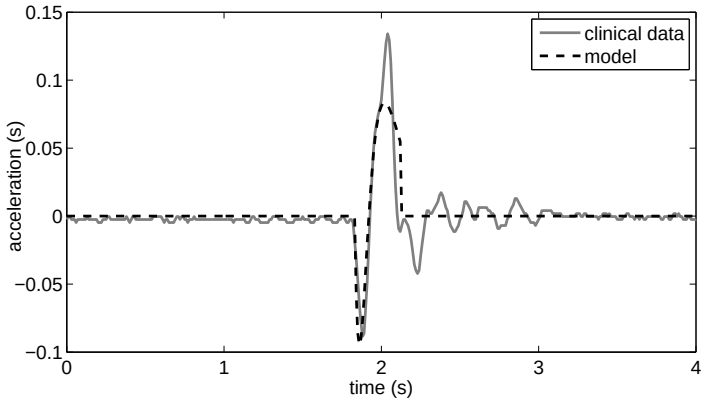

Figure 27: Model fitted to real seizure waveform.

is able to analyse the frequency behavior of f during the time interval for which h is localized.

$$\mathrm{STFT}_h[f](t,\omega) = \frac{1}{\sqrt{2\pi}} \int_{-\infty}^{\infty} f(\tau) h^*(\tau - t) e^{-i\omega\tau} d\tau \,. \tag{6.2}$$

As output the spectrogram is estimated as in (6.3).

$$\mathrm{SP}_h[f](t,\omega) = |\mathrm{STFT}_h[f](t,\omega)| \,. \tag{6.3}$$

For $h(t)$ a Hanning window is chosen, since this is often used with good results. A myoclonic seizure can last shorter than one second, therefore a large time resolution is desirable. The sample frequency of the ACM-signals used is 100 Hz, this limits the choice for a window length. A window length of 50 samples is chosen. This corresponds to a frequency resolution of 2 Hz. A shift of one sample with the STFT is chosen. A disadvantage of using the STFT for myoclonic seizure detection is the trade off between time and frequency resolution.

6.5.2 *Wigner distribution*

The Wigner distribution (WD) is a quadratic energy distribution, which distributes the energy of the signal over the time and frequency variables without windowing. This windowing limits the resolution of the time-frequency decomposition in case of the STFT and the CWT [115]. To our knowledge the application of this technique to ACM-signals is new in literature.
It is known that the Wigner distribution, among other favorable properties, achieves the best results in terms of spread in the time-frequency plane, compared to other quadratic time-frequency distributions that belong to the same

class [116].
For the WD, the Fourier transform is taken of the product of a signal f with a translated version of itself ($*$ denotes the complex conjugation):

$$WD[f](t,\omega) = \frac{1}{\sqrt{2\pi}} \int_{-\infty}^{\infty} f(t+\frac{\tau}{2}) f^*(t-\frac{\tau}{2}) e^{i\omega\tau} d\tau \,. \tag{6.4}$$

In contrast to the STFT and the CWT, the WD is a nonlinear operation. An advantage of the WD is that there is a good time-frequency resolution. Since the WD is an energy distribution a link can be made to mechanical energy, that is expected to be different between normal movements and epileptic movements. A disadvantage is that artefacts occur when multi-component signals are analyzed, because of the quadratic character of the distribution. These artefacts are known as cross-terms. These cross-terms can interfere with the actual signal terms and make it difficult to interpret the time-frequency plot. To avoid interference terms between positive and negative frequencies the signal is transformed to its analytical version [117].

6.5.3 *Continuous wavelet transform*

The continuous wavelet transform (CWT) of a signal $f(t)$, at the scale a and position t is defined as:

$$CWT_h[f](t,a) = \frac{1}{\sqrt{a}} \int_{-\infty}^{\infty} f(\tau) h^* \left(\frac{t-\tau}{a} \right) d\tau \,, \tag{6.5}$$

where $h(t)$ is the wavelet base and $*$ denotes the complex conjugation [115]. While the STFT uses a single analysis window, the wavelet transform uses short windows for analyzing high frequencies and long windows for analyzing low frequencies. As the scale changes, the wavelet is localized better in time, but worse in frequency and vice-versa. Nevertheless the use of various scales seems appropriate since movements can have various durations and intensities and thus take place on various scales. Furthermore, the shape of the pattern observed during a myoclonic seizure resembles a wavelet. A disadvantage of using the CWT for myoclonic seizure detection could be the bad time localization at higher scales. As output, the absolute wavelet coefficients are plotted in a scalogram:

$$SC_h[f](t,a) = |CWT_h[f](t,a)| \,. \tag{6.6}$$

The output is calculated for scales 2–256. This choice is made because the lower boundary for frequencies in normal movements is approximately 0.3 Hz [94]. The scale of 256 corresponds to a frequency of 0.26 Hz. A wavelet base is used, that is suitable for the signal pattern of interest. Therefore the fifth member of the Daubechies wavelet is used.

6.5.4 *Model based matched wavelet transform*

Based on Eq. 6.1 a matched wavelet transform can be defined. In this case the wavelet base $h(t)$ is formed by:

$$h(t) = t(e^{-t} - \frac{1}{A}e^{\frac{-t}{B}})\chi_{[0,\infty)}(t)\ , t \in R. \tag{6.7}$$

This function satisfies the admissibility condition if $A = B^2$, see [33] for more details.
In a previous study, where the model is fitted to clinical data, it is shown that this condition is met [32]. From this study the value 1.023 for B is obtained. For the matched wavelet transform, the wavelet transform is performed with a time reversed version of $h(t)$. In this case the highest value occurs when the signal waveforms matches the model best. Scale a is proportional to τ_0. Scale 1 corresponds to a value of τ_0= 10 ms. It was found that the values for τ_0 in a myoclonic seizure vary between 20 and 70 ms, therefore scale 2 to 7 are important for the analysis of myoclonic seizures. For the distinction between other movements that are longer in duration also the higher scales are important, therefore in our analysis we include scales up to 50. As output, again, the absolute wavelet coefficients are plotted in a scalogram.

6.6 PATIENT DATA

For analysis and evaluation ACM-data are used from 36 mentally retarded patients who suffer from refractory epilepsy. The patients are monitored with the setup described in our previous clinical study [30], with five 3-D sensors placed on the limbs and the sternum. The sampling frequency f_s of the ACM-signals is 100 Hz. For each patient at least one and maximal three video fragments per seizure type (myoclonic, tonic, clonic) are selected. In these fragments the patients should be in the scope of the camera. This resulted in 156 video fragments with a total duration of 3.6 hours. Three experts divided the corresponding ACM-signals into classes using both video and accelerometric information. Available classes were: no movement, myoclonic seizure waveform, tonic seizure waveform, clonic seizure waveform, normal movement, and unclear. For the evaluation study, only events where two experts agreed on were selected. Events marked as 'unclear' were also excluded from the evaluation. In total 30 minutes of data were excluded.
The four time-frequency methods are tested for their suitability to detect myoclonic seizures in a linear discriminant setup. Therefore the data are divided into a training and a test set. We aim for an approach that is robust among patients. Therefore the training data consists of data from other patients than the test data. For training, data from the first 15 patients are used (100.17 minutes). For testing data from the other 21 patients are used (79.2 minutes). The composition of these data sets is listed in Table 11.

Since our model-based approach is based on a model for arm-movements,

Table 11: Composition of Train- and Test data

A. Train data

TYPE	NUMBER OF EVENTS	TOTAL DURATION (MIN)	MEAN DURATION (MIN)
no movement	116	56.2	0.48
movement	72	32.8	0.46
myoclonic	29	0.89	0.03
tonic	39	8.38	0.21
clonic	13	1.9	0.15

B. Test data

TYPE	NUMBER OF EVENTS	TOTAL DURATION (MIN)	MEAN DURATION (MIN)
no movement	98	50.7	0.52
movement	39	20.3	0.52
myoclonic	35	1.1	0.03
tonic	30	4.8	0.16
clonic	7	2.3	0.32

only data from the arm-sensors are included. From the six arm-sensors automatically the sensor is chosen on which the movement has the highest amplitude. The included sensor therefore can vary per patient and per seizure. From video observations is known that during a myoclonic seizure, in most cases the x-direction is the most dominant movement direction. The characteristic waveform is most clearly visible and has the highest amplitude in this direction. This hypothesis was confirmed with a statistical analysis, where myoclonic data of all the six sensors were analyzed with histograms.

6.7 TIME-FREQUENCY ANALYSIS ACCELEROMETER PATTERNS

6.7.1 *Myoclonic waveforms*

Figure 28 shows time-frequency and time-scale representations that are typical for ACM-patterns associated with myoclonic seizures. The original ACM-signal that belongs to this output is depicted in Fig. 26 A. There is a clear distinct area in the spectrogram of the STFT. The frequencies where most of the power is concentrated lie for all seizures in a range of 4–6 Hz. In the plot of the WD, there is also a distinct area, but there are more high frequencies present. The frequencies where most of the power is concentrated varies from 5–8 Hz. For the scalogram of the CWT the observations are similar, the coefficients with the highest values lie in the 8–60 range of scales. The scale where the coefficients are maximal lies for all the seizures in a range of 9–39. For the scalogram of the MOD, the coefficients with the highest values lie in the 2–8 range of scales. This corresponds to the findings presented in [32].

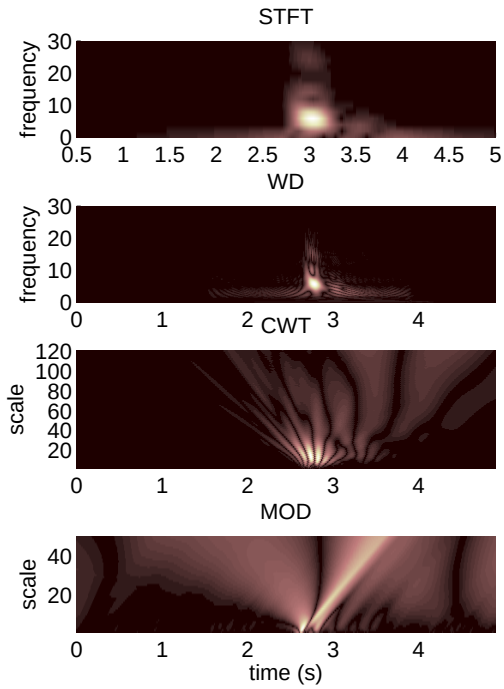

Figure 28: Time-frequency representations of myoclonic pattern. During the seizure, there is an isolated area with high values visible in each plot.

6.7.2 *Normal movements*

Figure 29 shows a typical output for normal movements. The original ACM-signal that belongs to this output is depicted in Fig. 26 C. Most of the power in the spectrogram is concentrated beneath 2 Hz. In the case of the WD, the frequency resolution is better and the main power is concentrated beneath 0.8 Hz. In the scalogram of the Daubechies wavelet, the highest values occur in the scales ranging from 74–256. For the model based wavelet the range is 10–50. For normal movements that are more rhythmical and contain sharper peaks it was observed that in the spectrogram high power values up to 30 Hz occur. For the WD, there is a noisy pattern visible, containing a lot of frequencies (interference). In the scalograms high coefficient values occur also in the lowest scales. Thus these sharp peaks seem to differ from the peaks in myoclonic seizures. They have a broader frequency pattern, more like a pulse. They have higher wavelet coefficients at lower scales, also more like a pulse. Whereas myoclonic seizures have a more isolated frequency pattern

(4–10 Hz) and higher wavelet coefficients in an isolated range of scales 8–60 or 2–8 depending on the wavelet used.

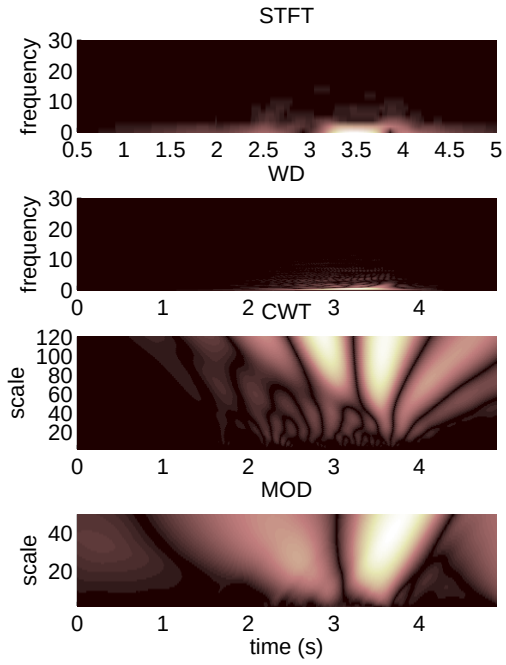

Figure 29: Time-frequency representations of normal movement. For STFT and WD, most of the power is concentrated in the lowest frequency band. For CWT and MOD we see high powers in the higher scales (low frequencies).

6.8 EVALUATION OF TIME-FREQUENCY FEATURES IN DETECTION SETUP

6.8.1 *Detection setup*

To evaluate their value for the detection of myoclonic seizures, for each time-frequency measure, the spectral powers or absolute wavelet coefficients are tested as features in a 'two-class' detection setup. The two classes are: 'myoclonic seizure', and 'other'. Hence, tonic, clonic, no movement and normal movements are regarded as one class. The choice for only two classes can cause that some of the false detections are actually one of the two other motor seizure types. In the future, however, we aim for a detection setup that consists of a number of 'two class' modules, each module for a specific movement type. Eventually, all the modules together will provide a detection

system consisting of more classes.
As classification method Fisher's linear discriminant analysis is used [118]. This is a classification method that projects the multi-dimensional feature space onto one line. The projection maximizes the distance between the means of the two classes while minimizing the variance within each class. Classification is performed in the one-dimensional space that is thus created. The performance per feature set is expressed in the percentage of myoclonic seizures correctly classified (SEN), the number of false detections (FD), the positive predictive value (PPV), which is the ratio between correct detected myoclonic seizures and all events that are classified as a myoclonic seizure, and the specificity (SPEC), that is the percentage of the data without myoclonic seizures that is correctly discarded. Detected events are defined in a similar way as in [31], but in this case the time-basis is 0.1 second instead of one second.

6.8.2 *Detection Results*

Table 2 shows the performance for each feature set. Highest sensitivities (SEN) are seen with the continuous wavelet transform (CWT) and the model based matched wavelet (MOD). The sensitivity of the Wigner distribution (WD) is poor. The performance of the short-time Fourier transform (STFT) is in between the results of the wavelet methods and the Wigner distribution. All

Table 12: Detection performance for each feature set

FEATURE SET	SEN	PPV (FD)	SPEC
STFT	0.71	0.16 (136)	0.89
WD	0.34	0.15 (67)	0.93
CWT	0.80	0.16 (148)	0.87
MOD	0.80	0.15 (155)	0.85

four methods have a similar value for the PPV. Specificity (SPEC) obtained using these methods varies between 85 and 93 %. These are the percentages of data without myoclonic seizures that are discarded correctly. Table 13 shows the number of false detections and total duration of the false detections per movement type. Here can be seen that STFT, CWT and MOD detect all the clonic seizures in the data set. WD detects 5 out of 7 clonic seizures. Furthermore some of the false detections are at the onset of a tonic seizure. Most of the false detections are in the normal movement periods. The analysis of these patterns reveals that these events are sharp peaks in normal movements, that occur during a jerky movement or when the patients arm bumps into a

surrounding object. Slow normal movements are successfully distinguished from myoclonic motor activity.

Table 13: False detection number and total duration per movement type

	STFT		*WD*	
Movement type	number	total duration (min)	number	total duration (min)
movement	91	4.6	45	3.6
no movement	26	1.3	9	0.4
tonic	12	0.5	8	0.35
clonic	7	2.1	5	1.5
	CWT		*MOD*	
Movement type	number	total duration (min)	number	total duration (min)
movement	92	6.0	101	6.8
no movement	37	1.5	35	1.6
tonic	12	0.61	12	0.66
clonic	7	2.2	7	2.2

6.9 DISCUSSION

Accelerometric signals measured in patients with epilepsy are analyzed using the short-time Fourier transform (STFT), the Wigner distribution (WD), the continuous wavelet transform (CWT), and a newly introduced model based matched wavelet transform (MOD). ACM-waveforms associated with myoclonic seizures have similar time-frequency characteristics across all patients. During myoclonic seizures most of the spectral power is in the 4–10 Hz range and there is an isolated area visible in time-frequency representations of both the STFT and the WD, although there are more interference patterns visible in the case of the WD. For the CWT and MOD there is also a clear isolated area of coefficients with high values at scales 8–60 and 2–8 respectively. Normal movements have most of their spectral power in the 0–2 Hz range in the spectrogram of the STFT. For the WD (that has a better frequency resolution) the range is 0–0.8 Hz. For the CWT, the wavelet coefficients have the highest values in the scales above 74 and for MOD most of the power is in the scales above 10. In normal movements sometimes also more rhythmical sharper waveforms occur but then still there are differences visible with the myoclonic pattern. The sharp peaks in normal movements have a broader frequency pattern (up to 30 Hz), and they have higher wavelet coefficients at lowest scales.

Our quantitative results show that it is possible to distinguish between myo-

clonic seizures and other movements. Sensitivities of both wavelet based methods are higher compared to the other two methods.
Using the STFT leads to a sensitivity of 71 % but PPV is 0.16. There were 136 false detections detected. This is mainly caused by the fact that most of the difference between the movement types occurs in the 0–2 Hz frequency band, and for the STFT this is just one bin. The WD performs poorly, only 34% of the myoclonic seizures is detected. The PPV is 0.15 and 67 false detections were detected. This poor performance could be caused by the cross-terms that are introduced by the WD. In literature much can be found about solutions to decrease the contribution of these cross-terms [119]. Applying such a solution could contribute to a valuable set of features.
Using the CWT leads to a sensitivity of 80% with a PPV of 0.16 and 148 false detections. The model based method MOD has a similar performance with a sensitivity of 80%, a PPV of 0.15 and 155 false detections.
As we can see all the methods have a similar PPV, and both wavelet methods, CWT and MOD, have the best sensitivity for detecting myoclonic seizures. The purpose of the methods under study, is to support off-line analysis for diagnostic and evaluation purposes. The total duration of all false detections together varies per method between 5.8 and 11.3 minutes. The total amount of data in the test set was 79.2 minutes and 1.1 minutes of these data were actual myoclonic seizures. In this perspective, the amount of data that needs further analysis is considerably reduced. After analysis of the false detections, it is observed that some of the false detections were actual motor seizures.
STFT, CWT and MOD detected all clonic seizures in the set. The WD detected 5 of the 7 clonic seizures. By definition clonic seizures consist of myoclonic jerks recurring at a regular repetition rate [3]. The clonic events are longer in duration and the ACM-amplitude is higher than during a myoclonic seizure. Therefore on forehand, we decided to treat them as two different classes. Nevertheless these results imply that similar features can be used for the detection of clonic patterns. This will be a topic for further research.
Tonic seizures are more block-shaped in appearance, more like slow normal movements, but in some cases also a false detection was seen at the onset of a tonic seizure. This corresponds with findings of a clinical study that shows that 67% of the tonic seizures in that study started as a myoclonic seizure but evolved into a tonic seizure [30].
The majority of the false detections were sharp peaks during normal movements. Slow normal movements are never falsely detected. This could be expected since the analysis results showed that slow movements have very distinct characteristics from myoclonic patterns. Sharp peaks on the other hand resemble myoclonic seizures. In our analysis we observed some difference in the higher frequencies and lowest scales but our experimental results in this stage do not confirm this observation. In future work we could focus on features that distinguish between sharp peaks in normal movements and myoclonic seizures.

The results obtained for CWT and MOD are similar, but an advantage of our newly introduced model is that it contains parameters that have a physiological meaning. It was especially designed for the detection of myoclonic seizures. In this setup we used 50 scales and obtained similar results as with the CWT using 255 scales. For both methods this large number of scales is not ideal. From the analysis is section 6.6 it can be observed that mainly the lower scales and the highest scales are important. Therefore future work will also focus on the optimization of the number of features.
Finally, in the future our detection algorithm can be incorporated, along with other modules in a system that can also be used for a real-time alarm system. The audio-triggered alarm system that is currently used in our institute detects seizures with a sensitivity $< 30\%$ and positive predictive value (PPV) $< 5\%$ [92], can then be improved significantly.

6.10 CONCLUSION

This chapter compares a newly introduced model based matched wavelet (MOD) with the short-time Fourier transform (STFT), the continuous wavelet transform (CWT), and the Wigner distribution (WD) for detecting myoclonic seizures in accelerometric (ACM) data. The choice for time-frequency measures was made because of the nonstationary character of the patterns of interest. To our knowledge this is the first attempt to detect myoclonic seizures based on accelerometric recordings. This chapter demonstrates that time-frequency measures can contribute to the detection of myoclonic waveforms from accelerometry data from epilepsy patients. Especially wavelet based features are able to detect the seizures with a high sensitivity. An extra advantage of our model based matched wavelet is that it consists of parameters that are related to seizure duration and intensity and are physiological meaningful. Also the model can be adapted so that it is useful for other motor seizure types. Hence, our model based matched wavelet is a promising tool for the detection of myoclonic seizures from accelerometric signals, and may be extended to make part of a real-time alarm system.

7

AUTOMATED DETECTION OF TONIC SEIZURES USING 3-D ACCELEROMETRY

7.1 ABSTRACT

In this chapter a first approach is presented for the detection of ACM-patterns associated with tonic seizures. Tonic seizures are a type of motor seizures where the muscles go into tetanic contraction. In contrast to other motor seizures, during tonic seizures the patient is not moving much, nevertheless the muscles are heavily contracting. In ACM-signals a tonic seizure is characterized by a block-like pattern that indicates a slow change of posture. On top of this block-like pattern a small tremor is visible. First it is shown that during tonic seizures the typical ACM-pattern is mainly caused by change of position towards the field of gravity and that the acceleration caused by movement is negligible. To this end a mechanical model of the arm and physiological information about muscle contraction during tonic seizures are used. Then for the dominant arm sensor, six features are computed that represent the main characteristics of ACM-patterns associated with tonic seizures. Linear discriminant analysis is used for classification. For training and evaluation the algorithm ACM-data are used from mentally retarded patients with severe epilepsy. It was possible to detect tonic seizures with a success rate around 0.80 and with a positive predictive value (PPV) of 0.35. A PPV of 0.35 implies that one out of three alarms is genuine. For off-line analysis this is acceptable, especially when 42 % of the false alarms are actually motor seizures of another type. The missed seizures, were not clearly visible in the ACM-signal. For these seizures additional ACM-sensors or a combination with other sensor types might be necessary. The results show that our approach is useful for the automated detection of tonic seizures and that it is a promising contribution in a complete multi-sensor seizure detection setup.

7.2 INTRODUCTION

Epilepsy is a neurological disorder that expresses itself in recurrent seizures that temporarily impair brain function. The seizures are caused by hypersynchronous neuronal discharges in the brain. Most of the people with epilepsy can be treated successfully, with drug therapy or neurosurgery. Still, 25% of the people affected can not be treated and have recurrent seizures [1]. A large part of this group of refractory patients, is also mentally retarded. A large number of these people is institutionalized. In these cases, seizure detection

is important for the management of daily care. Information about seizure frequency can be used to evaluate treatment effects and detections can be used to trigger an alarm during severe seizures that require medical assistance. It is known that in mentally retarded subjects, seizures often manifest themselves in movements [91]. Therefore in mentally retarded subjects it is feasible to use accelerometers (ACM) for automated detection of epileptic seizures [30]. The clinical manifestations of seizures depend upon the location and extent of the propagation of the discharging cortical neurons. When the motor cortex is involved this results in seizures that express themselves with movement, so called *motor* seizures [3]. When the intensity of this stimulation is high, the muscles can go into tetanic contraction [10]. This happens during a tonic seizure or during the tonic phase of a tonic clonic seizure. In a previous clinical study, we found that 64% of all the motor seizures in our population consisted of a tonic element [30]. In contrast to other motor seizures, during tonic seizures the patient is not moving much, nevertheless the muscles are heavily contracting. In ACM-signals a tonic seizure is characterized by a *block-like* pattern, that indicates a slow change of posture. On top of this block-like pattern a small tremor can be visible. Figure 30 A. shows a tonic seizure. Figure 30 B. shows a tonic-clonic seizure. The block-like change of posture is very subtle and short and it evolves into a clonic phase with a higher amplitude and frequency. Figure 30 C. and D. show two examples of non-epileptic movements. Figure 30 C. represents a movement were the subject is turning pages of a book. Figure 30 D. shows an example of high frequency bursts caused by banging with a toy on a table.

This chapter presents a first approach for the detection of tonic patterns from ACM-signals measured with one 3-D sensor placed on one arm. The purpose of the methods under study, is to support off-line analysis for diagnostic and evaluation purposes. In epilepsy related fields, ACM is only sporadically mentioned in published literature and then ACM is not used for seizure detection [24], [25], [26]. Seizure detection literature dominantly describes seizure detection based on the EEG-signal [27]. For the detection algorithm a supervised learning approach is used. Features are selected that represent the most important characteristics that distinguish between tonic movements and other movement types. For classification linear discriminant analysis is chosen. Linear discriminant analysis is a widely used method to classify multidimensional data with good results [120, 121].

First our features are calculated for ACM-signals obtained from refractory epilepsy patients that were annotated by three experts. The optimal combination of features is determined by evaluating all possible combinations of features on training data in a linear discriminant analysis setup. Second, to study the robustness across patients, the optimal combination of features is evaluated for its value for seizure detection on data from other patients.

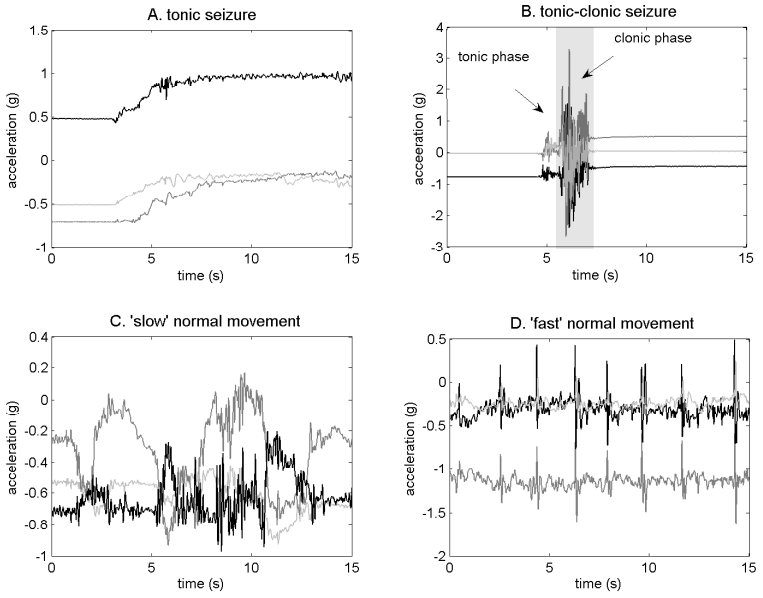

Figure 30: Examples of typical ACM-patterns, measured with one 3-D sensor on an arm. A. Block-like pattern associated with tonic seizure. B. Tonic-clonic seizure. C. 'Slow' normal movement. D. 'Fast' normal movement.

7.3 FEATURE EXTRACTION

EEG-technicians are able to visually 'detect' tonic seizures from accelerometric (ACM) patterns because of the following features:

- There is a slow change in position of the limbs of the patients during a tonic seizure, this results in a block-shaped pattern in the ACM-signal, as can be seen in Fig. 30, that is slower than a normal change of posture.
- A small tremor of the limbs is visible, on top of the change of posture, when the seizure evolves to a clonic phase, this tremor may evolve in jerking of the limbs (clonic part of the seizure).
- Furthermore often more body parts can be involved, so the movement pattern is synchronously visible at more than one 3-D ACM-sensor.

Before exploring the combination of multiple ACM-sensors, this chapter focusses on detection based on one 3-D sensor placed on one arm. First we need to see if it is possible to detect the characteristic pattern that is associated with tonic seizures in only one sensor. To study the relations between all involved sensors, is a topic for future research. The arms are chosen since the

characteristic patterns are best visible on the arm-sensors. Thus, the two most important features of ACM-patterns associated with a tonic seizure, are a slow change in posture, represented by a block-like pattern in the ACM-signal, and a low amplitude tremor. Other movement patterns in general are much higher in amplitude and frequency. Changes of posture that are not associated with epilepsy, can also result in block-like patterns, but our hypothesis is that they vary in slope and duration and therefore can be distinguished from tonic seizures. In the next section a number of features is described that might contribute to the detection of ACM-patterns that are associated with tonic seizures. First the model for myoclonic seizures is used to explain the ACM-patterns that can be seen during tonic seizures. Then a set of features is described that is based on the descriptions of the experts. Tonic seizures have a duration between 10 and 20 seconds, but can vary between 2 seconds and 60 seconds [3]. Thus tonic seizures are relatively long in duration compared to myoclonic seizures and normal movements. For feature extraction therefore a time window of 10 seconds is chosen. All features are computed for the dominant arm sensor.

7.3.1 *Model for motor seizures*

From other research areas it is known that features that incorporate morphological characteristics of the pattern of interest are most successful for pattern recognition [29]. To this purpose we developed an analytical model that describes accelerometric patterns associated with myoclonic seizures [32]. The model was developed in such a way that it can be used for other motor seizure types. The model consists of several parts. The first part describes the innervation pattern that travels down from the brain to the muscles. Second, a muscle force function is defined to describe the reaction of the muscles to the innervation. Then the muscle force is applied to a mechanical system that results in movement and an accelerometer output. During a myoclonic seizure the innervation pattern of the muscles is a short pulse train, in the model this is represented by a single pulse. The muscle response to a pulse is defined by:

$$F_{ag}(t) = F_{sum}(\frac{t}{\tau})e^{\frac{-t}{\tau}} , \tag{7.1}$$

where $F_{ag}(t)$ is the agonistic muscle response, F_{sum} is a constant that indicates the force that can be produced by the muscle and τ is a general time constant for all motor units together.
During tonic seizures the muscles are innervated with a long pulse train of high frequency [10]. In our model this is represented by a block ($u(t) = 0$ if $t < 0$ or $t > a$ and $u(t) = 1$ if $0 \leqslant t \leqslant a$). The muscle force function and mechanical system are similar as with myoclonic seizure [32] Therefore for

tonic seizures the muscle force response is:

$$F_{ag} = F_{sum}(1 - (\tau t - 1)e^{\frac{-t}{\tau}}) \tag{7.2}$$

For physiological values of τ, the value of Eq. 7.2 goes rapidly to F_{sum}. For the antagonist muscle the response yields:

$$F_{ant} = AF_{sum}(1 - (B\tau t - 1)e^{\frac{-t}{B\tau}}) \tag{7.3}$$

Where A and B are dimensionless constants approximately equal to 1. The value of Eq. 7.3 goes rapidly to AF_{sum}. Thus the net value of both muscles working together is approximated by $(1 - A)F_{sum}$. A has a value close to 1 therefore the net muscle force is very small. Hence, the arm is moving very slowly in one direction.
An accelerometer signal measured during human movement, consists of a part that represents accelerations due to the actual movements of the body and a part that represents the position of the sensor in relation to the gravity field. When there is no movement, the latter causes an offset in the signal between -1 and 1 g. During a change of posture, the position in relation to the gravity field can change, and thus the offset changes. For a simple 2-D planar rotation of the arm, in the field of gravity, the acceleration (A_t) in the direction of the movement then yields:

$$A_t(t) = -R\alpha(t) - g\sin(\theta(t)); \tag{7.4}$$

where R is the distance between the elbow and the accelerometer, $\alpha(t)$ is the angular acceleration, g is the gravitational constant and $\theta(t)$ is the angular displacement. Using kinetic relations $\alpha(t)$ can be replaced by:

$$\alpha(t) = \frac{4.5}{BMBL^2}(F_{ag} - F_{ant}) \tag{7.5}$$

where BM is body mass and BL is body length. Filling Eq. 7.5 in Eq. 7.4 leads to:

$$A_t(t) = \frac{4.5}{BMBL^2}((1 - A)F_{sum}) - g\sin(\theta(t)) \ . \tag{7.6}$$

From this Eq. can be seen that the acceleration caused by movement is much smaller as the acceleration caused by gravity. Thus the typical *block-like* pattern is mainly caused by the gravity component that slowly changes.
Luinge et al. [122] estimate the gravity component with a Kalman filter, but the gravity component is mostly estimated using a low-pass filter [14, 11]. Because for the detection of tonic seizures we are not exactly interested in the

kinematics of the arm, we use the filter method. For this end each ACM-signal x_i is filtered with a first order low-pass filter with a cut-off frequency of 0.5 Hz. x_i represents one of the three signals from a 3-D accelerometer, $i \in \{1, 2, 3\}$. The resulting signal x_{islw} is used to calculate features that represent the typical block-like pattern that is associated with tonic seizures.

7.3.2 *Features for block-like pattern*

The most important feature of ACM-patterns associated with tonic seizures is the block-like characteristic caused by a slow change of posture of the limb. The posture of the limb is approximated with x_{islw}, for the change of posture we can therefore use the first derivative (jerk), or the variance. Furthermore because during a tonic seizure the movement is extremely slowly, the amplitude of the ACM-signal is between -1 and 1 g. During other movements there is more variation and the amplitude can be up to 2-3 g [94], therefore the distance between the minimal and maximal value of x_{islw} is also a good indicator for tonic seizures.
The jerk Jy_{slw} is defined as :

$$Jy_{slw}[n] = \sqrt{\sum_{k=1}^{3} \left(\frac{x_{kslw}[n] - x_{kslw}[n-1]}{\Delta t} \right)^2} \tag{7.7}$$

where Δt is the sampling interval .
During a tonic seizure the arm very slowly changes position, thus the value of $J_{y_{slw}}$ is low. During other movement types the velocity of the position changes is much faster and thus also $J_{y_{slw}}$. Per segment of N samples we calculate the mean magnitude of the jerk $\overline{J_y}$. For a segment length of 10 seconds with a sampling frequency f_s of 100 Hz this means that $N = 1000$ samples.

$$\overline{J_{y_{slw}}} = \frac{1}{N} \sum_{n=1}^{N} Jy[n] \ , \ N = 1000 \ . \tag{7.8}$$

The magnitude Y_{slw} for the dominant arm sensor is:

$$Y_{slw}[n] = \sqrt{\sum_{1}^{3} x_k{}^2_{slw}[n]} \ . \tag{7.9}$$

The variance of the magnitude $S^2_{Y_{slw}}$ for each segment is:

$$S^2_{Y_{slw}} = \frac{1}{N-1} \sum_{n=1}^{N} (Y_{slw}[n] - \overline{Y_{slw}})^2 \ , \ N = 1000 \ , \tag{7.10}$$

with $\overline{Y}$ the mean magnitude:

$$\overline{Y_{slw}} = \frac{1}{N}\sum_{n=1}^{N} Y_{slw}[n]\ , N = 1000\ . \tag{7.11}$$

Since $J_{y\,slw}$ is a linear measure and $S^2_{Y\,slw}$ quadratic the square root $S_{Y\,slw}$ is used. The hypothesis is that the change of posture is unnaturally slow, thus $S_{Y_{slw}}$ is lower for tonic seizures than for other movement types
For the distance between minimum and maximum signal values, the range R_y is defined as:

$$R_y = \sqrt{\sum_{k=1}^{3} |max(x_{k\,s}lw[1:1+L]) - min(x_{k\,s}lw[1:1+L])|^2}\ . \tag{7.12}$$

The range $R_{y\,s}lw$ between the maximum and minimum value is in a smaller range for tonic seizures than for other movement types.

7.3.3 *Features for tremor*

The block-like pattern is often accompanied by a subtle tremor, therefore also the fast signal component x_{ifst} is used, to calculate features that are indicative for this tremor. To create x_{ifst}, x_{islw} is subtracted from the original signal x_i. Then the variance is also calculated for this fast component ($S_{Y_{fst}}$).

7.3.4 *Features for other movements*

For a discriminative feature set, features need to represent characteristics of both tonic seizures and other movement types, this can also be motor seizures of another type. Therefore features based on our model for myoclonic and clonic seizures are included.
The continuous wavelet transform (CWT) of a signal $f(t)$, at the scale a and position t is defined as:

$$CWT_h[f](t,a) = \frac{1}{\sqrt{a}}\int_{-\infty}^{\infty} f(\tau)h^*\left(\frac{t-\tau}{a}\right)d\tau\ , \tag{7.13}$$

where $h(t)$ is the wavelet base and $*$ denotes the complex conjugation [115]. In this case the wavelet base $h(t)$ is formed by our model:

$$h(t) = t(e^{-t} - \frac{1}{A}e^{\frac{-t}{B}}) \tag{7.14}$$

This function satisfies the admissibility condition if $A = B^2$, see [33] for more details.

To compare the performance with the other features, that are computed for the discrete signals $x_i[n]$, the sampled versions of Eq. 7.13 and 7.14 are used. Per sensor i the scalogram $SC_h[x_i](n,a)$ is calculated using our model based wavelet. Then the scalograms of the three 1-D sensors are summated:

$$SC_h[x_i](n,a) = |CWT_h[x_i](n,a)|^2 \,, \tag{7.15}$$

and

$$SCT(n,a) = \sqrt{\sum_{i=1}^{3} SC_h[x_i](n,a)} \,. \tag{7.16}$$

Frequencies of movements during daily activities, dominantly lie between 0.3 and 3.5 Hz [123]. Frequencies of clonic seizures typically lie in the range of 2–5 Hz [3] and accelerometer patterns of myoclonic seizures lie in the range of 4–6 Hz [34].
For myoclonic (and clonic) seizures most of the power is in the range of scales 2-10. Our hypothesis is that during tonic seizures the power is concentrated in the higher scales ($\leqslant$ 0.5 Hz) because of the slow change of posture. Hence the model based wavelet is used to calculate a scalogram for the scales 1-50. For the detection of tonic seizures the ratio between the power in scale 2–10 and the total power (ER_{high}) and the ratio between the power in scale 20–50 and the total power (ER_{low}) can be useful features:

$$ER_{high}[n] = \frac{\sum_{a=2}^{10}(SCT(n,a))}{\sum_{a=1}^{50}(SCT(n,a))}, \tag{7.17}$$

$$ER_{low}[n] = \frac{\sum_{a=20}^{50}(SCT(n,a))}{\sum_{a=1}^{50}(SCT(n,a))} \,. \tag{7.18}$$

ER_{high} because it is an important feature to discriminate between tonic movements and myoclonic, clonic and fast normal movements. ER_{low} because it is an important feature to distinguish slow (block-like) movements from the other movements. Per segment of 1000 samples the mean values of ER_{high} and ER_{low} are determined:

$$\overline{ER_{high}} = \frac{1}{N}\sum_{n=1}^{N} ER_{high}[n] \,, N = 1000 \,, \tag{7.19}$$

and

$$\overline{ER_{low}} = \frac{1}{N}\sum_{n=1}^{N} ER_{low}[n] \,, N = 1000 \,. \tag{7.20}$$

7.4 CLASSIFICATION

To establish their value for the detection of tonic seizures the features are evaluated in a 'two-class' detection setup. The two classes are: 'tonic seizure', and 'other movements'. Hence, myoclonic, clonic, and normal movements are regarded as one class. As classification method Fisher's linear discriminant analysis is used [118]. This is a classification method that projects the multi-dimensional feature space onto one line. The projection maximizes the distance between the means of the two classes while minimizing the variance within each class. Classification is performed in the one-dimensional space that is thus created.

7.5 EVALUATION

7.5.1 *Patient data*

For evaluation ACM-data are used from 36 mentally retarded patients who suffer from refractory epilepsy. The patients are monitored with the setup described in our previous clinical study [30], with five 3-D sensors placed on the limbs and the sternum. The sampling frequency f_s of the ACM-signals is 100 Hz. For each patient at least one and maximal three video fragments per seizure type (myoclonic, tonic, clonic) are selected. In these fragments the patients should be in the scope of the camera. This resulted in 156 video fragments with a total duration of 3.6 hours. Three experts divided the corresponding ACM-signals into classes using video and accelerometric information. Available classes were: no movement, myoclonic seizure waveform, tonic seizure waveform, clonic seizure waveform, normal movement, and unclear. To get an indication of the value of a standard based on these annotations the interrater agreement is computed for each pair of experts. The measure that is used for the agreement is Cohen's kappa κ [105]. This statistic is most often used to measure agreement and takes into account the agreement that can occur by chance. The range of κ is from -1 till 1, with larger values indicating better reliability. For the evaluation study, only events were selected, where two experts agreed on. Events marked as 'unclear' were excluded from the evaluation. For a seizure event to be included, the seizure needed also to be visual in the EEG-signal. This resulted in a data set containing data of 18 patients, 27 tonic seizures, 10 clonic seizures, 16 myoclonic seizures and 36 normal movements.
The data is divided into three groups. We aim for an approach that is robust among patients. Therefore the groups have no overlap in patients. From these three groups, three training sets are created that are composed of data of two groups. For each training set, the data of the remaining third group of patients is used for testing.

7.5.2 *Performance measures*

The performance per feature set is expressed in the sensitivity (SEN) the percentage of myoclonic seizures correctly classified, the number of false detections (FD), and the positive predictive value (PPV), which is the ratio between correct detected tonic seizures and all events that are classified as a tonic seizure. Detected events are defined in a similar way as in [31], but in this case the time-basis is 10 seconds instead of one second.

7.5.3 *Optimal combination of features*

The three training sets are also used for the determination of the optimal combination of features. To this end per training set the detection performance of each combination of features is calculated. The optimal feature set, is the feature set where all training sets obtain a PPV > 0.4 and where lowest sensitivity of the three training sets is maximal.

7.6 RESULTS

7.6.1 *Interrater agreement*

Table 14 lists the values of κ for each pair of experts. The annotations were made based on information based on both video and ACM. The agreement can be considered moderate if κ lies between 0.41 and 0.6 and good if κ lies between 0.61 and 0.8 [106]. Thus, with a mean value of 0.50 the agreement of our experts can be considered moderate. This results is in agreement with the findings of Parra et al. [124], who studied interrater agreements of three epileptologists when they rated 138 seizures from 60 patients using the same semiological seizure classification suggested by Lüders et al. [3] that was also used by our experts. For the validation of our algorithm only events are used where at least two experts agreed on plus that the seizure needed also to be visible in the EEG signal.

Table 14: Interrater agreement κ for tonic seizures for each pair of experts

raters	agreement (κ)
1 and 2	0.41
2 and 3	0.45
1 and 3	0.63
mean	0.50

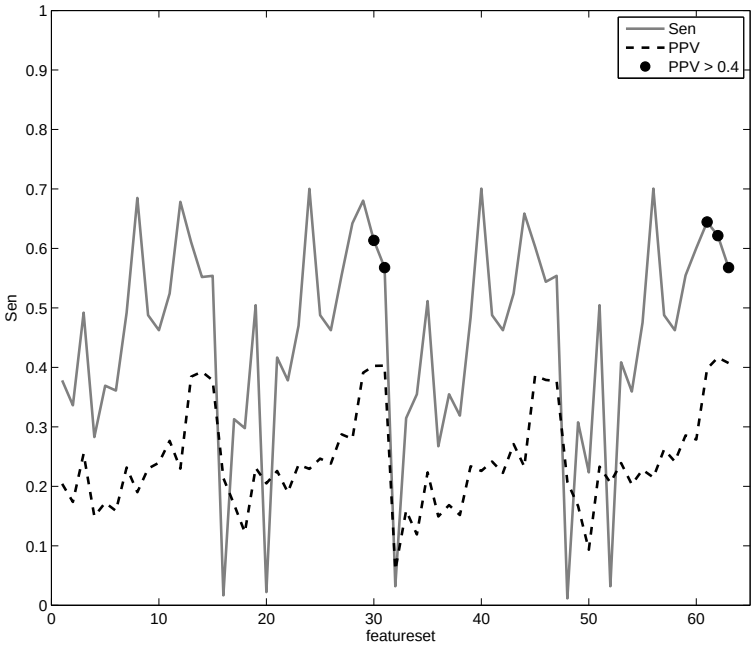

Figure 31: Minimal values (for the three training data sets) of performance measures SEN and PPV per combination of features.

7.6.2 *Feature selection*

Per training set the detection performance of each combination of features is calculated. Since there are six features, there are $(2^6) - 1 = 63$ combinations. Figure 31 shows the minimal PPV and SEN of the three feature sets for every feature set. The other two training sets thus have higher values for PPV and SEN for the corresponding feature set. Sensitivity values with a corresponding PPV > 0.4 are marked with a '$\bullet$'. Hence we see that there are five feature sets with a PPV > 0.4. The feature set with the maximal sensitivity is the 60^{th} combination. This combination contains all features, except $\mathrm{ER}_{\mathtt{high}}$.

7.6.3 *Detection performance*

Table 15 shows the detection performance on the training data itself with the optimal feature set. Sensitivities are high. All tonic seizures except one are detected. The one that is missed has a duration less than a second, and therefore is difficult to detect with our window choice of 10 seconds.

The positive predictive values lie around 0.40. Table 16 shows the detection

Table 15: Detection performance results on training sets

Training set	TP	FN	FD	Sen	PPV
1	7	1	14	0.88	0.33
2	12	0	19	1.00	0.39
3	14	0	18	1.00	0.44
overall	33	1	51	0.97	0.40

performance on the three test sets. The values for SEN and PPV are slightly lower than in the training phase. 80 % of the tonic seizures is detected with a PPV of 0.35. Analysis of the false detections shows that 42% of the false

Table 16: Detection performance results on test sets

Test set	TP	FN	FD	FD_{sz}	Sen	PPV
1	11	3	13	4	0.79	0.46
2	7	2	14	5	0.78	0.33
3	6	0	18	10	1.00	0.25
overall	24	5	45	19	0.83	0.35

positives is also a seizure. The other false positives are very slow change of postures that have a long plateau. Based on ACM alone these false positives are visually difficult to distinguish from real tonic seizures.
The five seizures that were missed were very subtle, in four cases there was no block-shaped pattern, and no clear movement visible in the ACM-signal. The remaining missed seizure is really short in duration ($<$ 1 s).

7.7 DISCUSSION

In this chapter six features were defined based on the description of experts of the characteristic patterns that can be observed in 3-D accelerometry(ACM)-signals associated with tonic seizures [30]. It was found that a combination of five of the features was optimal, and that it was possible to detect tonic seizures from ACM-signals. This led to a sensitivity (SEN) of 0.83 and a positive predictive value (PPV) of 0.35.

The variance and the jerk of the slow signal component ($<$ 0.5 Hz), the range from minimal to maximal signal value as well as the power ratio of the higher scales (lower frequencies) in relation to the entire scalogram, are important features for the detection of tonic seizures. This because they are all

good indicators of the presence of the block-like pattern that is visible in the ACM-signal associated with a tonic seizure. Furthermore the variance of the fast signal component (> 0.5 Hz) is an important feature, because it describes the presence of the subtle tremor that can also be visible in the ACM-signal associated with a tonic seizure.
The sixth feature, the power ratio of the lower scales (higher frequencies) in relation to all scales, did not contribute much extra to the performance of the algorithm. This feature was added to describe the characteristics of fast normal movements as well, but this feature appears to be redundant.

Four of the five tonic seizures that were missed, did not have the characteristic block-like appearance in the ACM-signals. During a tonic seizure the muscles go into tetanic contraction. Both agonist and antagonist muscles contract heavily. Usually there is still a net force effect in one direction, and then the affected limbs move slowly, but it can also happen that the net effect is zero. Then there is no movement effect. It can also be the case that the movement is blocked, because the limbs are fixed (for example against the body, or against furniture). In these cases, where the seizures are not clearly visible in ACM-signals, but the muscles are heavily contracted perhaps the measurement of the EMG might be more useful [10].
The other missed seizure was very short in duration (< 1 s). Since the majority of the tonic seizures in our population last between 5 and 10 seconds, a 10 seconds analyzing window was chosen. All features are averaged over these 10 seconds thus this window length was too long to detect this seizure.

A positive predictive value of 0.35 implies that one out of three alarms is genuine. For off-line analysis this is acceptable, especially when 42 % of the false alarms are actually motor seizures of another type (myoclonic or clonic).
Previously we reported that there are three characteristic pattern types visible during simple motor seizures [30]. In this study, it was also shown that a seizure can consist of a combination of these 'elementary' patterns. Figure 32 shows the flow diagram of the patterns during the simple motor seizures in our patient population. The transition of one pattern to another is not abrupt, but gradually. This can be seen in Fig. 33 where an accelerometer signal associated with an epileptic seizure is depicted. First there is a small twitch visible that is associated with a myoclonic seizure, then the typical block-like shape associated with a tonic seizure is visible. This gradually changes into a clonic phase, thus both the jerking of the clonic phase as well as the block-like pattern are present in the signal.
Thus besides that there are three types of clearly distinguishable ACM-patterns associated with motor seizures, there are also patterns that are a mix of these types. An algorithm trained for the detection of a specific seizure type will also detect patterns that are of a mixed seizure type. For experts, this distinction is just as difficult. The mean interrater agreement for our experts

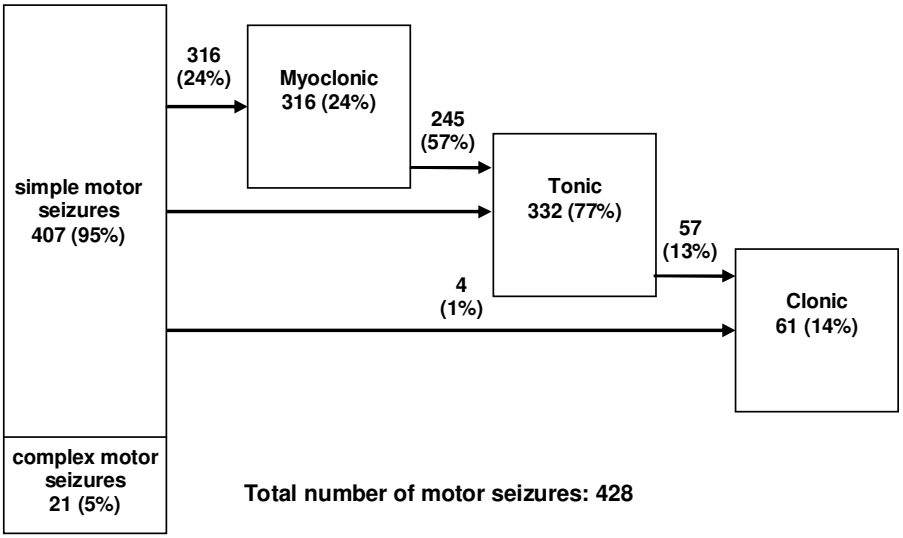

Figure 32: Flow diagram of seizure patterns during simple motor seizures in our population [30].

on the data used for the evaluation was 0.50. This is a value that is similar to agreement values found in literature [124].

In our seizure detection setup we have chosen for a modular approach,

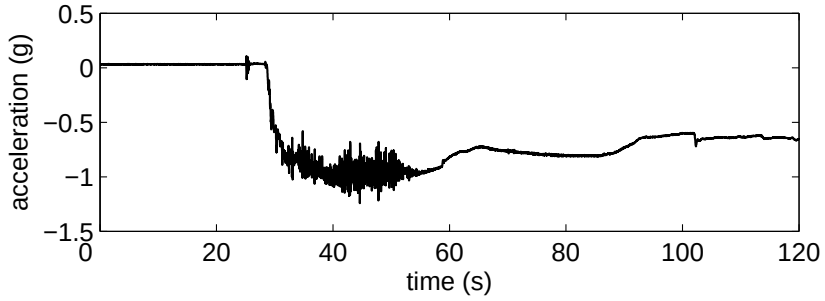

Figure 33: Example of motor seizure consisting of a mix of elementary patterns.

where patterns associated with myoclonic, tonic and clonic seizures are separately handled. Nevertheless there is a percentage of seizures that manifests in patterns that are a mix of the three types. Thus a part of the false positives from the separate modules will point to other motor seizure types. For automatic analysis this is not a problem, since these are events that are also clinically relevant. To separate these mixed forms (if this is of clinical interest)

from the purely elementary movements is possible in a post processing step using features like duration of event or amplitude.
The false positives that were not of a mixed seizure type, were slow changes of posture, that based on the ACM-signal from one arm alone, visually can not be distinguished from patterns associated with tonic seizures. Experts also had all five 3-D ACM-signals, video and EEG available. Inclusion of new features will not be useful to decrease the amount of false positives. Using information from accelerometers placed on the other limbs might contribute to a higher SEN and PPV in these cases. For the missed seizures that did not have the characteristic appearance in the ACM-signal a combination with other sensor types can be useful. The EMG-signal can be a useful source of information because during motor seizures both agonist and antagonist muscles are synchronously involved [10]. It is also possible to focus on another effect of the seizure, it is known that many tonic seizures are associated with an increase of heart rate, therefore heart rate is also a useful parameter for detecting tonic seizures [45].

7.8 CONCLUSION

This chapter shows the first quantitative results for the detection of tonic seizures based on 3-D accelerometry (ACM) recordings.
Features were defined that represent the block-like characteristic and the subtle tremor that is visible in ACM-signals associated with tonic seizures. It was possible to detect tonic seizures with a sensitivity (SEN) of 0.83 and a positive predictive value (PPV) of 0.35. The seizures that were missed, were not clearly visible in the ACM-signal. For these seizures additional ACM-sensors or a combination with other sensor types might be necessary. False alarms were either motor seizures of a mixed type or slow normal movements that visually can not be distinguished from tonic seizures based on one 3-D ACM-sensor alone. The results show that our approach is useful for the automated detection of tonic seizures based on 3-D accelerometry and that it is a promising contribution in a complete multi-sensor seizure detection setup.

8 RECOMMENDATIONS FOR FUTURE RESEARCH

The use of accelerometry for seizure detection is new. This thesis presents the first steps of the development of an accelerometry based seizure detection system. It shows the added value of accelerometry for seizure detection and the first results for algorithm development. Currently the motor activity detection algorithm described in chapter 4 is already implemented in clinical practice to improve the efficiency of off-line analysis. Using this algorithm a substantial part of the data can be excluded from further analysis in order to reduce the workload of the EEG-technicians. There are also plans for implementing the algorithms for myoclonic and tonic seizures in a similar setup. Ideally, in the future, these algorithms will be part of a real-time seizure warning system based on accelerometry and heart rate [125]. To reach this goal, there are number of steps that can be taken:

8.1 IMPROVEMENT OF DETECTION ALGORITHMS

A model based wavelet was especially designed for accelerometer patterns associated with myoclonic seizures. Chapter 5 described the model itself and the mathematical properties of the wavelet that can be derived from the model. In chapter 6 this wavelet was compared to other time-frequency methods. The model based wavelet outperformed the short time Fourier transform and the Wigner distribution, but the detection performance was similar when the fifth Daubechies wavelet was used. Advantages of the model based wavelet over the Daubechies wavelet are:

- for the model only 50 scales instead of 255 scales were used,
- the model consists of physiological parameters such as body mass, body length, seizure intensity and seizure duration,
- the model can also be used for other motor seizure types.

Future research needs to focus on the optimization of the use of this model based wavelet. The optimum number of scales needs to be determined and possibly other features can be derived from the wavelet coefficients.
For detection of tonic seizures our physiological model was used to show that the pattern in the accelerometer signals associated with tonic seizures is mainly caused by the gravity component of the signals. The gravity component was estimated using a low-pass filter, and features were selected based on the description of ACM-patterns associated with myoclonic seizures by

human experts. The feature selection process could be improved by estimating the gravity component with a more sophisticated method [122], thus acquiring more detailed kinematic information. Furthermore detection of tonic seizures would benefit from the combination of heart rate and accelerometry. The movement patterns associated with tonic patterns are relatively slow, it is known however that heart rate increases during tonic seizures [45]. Thus fusion of these two modalities would improve detection performance.
This thesis describes detection methods for myoclonic and tonic movement patterns. The third category: clonic movement patterns has not been covered yet. The choice to tackle myoclonic and tonic patterns first is that these two elementary patterns differ most from each other. The clonic movement pattern lies more in between. By definition clonic seizures consist of myoclonic jerks recurring at a regular repetition rate [3]. Furthermore tonic seizures often evolve into a clonic phase. We found that features for both myoclonic and tonic movement patterns were also sensitive to clonic seizures. Accelerometry patterns associated with clonic seizures differ from myoclonic seizures in duration and amplitude. Patterns associated with clonic seizures differ from tonic seizures in amplitude and frequency. Therefore in a post-processing step it should be possible to separate these. Then the methods described in this thesis can also contribute to the detection of clonic and tonic-clonic seizures.

8.2 OPTIMIZATION OF NUMBER OF SENSORS

For the movement detection algorithm all 5 3-D sensors were used. Sometimes one or two sensors were malfunctioning; in that case these sensors were excluded from the calculations. Nevertheless all movements that were scored by the experts were detected by the algorithm. This shows that not all the five 3-D sensors are needed for movement detection. On the other side, the detection algorithms for myoclonic and tonic seizures were based on only one 3-D sensor placed on the arm. The arm was chosen using a priori clinical knowledge, but for tonic seizures it was found that in 20% of the seizures 1 sensor was not enough. It is known that in generalized tonic and tonic-clonic seizures often the entire body is synchronously involved. The use of more sensors could give additional information whether a movement is associated with a seizure or not. Future research could therefore focus on the optimal number of ACM-sensors, and features computed using information from combination of sensors.

8.3 COMBINATION OF ACCELEROMETRY AND HEART RATE

For seizures that do not express themselves in motor phenomena 3-D ACM can never suffice. Therefore an ideal seizure detection system will consist of more sensor modalities. In our seizure detection programme we also use

ECG and EEG [45, 90]. Research needs to point out what combinations of sensor modalities are most suitable for various patient and seizure types. In our experience, heart rate and accelerometry is a valuable combination [125]. Future research will focus on the combination of the algorithms in this thesis with a heart rate based detection algorithm [45]. The eventual goal is a tailored seizure detection system that also takes into account prior clinical knowledge, so that per individual patient the best seizure detection is achieved, that not only can be used in a clinical environment but is also suitable for home monitoring purposes.

8.4 USE OF CLINICAL INFORMATION

In chapter 2 of this thesis it was also found that for both the adaptation of existing techniques and the development of new algorithms, clinical information should be taken more into account. This should also yield for the methods described in this thesis. A priori knowledge of seizure types should be incorporated in the detection algorithm. In this thesis this was done, by using only the ACM-signals measured on the arms for detecting the seizures. Furthermore the model incorporates parameters that represent body weight, body height, seizure duration and seizure intensity. The model is used as a wavelet without using these parameters. Explicit use of these parameters might improve detection performance. All methods described in this thesis were trained in such a way that they did not have to be trained for each patient individually. For the motor activity detection the linear threshold function is robust for fluctuations across patients. We also found that the model parameters of the model for myoclonic seizures, fitted to real data where in a certain range and that these parameters were physiological feasible. Nevertheless for myoclonic and tonic seizure patterns it is interesting to study individual differences. The use of patient specific information might contribute to an even better detection performance.

8.5 TYPES OF SEIZURES THAT CAN BE DETECTED

The methods described in this thesis are developed for the detection of motor seizures with elementary movement patterns (simple motor seizures [3]). In this thesis ACM-data was collected in mentally retarded subjects with severe epilepsy. This patient group is known to have simple motor seizures [91, 30]. As stated in chapter 2, it should be a topic of future research how detection methods developed for specific patient types can be extended to other patient types. This section discusses some possibilities of the application of the methods developed in this thesis to other patient groups. This depends on the occurrence of simple motor seizures in these patient groups.
The 'normal' adult epileptic patients (not mentally retarded) often experience

partial seizures. Of this group 33% have a focus outside the temporal lobe and often in the frontal lobe, in this case myoclonic seizures can occur. Clinical manifestations tend to reflect the specific area of seizure onset and range from behavioral to motor or tonic/postural changes. When the primary motor cortex is involved clonic or myoclonic movements can occur. When the supplementary motor area is involved, unilateral or asymmetric bilateral tonic posturing occurs. For the 67% of the patients that has seizures arising from the temporal lobe motor activity is not the main clinical symptom, however sometimes unilateral dystonic posturing of a limb also can be observed.
Generalized tonic-clonic seizures occur in all patient populations. These seizures are most harmful to the patient and home situations most important to detect. For these seizures the methods in this thesis are certainly useful.

BIBLIOGRAPHY

[1] H. Witte, L.D. Iasemidis, and B. Litt. Special issue on epileptic seizure prediction. *IEEE Transactions on Biomedical Engineering*, (50):537–539, 2003. (Cited on pages 1, 39, and 89.)

[2] C.D. Binnie, J.H.P. Aarts, P.T.E. Van Bentum-De Boer, and T. Wisman. Monitoring at the instituut voor epilepsiebestrijding Meer en Bosch. *Electroencephalograpy and Clinical Neurophysiology Suppl.*, 37(3):341–355, 1985. (Cited on pages 1 and 12.)

[3] H.O. Luders and S.N. Noachtar. *Epileptic Seizures, Pathophysiology and Clinical Semiology*. Churchill Livingstone, New York, 2000. (Cited on pages 2, 5, 6, 13, 14, 16, 26, 31, 40, 74, 87, 90, 92, 96, 98, 106, and 107.)

[4] Commission of Classification and Terminology of the International League Against Epilepsy. Proposal for revised clinical and electroencephalographic classification of epileptic seizures. *Epilepsia*, 22:489–501, 1981. (Cited on pages 2, 27, and 31.)

[5] J. Engel Jr. A proposed diagnostic scheme for people with epileptic seizures and with epilepsy: Report of the ILAE task force on classification and terminology. *Epilepsia*, 42:796–803, 2001. (Cited on pages 2, 14, 16, and 27.)

[6] H. Luders, J. Acharya, C. Baumgartner, S. Benbadis, A. Bleasel, R. Burgess, D.S. Dinner, A. Ebner, N. Foldvary, E. Geller, H. Hamer, H. Holthausen, P. Kotagal, H. Morris, H.J. Meencke, S. Noachtar, F. Rosenow, A. Sakamoto, B.J. Steinhoff, I. Tuxhorn, and E. Wyllie. Semiological seizure classification. *Epilepsia*, 39(9):1006–1013, 1998. (Cited on pages 2, 4, 31, 32, and 34.)

[7] M. Hallett. Myoclonus: Relation to epilepsy. *Epilepsia*, 26(Suppl.1): S67–S77, 1998. (Cited on pages 3, 31, 59, 60, 74, 76, and 77.)

[8] P. Brown and C.D. Marsden. Rhytmic cortical and muscle discharge in cortical myoclonus. *Brain*, 119:1307–1316, 1996. (Cited on page 3.)

[9] H.M. Hamer, H.O. Lüders, F. Rosenow, and I. Najm. Focal clonus elicited by electrical stimulation of the motor cortex in humans. *Epilepsy Research*, 51:155–166, 2002. (Cited on pages 4 and 5.)

[10] H.M. Hamer, H.O. Lüders, S. Knake, B. Fritsch, W.H. Oertel, and F. Rosenow. Electrophysiology of focal clonic seizures in humans:

a study using subdural and depth electrodes. *Brain*, 126:547–555, 2003. (Cited on pages 4, 5, 59, 90, 92, 101, and 103.)

[11] J. Fahrenberg, F. Foerster, M. Smeja, and W. Muller. Assessment of posture and motion by multichannel piezoresistive accelerometer recordings. *Psychophysiology*, 34(5):607–612, 1997. (Cited on pages 6, 40, 42, and 93.)

[12] M.J. Mathie, B.G. Celler, N.H. Lovell, and A.C.F. Coster. Classification of basic daily movements using a triaxial accelerometer. *Medical and Biological Engineering and Computing*, 42:679–687, 2004. (Cited on pages 6, 40, 42, and 43.)

[13] J.B. Bussmann, J.H. Tulen, E.C. van Herel, and H.J. Stam. Quantification of physical activities by means of ambulatory accelerometry: A validation study. *Psychophysiology*, 35:488–496, 1998. (Cited on pages 6, 24, 40, 42, and 54.)

[14] P. Veltink, H.B. Bussmann, W. de Vries, W.L. Martens, and R.C. Van Lummel. Detection of static and dynamic activities using uniaxial accelerometers. *IEEE Transactions on Rehabilitation Engineering*, 4(4):375–385, 1996. (Cited on pages 6, 24, 40, 42, 43, 76, and 93.)

[15] M. de Niet, J.B. Bussmann, G.M. Ribbers, and H.J. Stam. The stroke upper-limb activity monitor: Its sensitivity to measure hemiplegic upper-limb activity during daily life. *Arch Phys Med Rehabil*, 88:1121–1126, 2007. (Cited on page 6.)

[16] B. Najafi, K. Aminian, A. Paraschiv-Ionescu, F. Loew, C. Bula, and P. Robert. Ambulatory system for human motion analysis using a kinematic sensor: Monitoring of daily physical activity in the elderly. *IEEE Transactions on Biomedical Engineering*, 50(6):711–723, 2003. (Cited on pages 6, 40, and 76.)

[17] N.L. Keijsers, M.W. Horstink, and S.C. Gielen. Movement parameters that distinguish between voluntary movements and levodopa-induced dyskinesia in parkinson's disease. *Human Movement Science*, 22:67–89, 2003. (Cited on pages 6, 24, and 40.)

[18] R.J. Dunnewold, J.I. Hoff, H.C. van Pelt, P.Q. Fredrikze, E.A. Wagemans, and B.J. van Hilten. Ambulatory quantitative assessment of body position, bradykinesia, and hypokinesia in parkinson's disease. *Journal of Clinical Neurophysiology*, 15(3):235–242, 1998. (Cited on pages 6, 40, 42, and 54.)

[19] H. Wharrad and D. Jefferson. Distinguishing between physiological and essential tremor using discriminant and cluster analyses of parameters

derived from the frequency spectrum. *Human Movement Science*, 19: 319–339, 2000. (Cited on pages 6 and 40.)

[20] T. Thielgen, F. Foerster, G. Fuchs, A. Hornig, and J. Fahrenberg. Tremor in parkinson's disease: 24-hr monitoring with calibrated accelerometry. *Electromyogr. Clin. Neurophysiol.*, 44:137–146, 2004. (Cited on pages 6, 40, and 76.)

[21] N. Vogels, K.R. Westerterp, D.L.A. Posthumus, F. Rutters, and M.S. Westerterp-Plantenga. Daily physical activity counts vs structured activity counts in lean and overweight dutch children. *Physiology and Behavior*, 92:611–616, 2007. (Cited on page 6.)

[22] M. Ermes, J. Pärkkä, J. Mäntyjärvi, and I. Korhonen. Detection of daily activities and sports with wearable sensors in controlled and uncontrolled conditions, 2008. (Cited on page 6.)

[23] A.K. Bourke, J.V. O'Brien, and G.M. Lyons. Evaluation of a threshold-based tri-axial accelerometer fall detection algorithm. *Gait and Posture*, 26:194–199, 2007. (Cited on page 6.)

[24] J.D. Frost, R.A. Hrachovy, P. Kellaway, and T. Zion. Quantitative analysis and characterization of infantile spasms. *Epilepsia*, 19:273–282, 1978. (Cited on pages 6, 24, 40, and 90.)

[25] E.M. Mizrahi. Pediatric electroencephalographic video monitoring. *Journal of Clinical Neurophysiology*, 16(24):100–110, 1999. (Cited on pages 6, 40, and 90.)

[26] M. Rinnerthaler, G. Luef, J. Mueller, K. Seppi, J. Wissel, E. Trinka, G. Bauer, and W. Poewe. Computerized tremor analysis of valproate-induced tremor: A comparative study of controlled-release versus conventional valproate. *Epilepsia*, 46(2):320–323, 2005. (Cited on pages 6, 40, and 90.)

[27] T.M.E. Nijsen, J.B.A.M. Arends, P.A.M. Griep, P.J.M. Cluitmans, and P.A.J.M. Boon. Seizure detection in long-term monitoring, from clinical to home environment. *Submitted to Clinical Neurophysiology*, January 2008. (Cited on pages 6, 10, 11, 75, and 90.)

[28] M. McKinney and J. Breebaart. Features for audio and music classification. *4th International Conferences on Music Information Retrieval (ISMIR2003), 26-30 October 2003 Baltimore Maryland USA*. (Cited on pages 8 and 76.)

[29] A. Aarabi, F. Wallois, and R. Grebe. Automated neonatal seizure detection: a multistage classification system through feature selection based

on relevance and redundancy analysis. *Clinical Neurophysiology*, 117: 328–340, 2006. (Cited on pages 8, 16, 18, 76, and 92.)

[30] T.M.E. Nijsen, J.B.A.M. Arends, P.A.M. Griep, and P.J.M. Cluitmans. The potential value of 3-D accelerometry for detection of motor seizures in severe epilepsy. *Epilepsy and Behavior*, 7:74–84, 2005. (Cited on pages 10, 13, 15, 16, 19, 21, 22, 23, 40, 41, 58, 63, 74, 75, 81, 87, 90, 97, 100, 101, 102, and 107.)

[31] T.M.E. Nijsen, P.J.M. Cluitmans, J.B.A.M. Arends, and P.A.M. Griep. Detection of subtle nocturnal motor activity from 3-d accelerometry recordings in epilepsy patients. *IEEE Transactions on Biomedical Engineering*, 54(11), 2007. (Cited on pages 10, 39, 68, 73, 85, and 98.)

[32] T.M.E. Nijsen, R.M. Aarts, J.B.A.M. Arends, and P.J.M. Cluitmans. Model for arm movements during myoclonic seizures. *29th Annual International Conference of the IEEE EMBS*, pages 1582–1585, 2007. (Cited on pages 10, 57, 76, 77, 78, 81, 82, and 92.)

[33] T.M.E. Nijsen, A.J.E.M. Janssen, and R.M. Aarts. Analysis of a wavelet arising from a model for arm movements during epileptic seizures. *ProRisc*, 2007. (Cited on pages 10, 57, 81, and 95.)

[34] T.M.E. Nijsen, R.M. Aarts, P.J.M. Cluitmans, and P.A.M. Griep. Time-frequency analysis of accelerometry data for detection of myoclonic seizures. *Submitted to IEEE Transactions on Information Technology in Biomedicine*, January 2008. (Cited on pages 10 and 96.)

[35] A.M. Beun, T. Gutter, and J. Overweg. Home EEG and video monitoring in epilepsy: first experiences. *Clinical Neurology and Neurosurgery*, 96: 257–260, 1994. (Cited on page 12.)

[36] S. Ried, P. Hilfiker, I.W. Mothersill, and G. Krämer. From clinical observation to long-term monitoring: diagnostic developments in conservative epileptology. *Epilepsia*, 41(Suppl. 3):S2–S9, 2000. (Cited on page 12.)

[37] C.E. Elger and W. Burr. Advances in telecommunications concerning epilepsy. *Epilepsia*, 41(Suppl. 5):S9–S12, 2000. (Cited on page 12.)

[38] T.P. Sutula, J.C. Sackellares, J.Q. Miller, and F.E. Dreifuss. Intensive monitoring in refractory epilepsy. *Neurology*, 31(3):243–247, 1981. (Cited on page 12.)

[39] J.R. Johansen, G. Lindahl, and P. Sandstedt. Home-video observation of seizures in children with epilepsy–impact on quality of family life. *Seizure*, 8:356–357, 1999. (Cited on page 12.)

[40] R.P. Shaw, S.G. Zelenski, and N. Page. Regulatory issues in the managment of developmentally disabled patients. *Epilepsy and Behavior*, 3: S45–S48, 2002. (Cited on page 12.)

[41] J. Gotman and P. Gloor. Automatic recognition and quantification of interictal epileptic activity in the human scalp EEG. *Electroencephalography and Clinical Neurophysiology*, 41:513–529, 1976. (Cited on page 12.)

[42] D. Raskovic, T. Martin, and E. Jovanov. Medical monitoring applications for wearable computing. *The Computer Journal*, 47(4):495–504, 2004. (Cited on page 12.)

[43] F. Axisa, P.M. Schmitt, C. Gehin, G. Delhomme, E. McAdams, and A. Dittmar. Flexible technologies and smart clothing for citizen medicine, home healtcare, and disease prevention. *IEEE Transactions on Information Technology in Biomedicine*, 9(3):325–336, 2005. (Cited on page 12.)

[44] N.B. Karayiannis, G. Tao, Y. Xiong, A. Sami, B. Varughese, J.D. Frost Jr., M.S. Wise, and E.M. Mizrahi. Computerized motion analysis of videotaped neonatal seizures of epileptic origin. *Epilepsia*, 46(6):901–917, 2005. (Cited on pages 13, 15, 16, 21, and 22.)

[45] W.J.C. Van Elmpt, T.M.E. Nijsen, P.A.M. Griep, and J.B.A.M. Arends. A model of hear rate changes to detect seizures in severe epilepsy. *Seizure*, 15:366–375, 2006. (Cited on pages 13, 15, 16, 21, 38, 103, 106, and 107.)

[46] J. Gotman. Automatic detection of seizures and spikes. *Journal of Clinical Neurophysiology*, 16(2):130–140, 1999. (Cited on page 13.)

[47] C.M.L. Lommen, J.W. Pasman, V.H.J.M. van Kranen, P. Andriessen, P.J.M. Cluitmans, L.G.M. van Rooij, and S. Bambang Oetomo. An algorithm for the automatic detection of seizures in neonatal amplitude-integrated EEG. *Acta Paediatrica*, 96:674–680, 2007. (Cited on pages 15 and 16.)

[48] B.R. Greene, P. de Chazal, G.B. Boylan, S. Connolly, and R.B. Reilly. Electrocardiogram based neonatal seizure detection. *IEEE Transactions on Biomedical Engineering*, 54(4):673–682, April 2007. (Cited on pages 15, 16, and 21.)

[49] N.B. Karayiannis, Y. Xiong, J.D. Frost Jr., M.S. Wise, R.A. Hrachovy, and E.M. Mizrahi. Automated detection of videotaped neonatal seizures based on motion tracking methods. *Journal of Clinical Neurophysiology*, 23(6):521–531, 2006. (Cited on pages 15 and 16.)

[50] B.R. Greene, G.B. Boylan, R.B. Reilly, P. de Chazal, and S. Connolly. Combination of EEG and ECG for improved automatic neonatal seizure

detection. *Clinical Neurophysiology*, 118(6):1348–1359, 2007. (Cited on pages 15, 16, and 21.)

[51] M.J.A.M. van Putten. Nearest neighbour phase synchronization as a measure to detect seizure activity from scalp EEG recordings. *Journal of Clinical Neurophysiology*, 20(5):320–325, 2003. (Cited on pages 15, 16, and 18.)

[52] A.J.C. Slooter, E.M. Vriens, F.S.S. Leijten, J.J. Spijkstra, A.R.J. Girbes, A.C. van Huffelen, and C.J. Stam. Seizure detection in adult icu patients based on changes in EEG synchronization likelihood. *Neurocritical Care*, 5(3):186–92, 2006. (Cited on pages 15, 16, 19, and 20.)

[53] A. Subasi. Application of adaptive neuro-fuzzy interference system for epileptic seizure detection using wavelet feature extraction. *Computers in Biology and Medicine*, 37:227–244, 2007. (Cited on pages 15 and 16.)

[54] H.S Liu, T. Zhang, and F.S. Yang. A multistage, multimethod approach for automatic detection and classification of epileptiform EEG. *IEEE Transactions on Biomedical Engineering*, 49(12):1557–1566, December 2002. (Cited on pages 15, 16, and 19.)

[55] H. Qu and J. Gotman. A patient-specific algorithm for detection of seizure onset in long-term EEG monitoring: possible use as a warning device. *IEEE Transactions on Biomedical Engineering*, 44(2):79–87, February 1997. (Cited on pages 15 and 16.)

[56] M.E. Saab and J. Gotman. A system to detect the onset of epileptic seizures in scalp EEG. *Clinical Neurophysiology*, 116:427–442, 2005. (Cited on pages 15 and 16.)

[57] H.C. Lee, W. van Drongelen, A.B. McGee, D.M. Frim, and M.H. Kohrman. Comparison of seizure detection algorithms in continuosly monitored pediatric patients. *Journal of Clinical Neurophysiology*, 2: 137–146, April 2007. (Cited on pages 15, 16, and 20.)

[58] J. Gotman. Automatic recognition of epileptic seizures in the EEG. *Electroenchephalography and Clinical Neurophysiology*, 54:530–540, 1982. (Cited on pages 16 and 18.)

[59] J. Gotman. Automatic seizure detection: improvements and evaluation. *Electroenchephalography and Clinical Neurophysiology*, 76:317–324, 1990. (Cited on pages 16, 19, 20, and 76.)

[60] A. Liu, J.S. Hahn, G.P. Heldt, and R.W. Coen. Detection of neonatal seizures through computerized EEG analysis. *Electroenchephalography and clinical Neurophysiology*, 82:30–37, 1992. (Cited on pages 16, 18, and 20.)

[61] F. Pauri, F Pierelli, G. Chatrian, and W.W. Erdly. Long-term EEG-video-audio monitoring: computer detection of focal EEG seizure patterns. *Electroenchephalography and Clinical Neurophysiology*, 82:1–9, 1992. (Cited on page 16.)

[62] H. Qu and J. Gotman. Improvement in seizure detection performance by automatic adaptation to the EEG of each patient. *Electroencephalography and Clinical Neurophysiology*, 86:79–87, 1993. (Cited on page 16.)

[63] A.J. Gabor, R.R. Leach, and F.U. Dowla. Automated seizure detection using a self-organizing neural network. *Electroenchephalography and Clinical Neurophysiology*, 99:257–266, 1996. (Cited on page 16.)

[64] N. Pradhan, P.K. Sadasivan, and G.R. Arunodaya. Detection of seizure activity in EEG by an artificial neural network: A preliminary study. *Computers and Biomedical Research*, 29:303–313, 1996. (Cited on page 16.)

[65] W.R.S. Webber, R.P. Lesser, R.T. Richardson, and K. Wilson. An approach to seizure detection using an artificial neural network. *Electroencephalography and Clinical Neurophysiology*, 98:250–272, 1996. (Cited on page 16.)

[66] W. Weng and K. Khorasani. An adaptive structure neural networks with application to EEG automatic seizure detection. *Neural Networks*, 9:1223–1240, 1996. (Cited on page 16.)

[67] I. Yaylali, H. Koçak, and P. Jayakar. Detection of seizures from small samples using nonlinear dynamic system theory. *IEEE Transactions on Biomedical Engineering*, 43(7):743–751, July 1996. (Cited on page 16.)

[68] J. Gotman, D. Flanagan, J. Zhang, and B. Rosenblatt. Automatic seizure detection in the newborn: methods and initial evaluation. *Electroenchephalography and Clinical Neurophysiology*, 103:356–362, 1997. (Cited on pages 16, 20, 21, and 22.)

[69] J. Gotman, D. Flanagan, B. Rosenblatt, A. Bye, and E.M. Mizrahi. Evaluation of an automatic seizure detection method for the newborn EEG. *Electroenchephalography and Clinical Neurophysiology*, 103:363–369, 1997. (Cited on page 16.)

[70] A.J. Gabor. Seizure detection using a self-organizing neural network: validation and comparison with other detection strategies. *Electroenchephalography and Clinical Neurophysiology*, 107:27–32, 1998. (Cited on pages 16 and 19.)

[71] A. Klatchko, G. Raviv, W.R.S. Webber, and R.P. Lesser. Enhancing the detection of seizures with a clustering algorithm. *Electroencephalography and Clinical Neurophysiology*, 106:52–63, 1998. (Cited on page 16.)

[72] M. Roessgen, A.M. Zoubir, and B. Boashash. Seizure detection of newborn EEG using a model-based approach. *IEEE Transactions on Biomedical Engineering*, 45(6):673–685, June 1998. (Cited on pages 16 and 19.)

[73] P. Celka. A computer-aided detection of EEG seizures in infants: a singular-spectrum approach and performance comparison. *IEEE Transactions on Biomedical Engineering*, 49(5):455–462, April 2002. (Cited on pages 16 and 20.)

[74] J. Altenburg, R.J. Vermeulen, R.L.M. Strijers, W.P.F. Fetter, and C.J. Stam. Seizure detection in the neonatal EEG with synchronization likelihood. *Clinical Neurophysiology*, 114:50–55, 2003. (Cited on pages 16, 18, and 20.)

[75] A. Shoeb, H. Edwards, J. Connolly, B. Bourgeois, T. Treves, and J. Guttag. Patient-specific seizure onset detection. *Epilepsy and Behavior*, pages 483–498, 2004. (Cited on page 16.)

[76] L.S. Smit, R.J. Vermeulen, W.P.F. Fetter, R.L.M. Strijers, and C.J. Stam. Neonatal seizure monitoring using non-linear EEG analysis. *Neuropediatrics*, 35:329–335, 2004. (Cited on page 16.)

[77] S. Faul, G. Boylan, S. Connolly, L. Marnane, and G. Lightbody. An evaluation of automated neonatal seizure detection methods. *Clinical Neurophysiology*, 116:1533–1541, 2005. (Cited on pages 16 and 20.)

[78] H. Firpi, E. Goodman, and J. Echauz. Epileptic seizure detection by means of genetically programmed artificial features. *Genetic Programming, Proceedings*, 3447:321–330, 2005. (Cited on pages 16 and 18.)

[79] A. Subasi. Epileptic seizure detection using dynamic wavelet network. *Expert Systems with Applications*, 29:343–355, 2005. (Cited on page 16.)

[80] A. Subasi and E. Erçelebi. Classification of EEG signals using neural network and logistic regression. *Computer Methods and Programs in Biomedicine*, 78:87–99, 2005. (Cited on page 16.)

[81] S.B. Wilson. A neural network method for automatic and incremental learning. *Clinical Neurophysiology*, 116:1785–1795, 2005. (Cited on page 16.)

[82] N. B. Karayiannis, G. Tao, J. D. Frost Jr, M. S. Wise, R. A. Hrachovy, and E. M. Mizrahi. Automated detection of videotaped neonatal seizures based on motion segmentation methods. *Clinical Neurophysiology*, 117: 1585–1594, 2006a. (Cited on page 16.)

[83] N.B. Karayiannis, A. Mukherjee, J.R. Glover, P.Y. Ktonas, J.D. Frost Jr., R.A. Hrachovy, and E.M. Mizrahi. Detection of pseudosinusoidal epileptic seizure segments in the neonatal EEG by cascading a rule-based algorithm with a neural network. *Journal of Clinical Neurophysiology*, 53 (4):633–641, April 2006. (Cited on page 16.)

[84] N.B. Karayiannis, Y. Xiong, G. Tao, J.D. Frost Jr., M.S. Wise, R.A. Hrachovy, and E.M. Mizrahi. Automated detection of videotaped neonatal seizures of epileptic origin. *Epilepsia*, 47(6):966–980, 2006. (Cited on pages 16 and 20.)

[85] M.A. Navakatikyan, P.B. Colditz, C.J. Burke, T.E. Inder, J. Richmond, and C.E. Williams. Seizure detection algorithm for neonates based on wave-sequence analysis. *Clinical Neurophysiology*, 117:1190–1203, 2006. (Cited on page 16.)

[86] A. Subasi. Automatic detection of epileptic seizure using dynamic fuzzy neural networks. *Expert Systems with Applications*, 31:320–328, 2006. (Cited on page 16.)

[87] A. Aarabi and F. Grebe, R.and Wallois. A multistage knowledge-based system for EEG seizure detection in newborn infants. *Clinical Neurophysiology*, 118:2781–2797, 2007. (Cited on page 16.)

[88] R. Hopfengärtner, F. Kerling, V. Bauer, and H. Stefan. An efficient, robust and fast method for the offline detection of epileptic seizures in long-term scalp EEG-recordings. *Clinical Neurophysiology*, 118:2332–2343, 2007. (Cited on pages 16 and 20.)

[89] M.S. Khlif, M. Mesbah, B. Boashash, and P. Colditz. Multichannel-based newborn EEG seizure detection using time-frequency matched filter. *Proceedings of the 29th Annual International Conference of the* IEEE EMBS, *Lyon, France*, pages 1265–1268, 2007. (Cited on page 16.)

[90] A.V. Sazonov. Implementation and evaluation of a method for automatic detection of epileptic seizures. Technical report, Stan Ackermans Institute, center for technological design, 2003. (Cited on pages 20, 21, 22, and 107.)

[91] K. Amano, J. Takamatsu, A. Ogata, C. Miyazaki, H. Kaneyama, S. Katsuragi, M. Deshimaru, S. Sumiyoshi, and T. Miyakawa. Characteristics of epilepsy in severely mentally retarded individuals. *Psychiatry and Clinical Neurosciences*, (54):17–22, 2000. (Cited on pages 22, 38, 40, 90, and 107.)

[92] D. Hendriksen. Evaluatie patientenbewakingssysteem en onderzoek naar gebruiksmogelijkheden t.b.v. diagnostiek. Technical report,

Epilepsy Centre Kempenhaeghe, Departement of Clinical Neurophysiology, 2003. (Cited on pages 24 and 88.)

[93] C.V. Bouten, K.R. Westerterp, M. Verduin, and J.D. Janssen. Assessment of energy expenditure for physical activity using a triaxial accelerometer. *Medicine and Science in Sports and Exercise*, 26(12):1516–23, 1994. (Cited on page 24.)

[94] C.V. Bouten, K.T. Koekkoek, M. Verduin, R. Kodde, and J.D. Janssen. A triaxial accelerometer and portable data processing unit for the assessment of daily physical activity. *IEEE Transactions on Biomedical Engineering*, 44(3):136–47, 1997. (Cited on pages 24, 80, and 94.)

[95] A.H. Goris, E.P. Meijer, A. Kester, and K.R. Westerterp. Use of a triaxial accelerometer to validate reported food intakes. *American Journal of Clinical Nutrition*, 73:549–53, 2001. (Cited on page 24.)

[96] A.Th. Willemsen, F. Bloemhof, and H.B. Boom. Automatic stance-swing phase detection from accelerometer data for peroneal nerve stimulation. *IEEE Transactions on Biomedical Egineering*, 37(12):1201–1208, 1990. (Cited on page 24.)

[97] F. Janssen, J. Arends, P. Griep, F. Tan, and P. Bijkerk. 3-d accelerometry and detection of seizures. *Epilepsia*, 43(s8):93, 2002. (Cited on page 24.)

[98] T. Nijsen, J. Arends, P. Griep, F. Tan, and P. Cluitmans. Detection of epileptic seizures: a model for motor phenomena. *Epilepsia*, 45(s3):95, 2004. (Cited on page 24.)

[99] Commission of Classification and Terminology of the International League Against Epilepsy. Proposal for revised classification of epilepsies and epileptic syndromes. *Epilepsia*, 30:389–399, 1989. (Cited on page 27.)

[100] Z. Li, A.M. da Silva, and J.P. Cunha. Movement quantification in epileptic seizures: A new approach to video-eeg analysis. *IEEE Transactions on Biomedical Engineering*, 49(6):565–573, 2002. (Cited on pages 40 and 55.)

[101] N.B. Karayiannis, S. Srinivasan, R. Bhattacharya, M.S. Wise, J.D. Frost, and E.M. Mizrahi. Extraction of motion strength and motor activity signals from video recordings of neonatal seizures. *IEEE Transactions on medical imaging*, 20(9):965–980, 2001. (Cited on pages 40 and 55.)

[102] S.M. Mahmud and A.I. Alrabady. A new descision making algorithm for airbag control. *IEEE transactions on vehicular technology*, 44(3):690–697, august 1995. (Cited on page 40.)

[103] Analog Devices. Analog devices' MEMS accelerometers help prevent information loss in new hard drive protection technology. News Release, december 2003. (Cited on page 40.)

[104] P. Shih and H. Weinberg. A useful role for de ADXL202 dual-axis accelerometer in speedometer-independent car-navigaton systems. *Analog Dialogue*, 35(4):1–3, August-September 2001. (Cited on page 40.)

[105] J. Cohen. A coefficient of agreement for nominal scales. *Educational and Psychological Measurement*, 20:37–46, 1960. (Cited on pages 42 and 97.)

[106] B. Dawson and R.G. Trapp. *Basic and Clinical Biostatistics*. Lange Medical Books / Mc Graw Hill, 2004. (Cited on pages 42, 51, 56, and 98.)

[107] N. Keijsers, M. Horstink, and S. Gielen. Online monitoring of dyskinesia in patients with parkinson's disease. *IEEE Engineering in Medicine and Biology Magazine*, 1, 2003. (Cited on page 42.)

[108] M. Epstein and W. Herzog. *Theoretical models of skeletal muscles: Biological and mathematical considerations*. Wiley, Chichester, 1998. (Cited on page 59.)

[109] J.M. Winters. *Multiple muscle systems : biomechanics and movement organization*. Springer, 1990. (Cited on page 59.)

[110] D.A. Winter. *Biomechanics and motor control of human movement*. Wiley-Interscience, Chichester, 1990. (Cited on pages 59, 62, and 63.)

[111] H. Veeger, B. Yu, K.N. An, and R.H. Rozendal. Parameters for modelling the upper extremity. *Journal of Biomechanics*, 30:647–652, 1997. (Cited on page 62.)

[112] P.E. Voorhoeve. *Physiologie van het centrale zenuwstelsel en de zintuigen*. N.V. Noord-Hollandsche Uitgeversmaatschappij, 1968. (Cited on page 63.)

[113] M. Holschneider. *Wavelets, An Analysis Tool*. Clarendon Press, Oxford, 1995. (Cited on pages 65, 70, and 71.)

[114] I. Daubechies. Ten lectures on wavelets. *SIAM, Philadelphia*, 1992. (Cited on page 65.)

[115] L. Sörnmo and P. Laguna. *Bioelectrical Signal Processing in Cardiac and Neurological Applications*. Academic Press, 2005. ISBN 0124375529. (Cited on pages 78, 79, 80, and 95.)

[116] W. Mecklenbräuker and F. Hlawatsch. *The Wigner Distribution - Theory and Applications in Signal Processing*. Elsevier, 1997. (Cited on page 80.)

[117] B. Boashash. *Time Frequency Signal Analysis and Processing*. Elsevier, Oxford, 1st edition edition, 2003. (Cited on page 80.)

[118] R.O. Duda, P.E. Hart, and D.G. Stork. *Pattern Classification*. Wiley-Interscience, New York, 2nd edition edition, 2001. (Cited on pages 85 and 97.)

[119] L. Stankovic, T. Alieva, and M. J. Bastiaans. Time-frequency signal analysis based on the windowed fractional Fourier transform. *Signal Processing*, 83:2459–2468, 2003. (Cited on page 87.)

[120] S.J. Raudys and A.K. Jain. Small sample size effects in statistical pattern recognition: recommendations for practitioners. *IEEE Transactions on pattern analysis and machine intelligence*, 13(3):252–264, 1991. (Cited on page 90.)

[121] A.K. Jain, R.P.W. Duin, and J. Mao. Statistical pattern recognition: a review. *IEEE transactions on pattern analysis and machine intelligence*, 22 (1):4–37, 2000. (Cited on page 90.)

[122] H.J. Luinge and P.H. Veltink. Inclination measurement of human measurement using a 3D accelerometer with autocallibration. *IEEE Transactions on Neural Systems and Rehabilitation Engineering*, (12):112–121, 2004. (Cited on pages 93 and 106.)

[123] M. Sun and J.O. Hill. A method for measuring mechanical work and work efficiency during human activities. *Journal of Biomechanics*, 26(3): 229–241, 1993. (Cited on page 96.)

[124] J. Parra, P.B. Augustijn, Y. Geerts, and W. van Emde Boas. Classification of epileptic seizures: A comparison of two systems. *Epilepsia*, 42(4): 476–482, 2001. (Cited on pages 98 and 102.)

[125] J.B.A.M. Arends, P.A.M. Griep, and I.Y. Tan. Patient monitoring system for the real-time detection of epileptic seizures, patent, NL1031958C, December 2007. (Cited on pages 105 and 107.)

SUMMARY

ACCELEROMETRY BASED DETECTION OF EPILEPTIC SEIZURES

Epilepsy is one of the most common neurological disorders. Epileptic seizures are the manifestation of abnormal hypersynchronous discharges of cortical neurons that impair brain function. Most of the people affected can be treated successfully with drug therapy or neurosurgical procedures. But there is still a large group of epilepsy patients that continues to have frequent seizures. For these patients automated detection of epileptic seizures can be of great clinical importance. Seizure detection can influence daily care or can be used to evaluate treatment effect. Furthermore automated detection can be used to trigger an alarm system during seizures that might be harmful to the patient. This thesis focusses on accelerometry (ACM) based seizure detection.

A detailed overview is provided, on the perspectives for long-term epilepsy monitoring and automated seizure detection. The value of accelerometry for seizure detection is shown by means of a clinical evaluation and the first steps are made towards automatic detection of epileptic seizures based on ACM. With accelerometers movements are recorded. A large group of epileptic seizures manifest in specific movement patterns, so called motor seizures.

Chapter 2 of this thesis presents an overview of the published literature on available methods for epileptic seizure detection in a long-term monitoring context. Based on this overview recommendations are formulated that should be used in seizure detection research and development. It is shown that for seizure detection in home environments, other sensor modalities besides EEG become more important. The use of alternative sensor modalities (such as ACM) is relatively new and so is the algorithm development for seizure detection based on these measures. It was also found that for both the adaptation of existing techniques and the development of new algorithms, clinical information should be taken more into account.

The value of ACM for seizure detection is shown by means of a clinical evaluation in chapter 3. Here 3-D ACM- and EEG/video-recordings of 18 patients with severe epilepsy are visually analyzed. A striking outcome presented in this chapter is the large number of visually detected seizures versus the number of seizures that was expected on forehand and the number of seizures that was observed by the nurses. These results underscore the need for an automatic seizure detection device even more, since in the current situation many seizures are missed and therefore it is possible that patients do not get the right (medical) treatment. It was also observed that 95% of the ACM-patterns during motor seizures are sequences of three elementary patterns: myoclonic, tonic and clonic patterns. These characteristic patterns are a starting point for the development of methods for automated seizure detection based on ACM.

It was decided to use a modular approach for the detection methodology and develop algorithms separately for motor activity in general, myoclonic seizures and tonic seizures. Furthermore, clinical information is incorporated in the detection methodology.

Therefore in this thesis features were used that are either based on the shape of the patterns of interest as described in clinical practice (chapter 4 and 7), or the features were based on a physiological model with parameters that are related to seizure duration and intensity (chapter 5 and 6).
In chapter 4 an algorithm is developed to distinguish periods with and without movement from ACM-data. Hence, when there is no movement there is no motor seizure. The amount of data that needs further analysis for seizure detection is thus reduced. From 15 ACM-signals (measured on five positions on the body), two features are computed, the variance and the jerk. In the resulting 2-D feature space a linear threshold function is used for classification. For training and testing the algorithm ACM data along with video data are used from nocturnal recordings in mentally retarded patients with severe epilepsy. Using this algorithm the amount of data that needs further analysis is reduced considerably. The results also indicate that the algorithm is robust for fluctuations across patients and thus there is no need for training the algorithm for each new patient.
For the remaining data it needs to be established whether the detected movement is seizure related or not. To this purpose a model is developed for the accelerometer pattern measured on the arm during a myoclonic seizure (chapter 5). The model consists of a mechanical and an electrophysiological part. This model is used as a matched wavelet filter to detect myoclonic seizures. In chapter 6 the model based wavelet is compared to three other time frequency measures: the short time Fourier transform, the Wigner distribution and the continuous wavelet transform using a Daubechies wavelet. All four time-frequency methods are evaluated in a linear classification setup. Data from mentally retarded patients with severe epilepsy are used for training and evaluation. The results show that both wavelets are useful for detection of myoclonic seizures. On top of that, our model based wavelet has the advantage that it consists of parameters that are related to seizure duration and intensity that are physiological meaningful. Besides myoclonic seizures, the model is also useful for the detection of clonic seizures; physiologically these are repetitive myoclonic seizures.
Finally for the detection of tonic seizures, in chapter 7 a set of features is studied that incorporate the mean characteristics of ACM-patterns associated with tonic seizures. Linear discriminant analysis is used for classification in the multi-dimensional feature space. For training and testing the algorithm, again data are used from recordings in mentally retarded patients with severe epilepsy. The results show that our approach is useful for the automated detection of tonic seizures based on 3-D ACM and that it is a promising contribution in a complete multi-sensor seizure detection setup.

SAMENVATTING

ACCELEROMETRY BASED DETECTION OF EPILEPTIC SEIZURES

Epilepsie is een van de meest voorkomende neurologische aandoeningen. Epileptische aanvallen zijn de manifestatie van abnormaal hypersynchrone ontladingen van neuronen uit de cortex waarbij de hersenfunctie verstoord wordt en waardoor men tijdelijk de controle over bepaalde lichaamsfuncties kan verliezen. De meeste mensen met epilepsie kunnen succesvol behandeld worden met medicatie of neurochirurgie. Toch is er nog een grote groep patiënten die ondanks behandeling nog steeds regelmatig aanvallen heeft. Voor deze patiënten is het automatisch detecteren van epileptische aanvallen erg van belang. Het detecteren van aanvallen kan invloed hebben op de dagelijkse verzorging. Informatie over de aanvallen kan ook gebruikt worden om de behandeling te evalueren. Verder kan automatische detectie van aanvallen gebruikt worden om een alarmsysteem aan te sturen zodat er ingegrepen kan worden bij aanvallen die gevaarlijk zijn voor de patiënt.
Dit proefschrift gaat in op het detecteren van epileptische aanvallen met behulp van accelerometrie (ACM). ACM-signalen geven verschillende bewegingspatronen weer, en een grote groep van epileptische aanvallen gaat ook met beweging gepaard, de zogenaamde motorische aanvallen. Een gedetailleerd overzicht wordt gepresenteerd van de vooruitzichten voor langdurige epilepsie monitoring en automatische detectie van aanvallen. De waarde van ACM voor het detecteren van aanvallen wordt aangetoond met een klinische evaluatie. Daarnaast zijn enkele stappen gezet voor het automatisch detecteren van epilepsie aanvallen met behulp van ACM.
In hoofdstuk 2 van dit proefschrift wordt een overzicht gegeven van de gepubliceerde literatuur over beschikbare methoden om epileptische aanvallen te detecteren in situaties waarin patiënten voor een lange periode gemonitord worden. Op basis van dit overzicht zijn aanbevelingen geformuleerd die gebruikt dienen te worden in onderzoek en ontwikkeling naar het automatisch detecteren van epileptische aanvallen. Voor het detecteren van epilepsie aanvallen thuis worden andere sensoren dan het EEG steeds belangrijker. Het gebruik van alternative sensoren (zoals ACM) is nieuw, net als de algoritme-ontwikkelingen voor signalen afkomstig van deze nieuwe sensor modaliteiten. Zowel voor het aanpassen van bestaande methodes als voor het ontwikkelen van nieuwe methodes dient meer rekening gehouden te worden met klinische informatie.
In hoofdstuk 3 wordt de waarde van ACM voor het detecteren van epileptische aanvallen is aangetoond door middel van een klinische evaluatie. 3-D ACM- en EEG/video-registraties van 18 patiënten met ernstige epilepsie worden hier visueel geanalyseerd. Een opvallend resultaat van dit hoofdstuk is dat er veel meer aanvallen visueel gedetecteerd zijn dan van te voren werd verwacht en dan er door de verpleging gemeld zijn. Dit resultaat benadrukt de behoefte aan een automatisch detectie systeem. In de huidige situatie worden veel aanvallen gemist en daardoor krijgen patiënten niet de juiste (medische) behandeling. In dit hoofdstuk wordt ook aangetoond dat 95% van de bewegingen tijdens motorische aanvallen samengesteld zijn uit een of

meerdere van drie elementaire patronen: myoclonische, clonische en tonische. Deze karakteristieke bewegingen zijn een goed aanknopingspunt voor het ontwikkelen van automatische detectie gebaseerd op ACM.
Op basis van deze uitkomst is een modulaire aanpak gekozen voor de detectie, namelijk om aparte algoritmen te ontwikkelen voor motorische activiteit in het algemeen, myoclone en tonische aanvallen. Bovendien wordt er zoveel mogelijk klinische informatie meegenomen in de detectie methodologie. Daarom worden er in dit proefschrift kenmerken (=features) gebruikt die of gebaseerd zijn op de te detecteren patronen zoals ze beschreven worden door clinici (hoofdstuk 4 en 7), of op een fysiologisch model met parameters die gerelateerd zijn aan de duur en intensiteit van de motorische aanval (hoofdstuk 5 en 6).
In hoofdstuk 4 wordt een algoritme beschreven dat onderscheid maakt tussen ACM-data met en zonder beweging. Wanneer er geen beweging is, is er ook geen motorische aanval. De hoeveelheid data die verder geanalyseerd dient te worden wordt zo gereduceerd. Van 15 ACM-signalen (gemeten op vijf posities op het lichaam) worden twee kenmerken berekend, de variantie en de 'jerk'. In de 2-D feature ruimte wordt een lineaire drempelfunctie gedefinieerd voor classificatie. Met dit algoritme wordt de hoeveelheid data die verdere analyse nodig heeft gereduceerd. De resultaten geven ook aan dat het algoritme robuust is voor variatie tussen patiënten en het is dus niet nodig om het algoritme per patiënt opnieuw in te stellen.
Voor de data die als beweging zijn geclassificeerd moet worden vastgesteld of de beweging een manifestatie van een epileptische aanval is of niet. Hiervoor is een model ontwikkeld dat de versnelling bij een myoclone aanval beschrijft (hoofdstuk 5). Het model bestaat uit een mechanisch en een elektrofysiologisch gedeelte. Dit model wordt in de analyse voorgesteld als een wavelet. In hoofdstuk 6 wordt deze wavelet vergeleken met drie andere tijdfrequentie methoden: de short time Fourier transformatie, de Wigner distributie en de continue wavelet transformatie met een Daubechies wavelet. Alle vier de tijdfrequentie methoden zijn geëvalueerd met een lineaire classificatie methode. Data van mentaal geretardeerde patiënten met ernstige epilepsie zijn gebruikt voor training en evaluatie. De resultaten laten zien dat beide wavelets (het model en de Daubechies wavelet) bruikbaar zijn om myoclone aanvallen te detecteren. Onze eigen model gebaseerde wavelet heeft als voordeel dat hij fysiologische parameters bevat die zijn gebaseerd op de duur en intensiteit van de aanval. Het model blijkt ook geschikt voor clonische aanvallen, die fysiologisch gezien ook beschreven worden als zich repeterende myoclonieën. Tenslotte beschrijft hoofdstuk 7 een studie naar het detecteren van tonische aanvallen uit ACM-data. Een aantal features is gedefinieerd die de belangrijkste karakteristieken bevatten die geassocieerd zijn met een tonische aanval. Lineaire discriminant analyse wordt gebruikt voor classificatie in de multi-dimensionale feature ruimte. Voor het trainen en evalueren wordt weer van data gebruik gemaakt die gemeten is in mentaal geretardeerde patiënten met ernstige epilepsie. De resultaten van deze studie laten zien dat onze aanpak bruikbaar is voor het automatisch detecteren van tonische aanvallen gebaseerd op 3-D ACM en dat het een veelbelovende bijdrage is in een multi-sensor detectie systeem.

CURRICULUM VITAE

Tamara Mathea Elisabeth was born on January 18^{th}, 1979 in Weert, the Netherlands. After graduating from secondary school (VWO) at the Philips van Horne Scholengemeenschap in Weert in 1998, she started to study Biomedical Engineering at the Eindhoven University of Technology. In 2001, she received the B.Sc. degree in Biomedical Engineering and later in 2004, the M.Sc degree in Biomedical engineering from the Eindhoven University of Technology. During her studies she got interested in biomedical signal processing. In 2002, she did an internship at Datex-Ohmeda in Helsinki, Finland. The subject of this internship was to study the adequacy of analgesia. To this end polygraphic data measured during surgery were used to find a measure for analgesia.
In 2003 she started to work on her M.Sc. graduation project at the Signal Processing Systems group of the department of Electrical Engineering of the Eindhoven University of Technology in collaboration with Epilepsy Centre Kempenhaeghe in Heeze. Here she started to work on accelerometry based seizure detection. In this masters project the basis for the model for myoclonic seizures was made.
After her graduation in 2004, she continued with this research, but now at Hobo-Heeze B.V. in order to pursue a Ph.D degree.

DANKWOORD

Aan het einde van dit proefschrift wil ik graag iedereen bedanken die een bijdrage heeft geleverd aan het tot stand komen van dit werk.

Allereerst wil ik mijn promotoren prof. dr. Ronald Aarts en prof. dr. Paul Boon bedanken. Ronald, bedankt voor de impuls die je aan mijn onderzoek hebt gegeven wat betreft de signaal-analyse kant. Verder wil ik je bedanken voor je praktische adviezen wat betreft het schrijven van papers en je commentaar in de laatste fase van het schrijven van dit proefschrift.
Paul, je interesse voor mijn onderzoek was erg motiverend, evenals de waardevolle adviezen bij het schrijven van het review artikel.
Verder wil ik mijn co-promotor dr. ir. Pierre Cluitmans bedanken. Pierre, bedankt voor onze vele discussies, vooral de discussie over de problematiek van het evalueren van algoritmes met klinische data kwam vaak terug. Maar vooral bedankt voor je optimisme en je continue vertrouwen in de goede afloop van dit project.

Natuurlijk mogen mijn begeleiders op Kempenhaeghe dr. Johan Arends en dr. ir Paul Griep niet vergeten worden. Johan, je enthousiasme en snelheid van denken werkten aanstekelijk. Door jou had ik al snel inzicht in de typische bewegingen tijdens 'simple motor seizures' en hoe deze weerspiegeld worden in de accelerometriesignalen. Paul, bedankt voor het me steeds bewust maken van het brede overzicht wat betreft de praktische kant van het onderzoek. Hierdoor kon ik de koppeling maken tussen mijn resultaten en de toepasbaarheid in de praktijk. Mede hierdoor zijn een aantal delen van mijn promotieonderzoek geïmplementeerd voor het gebruik ter ondersteuning van de diagnostiek, wat ikzelf als een hele mooie afronding van dit werk beschouw.
Een belangrijk onderdeel van mijn promotie-project is natuurlijk de accelerometrie data. Daarom wil ik alle mensen binnen Kempenhaeghe bedanken die ervoor gezorgd hebben dat ik beschikte over grote hoeveelheden geanalyseerde accelerometrie signalen, met in het bijzonder: Antonet Aarts voor haar betrokkenheid en inzet bij de vele patiënten registraties en Peter Bijkerk voor zijn ondersteuning aan de meetopstelling. Harrie Geeris, Riny Sijben, Marjan van Gerwen en Margret Verspaandonk wil ik bedanken voor het annoteren van de accelerometrie signalen.
Roy Krijn, wil ik bedanken voor het altijd snel oplossen van mijn Matlab-problemen. Dankzij zijn inspanningen konden de vele annotaties gemakkelijker worden uitgevoerd evenals het verwerken van deze annotaties.

Dr. ir. Guido Janssen wil ik bedanken voor zijn wiskundige bijdragen aan hoofdstuk 5 van dit proefschrift.

Verder wil ik alle collega's bedanken van zowel Kempenhaeghe als SPS voor hun betrokkenheid en voor de gezellige gesprekken, met in het bijzonder:
Andrei, Chiara, Harald, Joep, Lotty, Massimo, Petra, Rianne, Rik, Saskia en Tanya.

Mijn broer Ben (en Atelier de Biest) wil ik bedanken voor het mooie kleurige kunstwerk dat de kaft van dit proefschrift siert.

Mijn ouders wil ik bedanken voor hun onvoorwaardelijke vertrouwen in mijn kunnen, maar ook voor de vele gezellige etentjes waarbij ik even helemaal 'niets' hoefde.

En als laatste wil ik jou bedanken Remco, voor al je liefde en omdat je er altijd voor me bent wanneer dat echt nodig is. En bedankt dat je toch maar steeds de moeite neemt om me wiskundige adviezen toe te stoppen, terwijl je toch inmiddels moet weten dat ik daar te eigenwijs voor ben...

Bedankt !
Tamara